CONDENSATION OF AIR COMPONENTS IN HYPERSONIC WIND TUNNELS -- THEORETICAL CALCULATIONS AND COMPARISON WITH EXPERIMENT

Thesis by

Rolf D. Buhler

In Partial Fulfillment of the Requirements

For the Degree of

Doctor of Philosophy

California Institute of Technology

Pasadena, California

1952

ACKNOWLEDGMENTS

The writer wishes to thank his adviser, Dr. H. T. Nagamatsu, for his patient help and encouragement throughout this study. Dr. Nagamatsu's continued interest in this work was decisive for its successful completion.

Helpful suggestions and criticisms by many other staff members are gratefully acknowledged. In particular, Professor M. S. Plesset and Dr. F. Gilmore contributed very generously their time and special knowledge in the field.

It should be mentioned that many of the important ideas in this investigation evolved out of discussions with fellow students and members of the Hypersonic Wind Tunnel group, among them Messrs. P. D. Arthur, D. Coles, M. Eimer, J. Grey, P. Jackson, P. MacCready, and W. W. Willmarth. Mr. Jackson also did many of the lengthy computations.

The writer is indebted to the Staff of the GALCIT 10-Foot Wind Tunnel for their friendly cooperation in the preparation of charts and of the final thesis copy. In particular, the help of Miss J. Mainwaring, Mrs. L. Marks, and Mrs. C. Rade is gratefully acknowledged.

Thanks are due to the Hypersonic Wind Tunnel project sponsored by the U. S. Army Ordnance Department and U. S. Air Force for providing computer time and other assistance throughout this work.

During the latter phases of the study, the writer worked very closely with Mr. P. D. Arthur, whose friendship, help, and good ideas were invaluable.

Finally, many thanks to Miss Gerry Ellis who prepared the manuscript efficiently under extreme rush conditions.

ABSTRACT

The effect of condensation on the flow in hypersonic wind tunnels is bracketed by equilibrium saturated expansion and by instantaneous condensation. By calculation of shock waves with evaporation, direct comparison of theoretical and measured pressures is made possible. Satisfactory agreement between saturated expansion theory and experiment is obtained after the collapse of the supersaturated state.

The droplet growth theory (for free molecule regime) is re-examined, and a good approximate solution is obtained for the non-steady case (i.e., rapidly changing vapor properties). Limits of validity of the quasi-steady theory are defined, and an upper limiting (zero growth) drop size given for expanding flow.

A simplified method is presented for calculating the pressure time history of the collapse of the supersaturated state in nozzles. From this, most effective nucleus sizes for given total mass of impurities are calculated. Thus the earliest possible collapse in a nozzle due to impurities is estimated theoretically for low impurity concentrations. The agreement of the predicted trend with experimental results in nitrogen appears to justify the assumed mechanism of the collapse, which is condensation on existing foreign nuclei formed upstream of the collapse.

TABLE OF CONTENTS

LIST OF FIGURES

NOMENCLATURE

Symbol		Units
a	Isentropic velocity of sound in perfect gas, $\sqrt{\gamma RT}$	cm/sec.
a^*	Limiting "sound" velocity defined in Eq. II-8	
A	Nozzle (or streamtube) cross-sectional area at a point	cm^2
α	Angle of an infinitesimal oblique pressure wave	degrees
C	A parameter in the collapse calculation (Eq. V-5)	cm^{-1}
C_p	Constant pressure specific heat (in mechanical units)	erg/gm ^oK
C_v	Constant volume specific heat (in mechanical units)	erg/gm ^oK
γ	Specific heat ratio, taken as 1.40	
Γ	Maxwellian effusive stream (Eq. IV-4)	gm/cm^2 sec.
E	Evaporation parameter for discontinuities with phase change defined in Eq. III-10	
e	Internal energy (in mechanical units)	erg/gm
ε	Mass of impurities per unit mass of air or nitrogen	
η	Parameter in the collapse calculation (Eq. V-1)	
ϑ	Flow deflection due to an obluque wave	radians
$\Phi(M,E)$	Invariant for discontinuities with phase change (Eq. III-9)	
g	Fraction of mixture which is in condensed phase, assumed $\ll 1$.	
h	Specific enthalpy (in mechanical units)	erg/gm
J	Condensation germ formation frequency	sec^{-1} cm^{-3}
K	Eötvos constant	
κ	Surface tension parameter (page 53)	dynes/cm ^oK
L	Latent heat of evaporation (in mechanical units)	erg/gm
C_γ	A parameter used in the collapse calculation (Eq. V-5)	cm^{-1}

λ	Approximate constant related to specific heat of liquid phase (Eq. IV-8)	$erg/cm^3\ ^oK$
M	Mach number, used for condensation free flow only	
$\tilde{M}$	Dynamic pressure parameter, valid in two phase flow or in perfect gas (Eq. II-7)	
$\overset{o}{M}$	Mach number based on sound speed $\overset{o}{a}$ (Eq. II-8)	
ν	Number of Nuclei per unit mass of air or nitrogen	gm^{-1}
p	Free stream pressure	$dynes/cm^2$
p_o'	Pitot pressure	$dynes/cm^2$
p_o	Upstream stagnation pressure	$dynes/cm^2$
P_o	Upstream stagnation pressure	atmospheres
q	Dynamic pressure, $\frac{1}{2}\rho u^2$	$dynes/cm^2$
R	Gas constant per unit mass (in mechanical units)	$erg/gm\ ^oK$
r	Droplet radius	cm
r_o	Nucleus radius	cm
r_{zg}	Zero growth radius of droplet in nozzle (Eq. IV-17)	cm
ρ	Density of mixture (vapor and condensed phase)	gm/cm^3
ρ_L	Bulk density of condensed phase	gm/cm^3
ρ_V	Density of vapor alone	gm/cm^3
s	Specific entropy	$erg/gm\ ^oK$
σ	Wave angle of oblique shocks	degrees
t	Time	sec.
T	Absolute temperature	^oK
u	Free stream velocity	cm/sec
w	Total surface energy	erg/cm^2
x	Axial distance along nozzle, from throat	cm

Subscripts and Superscripts

The following subscripts and superscripts refer to

$( )_o$	the supply tank
$( )_1$	the point in the nozzle where saturation first occurs
$( )_2$	a point in free stream where condensation has taken place
$( )_3$	conditions just after shock with evaporation
$( )^*$	the nozzle throat
$( )^+$	the critical droplet radius
$( )_s$	the vapor saturated with respect to the liquid phase at the same temperature
$( )_v$	the vapor in general
$( )_D$	the droplet or crystal
$( )_E$	a droplet or crystal at quasi-steady equilibrium temperature
$( )_L$	the condensed phase in general
$( )_{QS}$	calculations under the quasi-steady assumption
$( )_N$	component normal to a discontinuity
$( )_T$	component tangential to a discontinuity

Several other symbols and notations are defined in the text, for use only in the immediate vicinity of their definition.

I. INTRODUCTION*

A. Early Theoretical Considerations on the Condensation of Air in Hypersonic Nozzles

The problem of condensation of oxygen and nitrogen in high speed wind tunnels was apparently first considered by Wagner (Ref. 1) in connection with the design of the Kochel tunnel. Wagner believed that the air would probably begin to condense near the saturation point because of foreign nuclei. In fact he set up (as this writer later discovered)the equations for the equilibrium saturated expansion of air. Wagner also considered the possibility of supersaturation and spontaneous self-nucleation. This work was continued by Grunewald (Ref. 2).

In this country, Epstein (Ref. 3) investigated both the spontaneous germ formation and the condensation on foreign nuclei. He came to the conclusion that the condensation on very small foreign nuclei would predominate over the self-nucleation. The assumptions regarding the nuclei (Cf. Section IV) are identical with those of the present paper, but the droplet growth formula is different due to an assumption regarding the droplet temperature. Puckett and Schamberg (Ref. 4) checked the calculations of Grunewald which were based on the Volmer theory of germ formation. They found an error in Grunewald's method and recomputed the saturation ratios required to give a germ formation frequency J of 10^3 in the nozzle. They came to

---

* A complete review of the literature on condensation problems is not intended here, since extensive reviews of this type have been made in several previous Theses (e.g., Charyk, Head, Gilmore).

the tentative conclusion that appreciable supersaturation might be reached in the tunnel. Further calculations based on germ formation theory were carried out by Charyk and Lees (Ref. 5). They also obtained very high saturation ratios for the values of J which they considered necessary for a condensation "shock" to occur. They stated, however, that saturation ratios above 1000 appeared unlikely physically. In addition they found that of the two major components of air, nitrogen would be more critical as far as self-nucleation is concerned.

The early thinking of these and other investigators of the hypersonic tunnel problem (except possibly Wagner and Epstein) was strongly influenced by the experimental and theoretical results on moisture condensation in nozzles. The previously observed condensation "shock" phenomenon in supersonic wind tunnels and in steam nozzles was first explained by Oswatitsch in a very extensive study (Refs. 6 and 7). He investigated all conceivable phases of the theoretical problem. In fact, most further theoretical work which has been done on the general problem of high speed condensation has, in principle, already been done, or at least outlined, in one of Oswatitsch's papers. A very brief review of his results is given because of their importance for this investigation.

In his explanation of the condensation shock, Oswatitsch showed that any foreign nuclei present in ordinary air were insufficient to keep the water vapor saturated in a nozzle of typical size. He therefore calculated germ formation frequencies in the nozzle. He integrated the growth of these droplets along the nozzle and thus found the order of magnitude of J required for the collapse of the supersaturated state. For heated steam, he obtained good agreement between theoretical and experimental results. For moisture in air, he was forced to use a semi-

empirical approach, determining the dependence of J on temperature from three experiments. The work of Oswatitsch showed that the significant contribution to the collapse came not from the germs formed at the point of measured pressure rise, but from those formed (in smaller numbers) some distance upstream. This means, in effect, that there is no simple correlation between the values of J at the measured collapse points in nozzles of different shape and size.* In fact, from the apparent delay caused by the necessary droplet growth, Oswatitsch estimated the depenence of the shock location (or saturation ratio) on the temperature gradient of the nozzle. The writer has extrapolated these results further and found quite good agreement with more recent experiments.** It is important for the present investigation that the quasi-steady theory of Oswatitsch predicted quite well the so-called non-steady effect, i.e., the dependence of the supersaturation on the temperature gradient in the nozzle, for water vapor.

Because of the behavior of moisture in supersonic tunnels, most investigators expected a condensation shock-like phenomenon to occur in air at high Mach numbers. Because of this, most of the efforts were spent on attempts to improve the theory of germ formation.

When the early experiments did not show any evidence of a shock-like collapse, (i.e., with pressure increase), all parties concerned with the problem began to re-examine the various aspects of the condensation phenomenon.

The present paper is part of this overall re-examination which has

---

* This statement is confirmed by the results of Head (Ref. 8) and others.

** Cf. Wegener and Smelt (Ref. 9).

been carried on in the past few years simultaneously in many places. Here the investigation is aimed at the specific problems of high Mach number wind tunnel operation, while some of the more general physical problems not immediately applicable to this have been left aside.

B. Early Experimental Evidence Leading up to the Present Study

During the initial periods of operation of the GALCIT-Army Ordnance Hypersonic Wind Tunnel, apparent discrepancies were discovered between the measured and the calculated static pressures along the nozzle. Other laboratories, particularly NACA (Langley Field), later M.I.T. and N.O.L., reported preliminary results of similar nature, though no actual data from these places were available for comparison during the early stages of this investigation. It must be pointed out that the actual magnitude of these discrepancies was difficult to ascertain because the static pressure, the clue to the problem, is difficult to measure reliably. To confuse matters further, it was found that the one reliable measurement which could be made, the pitot pressure, agreed well with values expected from the perfect gas theory, within a reasonable boundary layer correction.

Various hypotheses were offered to explain the discrepancies, among them:

(1) condensation of the air

(2) deviation from the assumed equation of state (without condensation)

(3) excessive viscous losses in the throat of the nozzle

(4) inherent systematic errors in the measured static pressures.

In 1949 Bogdonoff and Lees (Ref. 10) reported the results of a

very significant (though very tentative) experiment: up to 2% of carbon dioxide had been added to the supposedly highly supersaturated flow without any marked effect on the tunnel wall pressures.

Following this lead, the writer started preliminary droplet growth calculations. These indicated the order of magnitude of the number of particles required to cause appreciable condensation. This number was found to be much larger than the number of particles counted in ordinary air (by electron microscope and other methods), but quite within the possible range of numbers which could be expected from condensed impurities such as carbon dioxide and water. (Cf. page 65)

In this potential presence of nuclei formed in the nozzle by condensing impurities appears to lie the basic difference between the moisture and the air condensation problems. Such "secondary" nuclei, by their very nature of formation, are likely to occur in similar numbers and sizes as condensation "germs" formed spontaneously from oxygen and nitrogen.

During 1950, several symposia on the subject of condensation were arranged by various agencies, where a thorough exchange of information took place. There it was learned that in the NACA tunnel, the above-mentioned discrepancies disappeared as soon as the air was sufficiently heated (Ref. 11). This was soon thereafter confirmed by other groups, particularly those at N.O.L. (Ref. 12) and at M.I.T. (Ref. 13). Furthermore, very convincing light-scattering tests had been carried out at all these tunnels, showing a strong difference in the intensity of scattering between heated and cold runs.

Also in the summer of 1950, the simple thermodynamic calculations (Cf. Section II) of the writer were compared with the preliminary

pressure data from the N.O.L. tunnel. In this comparison, effective area ratios, based on the heated runs, were used. The agreement was very good and well within the accuracy with which this particular comparison can be carried out (Cf. Sections II and III).

Thus by the summer of 1950, it was well established that condensation of oxygen and nitrogen was taking place in hypersonic tunnels.

C. Reasons for this Study

From the viewpoint of the engineer, the following questions remained to be answered:

(1) How much supersaturation is reached before the collapse.

(2) How does this depend on the tunnel size and pressure.

(3) Would purification of the air (or nitrogen) increase the attainable supersaturation and make possible testing in supersaturated air.

(4) How close to the saturation point could one obtain reliable test data in a tunnel with ordinary air.

(5) Could useful hypersonic testing be done in partially condensed air, and how should tests be evaluated and correlated with free flight data.

It should be mentioned here that the heating of the air, while very desirable, does not solve all the problems of condensation in hypersonic tunnel operation. A look at the saturation point chart for air (Cf. Fig. I-1) shows that very high stagnation temperatures would be required if we want to stay above saturation at Mach numbers near 10 (about 1500°F for Mach number 10 at 100 atmospheres stagnation pressure). Tunnel design and operation at such high temperatures will be both

cumbersome and expensive. On the other hand, some investigators believe that for the study of the hypersonic flow regime, experiments at Mach numbers much higher than 10 would be desirable. For a general discussion of testing problems at very low densities, see Tsien (Ref. 14).

Various scientists have for a long time suggested the use of non-condensing gases in hypersonic tunnels, particularly helium. This obviously offers a solution and is being seriously considered in several places. Preliminary experiments with helium in hypersonic nozzles have been made by several investigators (Cf. Refs. 16 and 33). However, it is still considered very desirable to obtain experimental data in air at high Mach numbers. Therefore, the questions enumerated above will be of practical importance for some time to come.

In order to answer these questions, one needs a more thorough understanding of the condensation process in a nozzle and of the general behavior of the two-phase flow. In particular one should have at least reliable order-of-magnitude information on the following:

(1) Numbers and sizes of foreign nuclei in the air, including those formed in the nozzle by condensing impurities.

(2) Numbers and sizes of the droplets after the collapse has occurred.

(3) Rate of condensation or evaporation of the droplets in passing through waves (such as those produced by models) and in the viscous boundary layer.

The calculations presented here together with concurrent experimental studies (Refs. 15, 16, and 17) were made in an attempt to shed some light on these points, both to assist current engineering projects and, if possible, to contribute toward the eventual understanding of an

important physical phenomenon.

D. Breakdown of Some Important Theoretical Problems Connected with Condensation

According to the methods of approach which have been used in the past, the theoretical problems connected with high speed condensation may be roughly grouped into the following categories:

(1) Overall thermodynamic effects of condensation on high speed flow:
    (a) gradual (near equilibrium) condensation
    (b) instantaneous collapse of the supersaturated state (condensation shock)
    (c) gradual collapse of the supersaturated state
    (d) general gas dynamic behavior of a two-phase aggregate.

(2) Thermo-kinetic problems of the growth of droplets or crystals larger than the critical size:
    (a) growth of existing droplets or crystals in a pure vapor
    (b) growth of existing droplets or crystals in a mixture of a condensing and a non-condensing vapor
    (c) initial condensation on foreign particles of sufficiently large size. Wetting of nuclei and interaction between nucleus and condensing substance.

(3) Thermo-kinetic probability problems on the formation of new droplets and crystals, due to fluctuations:

(a) condensation germ formation in a pure vapor

(b) condensation germ formation in a mixture of condensible substances

(c) condensation on nuclei much smaller than critical size, and condensation on ions.

(4) Dynamic and thermodynamic behavior of small particles suspended in a high velocity gas jet:

(a) velocity and temperature lag of nuclei in a rapidly expanding flow, before the onset of condensation

(b) velocity and temperature of growing droplets in an expanding flow

(c) behavior of droplets during and after the passage through a shock wave.

The problems investigated in the present study (Cf. E below) belong in group (1) and group (2-a). In order to justify certain assumptions in this work, order-of-magnitude estimates on the dynamic behavior of particles have been made, which belong in group (4). Most of these are similar to the estimates made by Oswatitsch. They are not repeated here in detail. An estimate has also been attempted on the distance which droplets of 10^{-5} cm radius would travel after passing through a normal shock, before being completely evaporated. This estimate is open to many doubts and is not included here. However, the result would be important in connection with pitot tubes and total temperature probes.

The important and difficult problems of group (3) were left

aside. The writer felt that the simpler and more straight-forward calculations of (1) and (2-a) should be made first, for the purpose of orientation. This approach was also dictated by the necessity of outlining experimental procedures and methods for correlating experimental data in this condensation investigation. Also it was believed that correlation of the results from (1) and (2-a) with experiments should clarify somewhat the role of impurities in the collapse of the supersaturated state.

It is nevertheless clear that a complete understanding of the whole phenomenon would require solutions of the difficult small-particle problems of group (3). This concerns particularly the formation of the foreign nuclei and the very early stages of growth of the droplets or crystals. Here the nuclei have merely been assumed (or possibly proved) to be present.

It should be mentioned that much important fundamental work has been done in the past few years on problems connected with spontaneous germ formation. No review of this work is intended here, but a few important references will be mentioned for completeness. The status (in 1939) of the theory of spontaneous germ formation, initiated by Volmer and Weber and furthered by Becker and Döring and others, is summarized in the text of Volmer (Ref. 18). Reviews of this work are also given by Charyk (Ref. 19) and Stever (Ref. 13) and many others. More recently, critical examinations of the Becker-Döring theory applied to non-steady conditions have been made by Kantrowitz (Ref. 20), Probstein (Ref. 21), and Gilmore (Ref. 22). The work of Gilmore includes a very illuminating comparison of different droplet "radii" which have been used in connection with the calculations of the surface energy. The recent work of Buff and

Kirkwood (Ref. 23) and of Buff (Ref. 24) on the thermodynamics of interfaces is of importance. Finally the important contributions by Reed (Ref. 25) on the energy associated with small clusters of molecules should be mentioned.

In spite of the above-mentioned efforts and progress, a complete theory of germ formation for a mixture of condensible substances is not yet available, to the knowledge of the writer. The writer also believes that a process similar to the spontaneous pure germ formation must exist, whereby due to fluctuations there is a finite probability for nuclei of much smaller than "critical" size to grow. This may be important in applications where large numbers of very small nuclei can be present. The simple approach of beginning the average growth at the "critical supersaturation", as used here*, is thus likely to be a very crude approximation to the true physical facts, though it appears to give some correct qualitative trends.

E. Outline of This Paper

In Section II, thermodynamic calculations are given, indicating the overall effect of the condensation of the air on the flow in a nozzle. Two limiting cases are considered: equilibrium saturated expansion and instantaneous condensation. A simple limiting sound velocity is derived for the two-phase fluid, based on the assumption of complete equilibrium between droplets and vapor. Typical numerical results are given.

In Section III, relations for shock waves in a two-phase fluid

---

* Cf. Section IV, Paragraph A.

are given.* These relations are used to calculate pitot pressures and pressures caused by steep wedges. Typical shock wave charts are given indicating the sensitivity of various parameters to the reevaporation. On the basis of the theoretical pitot pressures, the saturated expansion and the instantaneous collapse results are compared with experimental data of Refs. 15 to 17.

In Section IV, a droplet growth formula, similar to that of Oswatitsch, is derived for the low-density case. All the terms, particularly the non-steady terms, are critically examined to determine the regions of validity of the quasi-steady growth calculations. An approximate solution of the non-steady case is given, valid in all cases where extreme pressure gradients are not encountered (i.e., excluding shock waves).

The corrected (non-steady) growth rates are numerically integrated along a typical five-inch wind tunnel nozzle. This integration is possible for the case where the vapor properties throughout the nozzle are known in advance, i.e., are not appreciably influenced by the condensation. This calculation gives an upper limit for the true droplet growth in the nozzle, for the purpose of order-of-magnitude estimates on the possible effect of a given number of nuclei.

In Section V, an attempt is made to predict the general nature of the collapse phenomenon by an approximate integration of the quasi-steady droplet growth during the collapse. From this an estimate is

---

* Note that in the substances considered (nitrogen and air), pressure waves always cause reevaporation, nearly isentropic expansion causes increased supersaturation or condensation.

made of the most effective nucleus size for a given total mass of the nuclei. Based on this nucleus size (and number), a theoretical estimate is made of the "earliest possible" collapse, for three concentrations of impurities (CO_2). This theoretical estimate is compared with the experimental collapse curves of Ref. 16. The effect of the nozzle size and stagnation pressure on the collapse is discussed qualitatively.

In Section VI, the most important results of this paper are briefly summarized, and certain unsolved problems are pointed out.

In Appendix I, some important physical properties of oxygen, nitrogen, and air are given for reference.

II. THERMODYNAMIC CALCULATIONS ON THE EFFECT OF CONDENSATION ON NOZZLE FLOW

A. Equilibrium Saturated Expansion

1. Assumptions

In the following calculations, it is assumed that a vapor (nitrogen or air) expands reversibly in a nozzle, and that during this process the vapor remains in complete mechanical and thermodynamic equilibrium with either its liquid or its solid phase. It was found later that Carl Wagner (Ref. 1) had already carried out similar calculations for the Koche tunnel. In the present investigation, these calculations were made mostly to obtain orders of magnitude and general trends rather than high numerical accuracy. Therefore, the physical properties of the vapor were approximated in a manner which greatly reduced the work of computation (see below).

The equilibrium flow described in this Section constitutes, of course, the simplest and most straight-forward limiting case which a condensing flow might approach. Experimental evidence now shows that certain regions of the actual flow in the tunnel are approximated fairly well by this simple equilibrium case, possibly within the accuracy with which the comparison between the theoretical and experimental values may be carried out.

At first sight, one would question the reasonableness of the equilibrium assumption. One might argue that very small condensed particles require supersaturation to exist, while larger ones could not follow the rapid temperature and velocity gradients of a typical expansion nozzle. Preliminary calculations show, however, that there

exists a "preferred region" of particle size with which the assumed properties of equilibrium could be satisfied very closely. Inspection of the saturation ratio chart based on the Thompson formula* (Cf. Fig. IV-2) shows the following, for typical wind tunnel temperatures: particles above 10^{-5} cm radius require no supersaturation of practical importance. Even for 3×10^{-6} cm radius, the required saturation ratio is very near unity. On the other hand, in the range of wind tunnel pressures considered, particles of 10^{-5} cm or less radius can follow any typical temperature and velocity gradient in a nozzle very closely (Cf. Section IV).

It may therefore be concluded that the assumed equilibrium could be satisfied quite well in a nozzle provided particles or droplets in the proper numbers and sizes are present. The fact that such particles could be present was pointed out in the discussion on nuclei.

Several other simplifying assumptions concern the physical properties of the substances treated, i.e., air and pure nitrogen. First, the best available vapor pressure curves were approximated by the integrated Clapeyron-Clausius equation, fitted over the region of interest. The vapor pressure curves used are discussed in Appendix I. The use of the simple logarithmic equation requires a constant latent heat over the range of temperatures considered. It further implies that the specific heat of the condensed phase must be equal to that of the vapor at constant pressure.

The vapor is treated as a perfect gas with constant specific heats,

---

* The assumptions used in the preparation of this chart are discussed in Section IV.

and constant specific heat ratio γ of 1.40. Note that here as throughout this paper, air is treated as a single vapor (rather than a binary mixture) with average properties of molecular weight, vapor, pressure, etc. (Cf. Appendix I)

The expansion in the nozzle is assumed to be frictionless and without heat transfer from the outside. These assumptions, however, apply only to the flow in the free stream, or, more specifically, to the particular stream tube under consideration. We thus share the dilemma common to all "one dimensional" channel flow considerations: if we consider the equations as applying only to a stream tube in the center of the channel, then the continuity equation becomes useless, because we have no way of knowing the cross sectional area of the streamtube at any point. If, on the other hand, we assume the flow uniform across the whole channel and use the geometric channel area, this involves very serious errors because of friction and heat transfer along the walls, and because of non-uniform flow due to the expansion. All these discrepancies from the ideal case can be lumped into a single factor, by defining an "effective" area ratio, based on the flow properties along the channel centerline. This approach is frequently used in gas dynamics. Conversely, we could use an "effective mean flow" based on the geometric area, as is done in pipe flow problems. Here the equations will be assumed to hold along a streamtube in the free stream. Where the term area ratio is used, it should be regarded as an effective area ratio based on the flow in the streamtube considered.

In the equation of state, the volume occupied by the condensed phase will be neglected compared with the total volume. This is justified

because the vapor phase is at rather low pressure, and in any practical case, the mass fraction g of the condensed phase must be of the order of a few per cent. The equations given therefore do not apply to the opposite limiting case of a few gas bubbles in a liquid.

2. Basic Equations

The specific enthalpy of the condensed phase must be defined as*

$$h_L(T) = h_V(T) - L$$

The energy equation for flow without external heat addition will therefore be

$$\frac{u^2}{2} + (1-g)h_V + g(h_V - L) = \text{Constant}$$

or for perfect gas

$$\frac{u^2}{2} + C_p T - Lg = C_p T_o$$

This is given below in differential form, which is convenient for combination with the momentum equation.

The basic equations for the conservation of mass, momentum, and energy in saturated flow then become

$$\frac{d\rho}{\rho} + \frac{du}{u} + \frac{dA}{A} = 0 \qquad \text{Continuity} \qquad (1)$$

$$u\,du + \frac{dp}{\rho} = 0 \qquad \text{Momentum} \qquad (2)$$

$$u\,du + C_p\,dT - L\,dg = 0 \qquad \text{Energy} \qquad (3)$$

---

* Note that the vapor has been assumed just saturated with respect to the condensed phase.

The assumed equation of state is

$$p = \rho_v RT = \rho(1-g)RT \tag{4}$$

where ρ_v is the density of the vapor alone and ρ is the density of the mixture of vapor and droplets.

The assumption of equilibrium saturation conditions together with the simplified vapor pressure equation give

$$p = p_s(T) \qquad \text{for} \qquad T \leq T_1$$

where

$$\ln \frac{p_s}{p_1} = \frac{L}{R}\left(\frac{1}{T_1} - \frac{1}{T}\right) \tag{5}$$

Here T_1 and p_1 refer to the point in the nozzle where the flow first becomes saturated, i.e., where the isentrope in the p - T plane crosses the saturation line.

We thus have five equations relating the six variables p, ρ, T, u, g, and A. On choosing a value for one of the variables, we can solve for the other five. It should be noted that A enters only into the continuity relation. We could thus just as well have omitted A and Eq. 1 altogether. This has been done in many of the calculations. In this respect, this reversible flow is different from the irreversible processes discussed later, e.g., condensation "shock" and shock with evaporation where the continuity relation is essential to the solution.

The results obtained are as follows: Eqs. 2, 3, 4, and 5 can be combined and integrated in closed form, giving

$$g = \frac{c_p}{L} T \ln \frac{T}{T_1} + \left(1 - \frac{T}{T_1}\right) \tag{6}$$

Using this, we can find all other variables (except A) as functions of T: p is given by Eq. 5, u by the energy equation in its integral form, ρ by Eq. 4.

If we wish to relate any of the above variables to the flow area, we write

$$\frac{A}{A_1} = \frac{\rho_1 u_1}{\rho u}$$

where ρ/ρ_1 and u/u_1 are now known functions of T. Some further details are given in Ref. 27.

An important parameter in fluid mechanics is the ratio of the dynamic pressure q to the free stream static pressure. A dimensionless parameter $\tilde{M}$ has been defined, the square of which is proportional to the above ratio:

$$\tilde{M}^2 = \frac{u^2}{\gamma p/\rho} = \frac{2}{\gamma} \frac{g}{p} \tag{7}$$

Clearly $\tilde{M}$ reduces to the ordinary Mach number for a perfect gas without condensation. $\tilde{M}$ retains some of the functions of the Mach number, in particular, it enters very naturally into all the shock relations of the two-phase fluid considered here (Cf. Section III).

3. Brief Comment on Sound Velocity and the Mach Number

Extensive literature exists on the sound velocity in gases at low temperatures, near the critical point, and the sound velocity in two and three-phase mixtures (such as fog). A review of this literature is not intended here. However, a brief discussion of the problem is indicated,

in order to clarify the meaning of several equations used here, and in order to show where the difficulties arise when we try to find the proper similarity parameter (corresponding to the Mach number) for two-phase flow in a hypersonic tunnel.

In an ideal gas which is assumed to be thermally perfect*, non-viscous, and non-heat-conducting, there is of course a unique sound velocity, $\sqrt{\gamma p/\rho}$, which is independent of the frequency and the shape of the disturbances as long as these waves are infinitesimal in strength.

In a real gas such as air at atmospheric temperature and pressure, this isentropic sound speed is still valid to a good approximation provided the frequency is not too high for a given pressure amplitude of the waves, i.e., provided that the temperature and pressure gradients produced by the waves are not too large. Also, when the wave length of the sound waves approaches the order of magnitude of the mean free path, relaxation effects become important. Thus, $\sqrt{\gamma p/\rho}$ approximates the "low frequency" sound velocity in real gases, although the term "low" may be applicable to frequencies up to several hundred thousand cycles per second. Thus, in a real gas, when the temperature is far above the critical, the sound velocity is still practically independent of the frequency over a wide range of "low" frequencies. (However, the sound velocity does, in this case, depend slightly on the pressure as well as on the temperature.) Consequently, in defining the Mach number for air at ordinary temperatures, we do not have to know the "frequency" of the disturbances since deviations from the condition of thermodynamic

---

* i.e., to follow the equation of state $p/\rho = RT$ without necessarily having constant specific heats.

equilibrium manifest themselves only at extremely high frequencies or low densities.

When a gas with small suspended particles is considered, matters become much more difficult. Epstein (Ref. 28) has shown that a pressure wave reflected at a solid wall or particle must in general result in viscosity and conduction as well as reflected pressure waves. It thus appears that even for a suspension of inert solid particles, the effects of viscosity and heat conduction on sound waves cannot be ignored.

In a two-phase fluid, such as a "fog" there enters, in addition, the possible condensation and evaporation during the passage of a sound wave. One would thus expect strong attenuation effects on sound waves. These effects have been studied extensively for water fogs in acoustic interferometers. The important fact here is that the attenuation as well as the sound speed in our two-phase suspension are likely to depend on droplet sizes and numbers, on the vapor density, the physical properties of the substance, and on the frequency of the sound wave. Since a pressure disturbance in a supersonic flow must have some characteristic spectrum of frequencies, it is very unlikely that a single, unique sound velocity should even exist for such disturbances in two-phase flow. Consequently one can hardly expect that a single, unique similarity parameter can, for the two-phase flow, take the place of the Mach number of perfect fluid gas dynamics. In fact, it is shown in Section III that for shock waves alone at least two parameters ($\tilde{M}$ and E) must be given in two-phase flow.

In spite of the above-mentioned difficulties and uncertainties, one sound velocity will be given here for this two phase fluid. It is

again based on a thermodynamically simple limiting case, that of complete equilibrium. Let us assume that either through condensation and evaporation on existing droplets or by formation of new ones, our vapor will always maintain its equilibrium with the condensed phase. Let us also assume, as is usual in the calculation of the sound velocity, that the heat conduction from and to the disturbance wave is negligible; further, that whatever droplets are suspended in the vapor will follow the velocity fluctuations of the vapor without appreciable lag. As usual we assume that in the steadily moving fluid, a stationary (oblique) disturbance exists, and then find what its speed of propagation must be. The disturbance thus must satisfy the following equations, writing u_N and u_T respectively for the normal and tangential velocity components:

$$\rho d u_N + u_N d\rho = 0 \qquad \text{Continuity} \qquad \text{(a)}$$

$$u_N d u_N + \frac{dp}{\rho} = 0 \qquad \text{Momentum} \qquad \text{(b)}$$

$$du_T = 0$$

$$u_N d u_N + C_p dT - L dg = 0 \qquad \text{Energy} \qquad \text{(c)}$$

$$\frac{dp}{p} - \frac{d\rho}{\rho} - \frac{dT}{T} + \frac{dg}{1-g} = 0 \qquad \text{State} \qquad \text{(d)}$$

$$\frac{dp}{p} - \frac{L}{RT^2} dT = 0 \qquad \text{Vapor Pressure} \qquad \text{(e)}$$

These equations are consistent only if the normal velocity u_N has a particular value. That is, the stationary disturbance, if it exists, must propagate at the speed

$$u_N = \overset{\circ}{a} = \left[\frac{(1-g)RT}{1 - \frac{2RT}{L} + \frac{\gamma}{(\gamma-1)} \frac{1}{(1-g)} \left(\frac{RT}{L}\right)^2} \right]^{\frac{1}{2}} \tag{8}$$

Also, the relation between the pressure change and the normal velocity change is now

$$\frac{dp}{p} = - \left[\frac{1}{1 - \frac{2RT}{L} + \frac{\gamma}{(\gamma-1)} \frac{1}{(1-g)} \left(\frac{RT}{L}\right)^2} \right] \frac{du_N}{u_N} \tag{9}$$

instead of the usual equation for a perfect gas:

$$\frac{dp}{p} = -\gamma \frac{du_N}{u_N}$$

The quantity $\overset{\circ}{a}$ must be valid for the limiting case of low frequency pressure fluctuations, and will be called "zero frequency sound" speed.

It is interesting to note that $\overset{\circ}{a}$ differs appreciably from the ordinary sound velocity even for arbitrarily small values of g. This, of course, is due to the fact that along the saturation line, the relation between p, and T differs greatly from the isentropic p - T relation for a perfect gas. For small values of g, one obtains

$$\frac{\overset{\circ}{a}}{\sqrt{\gamma RT}} \approx \frac{1}{\sqrt{\gamma\left(1 - \frac{2RT}{L}\right)}} \tag{10}$$

Thus for typical wind tunnel temperatures, $\overset{\circ}{a}$ is about 10% smaller than the perfect gas sound speed.

It appears that the sound speed should be a very sensitive indicator of the onset of two-phase flow. If $\overset{\circ}{a}$ is valid to sufficiently high frequencies, it should be possible to detect a change in sound speed by direct measurement, e.g., with a crystal.

Other "sound speeds" based on a variety of postulated processes have been derived in Ref. 32.

The Mach wave relation is immediately dependent on the pertinent sound velocity. From the fact that the tangential velocity is conserved, one gets for an infinitesimal oblique wave

$$\frac{du_N}{u_N} = -\frac{d\vartheta}{\sin\alpha\cos\alpha}$$

where α is the angle between the wave and the approaching free stream, and $d\vartheta$ is the flow deflection. The first momentum equation gives

$$\frac{dp}{p} = -\frac{\rho u^2}{p}\sin^2\alpha\,\frac{du_N}{u_N}$$

Combining these and using the definition of $\tilde{M}$, one gets as a general relation for an infinitesimal oblique wave (in this fluid)

$$\frac{dp}{p} = \gamma\tilde{M}^2\tan\alpha\,d\vartheta \tag{11}$$

Now $\tilde{M}$ can be determined by several independent methods to good accuracy (Cf. Section III). Thus, if one can find experimentally values of $\frac{1}{p}\frac{\Delta p}{\Delta\vartheta}$ for weak shock waves, the limiting value of this ratio as $\Delta p \longrightarrow 0$ will define an effective Mach angle α for the flow in question. Unfortunately, this and similar experiments with weak waves are difficult to carry out to sufficient accuracy to make the results convincing.

If we assumed $\overset{o}{a}$ to be the proper sound velocity for "Mach waves", then the theoretical wave relation becomes

$$\frac{dp}{p} = \frac{\gamma\tilde{M}^2}{\sqrt{\tilde{M}^2-1}}\,d\vartheta \tag{12}$$

where $\overset{o}{M} = u/\overset{o}{a}$. It is important to point out that the parameters $\overset{o}{M}$ and $\tilde{M}$

in this equation are independent of one another: $\tilde{M}$ depends only on speed, pressure, and density of the fluid, while $\overset{o}{M}$ depends on the slope of the vapor pressure curve, through the term RT/L (Cf. Eq. 8 above).

It has been considered that the process in a weak pressure wave in the two-phase fluid may be different for compression and expansion waves, i.e., that there might not be a unique Mach wave relation for all infinitesimal waves. This difficulty is to be expected if the two-phase flow in the tunnel does not reach a thermodynamic equilibrium state. However, if the flow is in an equilibrium state, the processes of condensation and evaporation must proceed at equal speed. Thus the assumptions made here regarding the sound velocity are consistent with those of the equilibrium expansion.

4. Results

The results of this section are useful primarily for gaining some insight into the two-phase flow and for order-of-magnitude estimates. For accurate comparison with experimental data, the results of the expansion alone are not sufficient because, of the six variables $p, \rho, T, u, g,$ and A, only p can be measured to a sufficient accuracy. Comparison with experiments requires theoretical calculation of at least one other measurable quantity. This will be discussed in the section on shock waves.

Nevertheless, charts of the saturated expansion results are included for reference. In Figs. II-1, 2, and 3, pressure ratio, free stream temperature, and amount of condensed phase are given as functions of the area ratio A/A^*. Here A^* is the cross-sectional area at the

throat. The curves are based on the (extrapolated) vapor pressures calculated by Wagner.

The ratio of dynamic to stagnation pressure for saturated flow was found to be practically identical with that of isentropic flow. The difference (about 2 or 3 per cent at extreme area ratios) is probably within the accuracy of the calculations. This result is most surprising.

Fig. II-4 shows the parameter $\tilde{M}$ as a function of the pressure ratio, while Fig. II-5 gives the ratio of $\overset{o}{M}$ to $\tilde{M}$.

B. Instantaneous Collapse of the Supersaturated State (Condensation "Shock")

Another simple limiting thermodynamic process is obtained if it is assumed that a supersaturated vapor condenses "instantaneously". While this assumption may not seem at all realistic, the results are useful because they set an upper limit to the degree of irreversibility, and hence the entropy increase, of a condensation process in a nozzle. Physically it is reasonable to expect that the final state after any condensation process in a nozzle must lie between the limits given by equilibrium expansion on one hand and instantaneous collapse on the other. This appears to be borne out by the experiments.

For the water vapor case, calculations of the so-called condensation shock have been carried out by many authors, including Heybey (Ref. 29) and Charyk (Ref. 19). In a somewhat more general way, Samaras (Ref. 30) has treated exothermic and endothermic discontinuities (in a compressible fluid), of which the condensation shock is a special case.

In the present calculations, both the change in amount of vapor

present and the heat released by condensation are considered. In this respect the calculations for air and nitrogen made here differ from those for water vapor in air. For the latter case, the amount of vapor condensed is very small while the latent heat of water is much higher than that of air (roughly by a factor of ten). Therefore, the moisture condensation shock is usually treated simply as a discontinuous heat addition.

The method of computation is straight forward and quite similar to that for shocks with partial evaporation (Cf. Section III). It will only be outlined here. First the fundamental assumptions involved will be given. It is assumed that

(1) No condensation has taken place ahead of the collapse.

(2) The vapor is saturated after the collapse.

(3) The saturation vapor pressure is given by the Clapeyron-Clausius equation with constant latent heat.

(4) The vapor phase is a perfect gas.

(5) After condensation, the volume of the condensed phase, g/ρ_L is neglected compared with the volume of the vapor, $(1 - g)/\rho_v$.

We designate by subscripts $_1$ and $_2$ the states before and after the collapse. The basic equations are

$$\rho_1 u_1 = \rho_2 u_2 \qquad \text{Continuity} \qquad (13)$$

$$\rho_1 u_1^2 + p_1 = \rho_2 u_2^2 + p_2 \qquad \text{Momentum} \qquad (14)$$

$$C_p T_1 + \frac{u_1^2}{2} = C_p T_2 + \frac{u_2^2}{2} - L g_2 \qquad \text{Energy} \qquad (15)$$

$$p_2 = \rho_2 (1 - g_2) R T_2$$
$$p_1 = \rho_1 R T_1 \quad , \quad (g_1 = 0)$$

State (16)

$$\ln \frac{p_2}{p_R} = \frac{L}{R} \left(\frac{1}{T_R} - \frac{1}{T_2} \right)$$

Vapor Pressure (17)

In the last equation, the subscript $_R$ designates an arbitrary reference point on the saturation curve.

Numerous methods for solving these equations have been suggested. None is very convenient because the vapor pressure equation is hard to combine with the others. One can, for instance, eliminate u_2 by the continuity equation, ρ_2 by the equation of state, and be left with momentum and energy expressed in terms of p_2, T_2, and g_2. We can now choose a set of values of p_2 and T_2 consistent with this (or any other) vapor pressure equation. When these values are substituted into the remaining two equations, a simultaneous solution can be obtained. The difficulty lies in the fact that a small error in T_2 or g_2 causes a very large error in p_2.

Another approach is to combine Eqs. 13 to 16 in such a manner as to obtain a relation between p_2 and T_2. This is then cross-plotted on the vapor pressure curve.

Results of a condensation shock calculation are shown in Fig. V-8, for the 1" x 1" nitrogen nozzle.* The results are there given as the locus of end points of instantaneous collapse calculations made for various points along the nozzle. It must be pointed out that no one particle will follow along this locus through the nozzle. In an instantaneous collapse, the vapor state would reach the collapse end point locus at one station. After that, the vapor will expand following

---

* See also Table I, page 95.

a curve which must run parallel to the equilibrium saturated expansion, at a higher pressure.

It will be seen that toward the end of the nozzle, the values of p/p_o' reached in a condensation shock would be 6 to 8 per cent higher than those reached in an equilibrium saturated expansion. The temperatures were slightly higher and the values of g appreciably lower than corresponding values along the saturated expansion.

III. SHOCK WAVES WITH EVAPORATION

In order to predict forces on a model in the tunnel, or even to determine reliably the state of the fluid in the two-phase flow, we have to calculate shock waves with evaporation.

For the case of moisture in air, such shock waves have already been studied by Head (Ref. 8). As mentioned before, for the moisture case the latent heat is much larger and the amount of condensing vapor is much smaller than in the present application, so that the moisture case may be treated simply as discontinuity with heat addition. For that case, of course, general methods have been developed by numerous authors. In a recently published paper (Ref. 37), Ross also treats oblique waves with "Energy Exchange and Change of State". Unfortunately, the paper was received too late to include here a comparison of results.

In the application considered here, a very appreciable fraction of the two-phase fluid (up to 15 or 20%) can be in the condensed state. Thus we have to consider both the change in the mass of vapor phase and the heat release due to the evaporation.

A. Assumptions

As before, the latent heat is taken as constant. Since this shock calculation is to be combined with the equilibrium saturated expansion, the same (constant) value of L/R must be used for both. Thereby much of the error introduced by use of the simplified vapor pressure equation is cancelled out in the reevaporation, and this may in part account for the surprisingly close agreement between theoretical and experimental results.

There are two distinct cases of "evaporation shocks", those with complete and those with partial reevaporation of the condensed phase. They differ both in the number of assumptions necessary and in the computational labor involved.

For complete evaporation shocks, the vapor pressure curve need not be known, only the latent heat. Such shocks can therefore be used as an experimental check on other calculations involving the saturation vapor pressure and various assumptions regarding the process of condensation. It is fortunate that many important measurements in the tunnel involve such strong shocks.

For partial evaporation shocks, one has to make an assumption as to the state of the fluid after the shock. Here this state is assumed to be just saturated, and the simplified vapor pressure equation is used as before.

As throughout this paper, the vapor phase is treated as a perfect gas.

B. Basic Equations

The states ahead of and after the shock are given the subscripts 2 and 3, respectively, to facilitate combination of the shock results with those of Section II. Both oblique and normal shocks are considered. The velocity and Mach number components normal and tangential to the wave are designated by subscripts $_N$ and $_T$ respectively. The basic equations thus are

$$\rho_2 u_{N2} = \rho_3 u_{N3} \qquad \text{Continuity} \qquad (1)$$

$$p_2 + \rho_2 u_{N2}^2 = p_3 + \rho_3 u_{N3}^2 \qquad \text{Momentum} \qquad (2)$$

$$u_{T2} = u_{T3} \qquad \text{Momentum} \qquad (3)$$

$$\frac{u_{N2}^2}{2} + C_p T_2 - L g_2 = \frac{u_{N3}^2}{2} + C_p T_2 - L g_3 \qquad \text{Energy} \qquad (4)$$

The tangential momentum equation has been used to eliminate u_t^2 from the last equation. The equation of state holds for both points (2) and (3):

$$p = \rho (1-g) RT \qquad (5)$$

A wave is called "complete evaporation" wave if $g_3 = 0$ ($g_2 \neq 0$), and "partial evaporation" wave when $g_2 > g_3 > 0$.

The above equations suffice to solve the normal shock with complete evaporation. If, for instance, the state of the fluid ahead of the shock is completely given, the unknowns are u_{N3}, p_3, ρ_3, T_3. $u_{T3} = g_3 = 0$. Equations 1, 2, 4, and 5 determine all the variables.

For normal shocks with partial evaporation, we need an additional assumption and equation to determine the unknown value of g_3:

$$p_3 = p_s (T_3) \qquad \text{Assumption}$$

$$\ln \frac{p_s}{p_r} = \frac{L}{R} \left[\frac{1}{T_r} - \frac{1}{T} \right] \qquad (6)$$

where again p_r T_r is an arbitrary point on the saturation curve.

First the relations for normal shocks will be given. Introducing again the dynamic pressure parameter $\tilde{M}$, where

$$\tilde{M}^2 = \frac{\rho u^2}{\gamma P} = \frac{u^2}{(1-g)\gamma RT}$$

we can reduce the number of variables in the problem as follows:

Continuity, state, and momentum equations can be combined to

$$\frac{P_3}{P_2} = 1 + \gamma \tilde{M}_{N2}^2 \left(1 - \frac{u_{N3}}{u_{N2}}\right) \tag{a}$$

The state and continuity equations combine to

$$\frac{P_3}{P_2}\frac{u_{N2}}{u_{N3}} = \frac{\tilde{M}_{N2}^2}{\tilde{M}_{N3}^2} \tag{b}$$

(a) and (b) combine to

$$\frac{P_3}{P_2} = \frac{1+\gamma \tilde{M}_{N2}^2}{1+\gamma \tilde{M}_{N3}^2} \tag{7}$$

and

$$\frac{u_{N3}}{u_{N2}} = \left(\frac{1+\gamma \tilde{M}_{N2}^2}{1+\gamma \tilde{M}_{N3}^2}\right)\left(\frac{M_{N3}}{M_{N2}}\right)^2 \tag{8}$$

Now the energy equation, after dividing by u_{N2}^2 and combining with Eq. 8 can be brought into the form

$$\frac{\tilde{M}_{N3}^2\left[\tilde{M}_{N3}^2 + \frac{2}{\gamma-1} + E_3\right]}{\left[\gamma \tilde{M}_{N3}^2 + 1\right]^2} = \frac{\tilde{M}_{N2}^2\left[\tilde{M}_{N2}^2 + \frac{2}{\gamma-1} + E_2\right]}{\left[\gamma \tilde{M}_{N2}^2 + 1\right]^2} \tag{9}$$

where

$$E(g,T) = \frac{2g}{1-g}\left(\frac{1}{\gamma-1} - \frac{L}{\gamma RT}\right) - \left(\frac{2}{\gamma-1}\right)\left(\frac{g}{1-g}\right)\left[1 - \frac{L}{C_p T}\right] \tag{10}$$

The relation (9) contains all the basic equations of the problem. It therefore must contain all possible solutions of evaporation or con-

densation shock problems. That is to say, the function

$$\Phi(\tilde{M}_N^2, E) = \frac{\tilde{M}_N^2\left[\tilde{M}_N^2 + \frac{2}{\gamma-1} + E\right]}{\left[\gamma\tilde{M}_N^2 + 1\right]^2}$$

must have the same value on both sides of any discontinuity involving a phase change in a single pure vapor. Φ is thus a fundamental invariant for all such discontinuities. It can be used for the condensation "shocks" of the previous Section as well as for evaporation shocks. It should be noted that Eq. 9 contains only one physical property of the vapor, namely γ. Considering E as a parameter, the same chart of Eq. 9 holds then for example for nitrogen, air, and any other diatomic gas, within the perfect gas assumption.

Not all solutions of Eq. 9 are physically possible discontinuities. In case any doubt exists as to the correct branch, the entropy change across the discontinuity should be checked.

C. Solution of Normal Shocks with Complete Evaporation of the Condensed Phase

In the present calculations, solutions of Eq. 9 were obtained graphically. Fig. III-1 shows a typical chart of the equation for $\gamma = 1.40$, with E as parameter. A similar but larger chart was used for most of the computations. For normal shocks at high Mach numbers, complete evaporation will always occur, making $E_3 = 0$. Therefore, only one curve is given on the subsonic side of Fig. III-1.

Typical values of E are given in Fig. III-2. Values obtainable in the 5" x 5" hypersonic wind tunnel lie in the interior of the dashed line in this figure; that is, the absolute value of E will always be

between 0 and 8, (usually less than 5).

Values of M_{N3}, the Mach number after the shock, are given in Fig. III-3.

If the fluid properties ahead of the shock are given, the solution is straight forward. One determines E_2 and $\tilde{M}^2_{N2}$, obtains M^2_{N3} from the chart. Equations 7 and 8 give the static pressure and velocity ratios across the shock, which is sufficient for finding any other desired quantities of the flow.

The static pressure ratios produced by plane shock waves with complete evaporation of the condensed phase are given in Figs. III-4a and b as function of the normal Mach number ahead of the shock. The factor $r(E, \tilde{M}_{N2})$ by which the static pressure ratio has to be multiplied to allow for the evaporation is plotted in Fig. III-4a. The dashed lines on this chart give the lower limit of the normal Mach number for which the shock is strong enough to produce complete evaporation, starting at various temperatures, T_2. It will be seen from Fig. III-4a that, for values of E encountered in the tunnel, the evaporation will alter the static pressure ratio of a shock by less than 5% for given $\tilde{M}$. It will also be seen on Fig. 4a that very strong shock waves (i.e., those with large normal Mach number, $\tilde{M}_{N2}$) are affected much less by the evaporation than weaker ones, as far as the static pressure ratio is concerned. Fig. III-4b (giving pressure ratios for shocks without phase change) is included here for convenience.

Since the above equations apply only to waves with complete evaporation, the charts of Figs. III-3 and III-4a cannot be used for arbitrarily low normal Mach numbers $\tilde{M}_{N2}$. In Fig. III-5, the lowest

pressure ratios (and hence values of $\tilde{M}_{N2}$) for which complete evaporation would take place are given for several temperatures. The method of calculating these pressure ratios and the assumptions which enter in are discussed below. $(p_3/p_2)_{min}$, the lowest pressure ratio for complete evaporation, depends mostly on the amount of condensed phase present in the flow and, to a lesser extent, on the temperature level. Also plotted in Fig. III-5 are the pressure ratios produced by complete evaporation shocks for various values of the normal Mach number component ahead of the shock, $\tilde{M}_{N2}$. (These latter curves give the same information as the curves of Fig. III-4.)

D. Remarks on Shock Waves with Partial Evaporation

For waves which are not strong enough to cause complete evaporation of the condensed phase, the solution is algebraically more involved. We have then one additional unknown, the amount of condensed phase left after the wave, g_3 (or E_3). Usually it should be reasonable to assume that the flow (a short distance) after the wave will be just saturated. This introduces some vapor pressure equation, e.g., Eq. 6, which is difficult to combine with the other equations. Also, the results contain the inherent uncertainties of this equation and assumption, and are therefore much less reliable than the corresponding results for complete evaporation.

A possible method of solution will be briefly outlined. Let it be assumed that the state of the fluid ahead of the shock is given and, in addition, that the vapor is just saturated there. This last assumption is reasonable here, though it is by no means necessary. The

vapor pressure equation then becomes

$$\ln \frac{P_3}{P_2} = \frac{L}{RT_2}\left(1 - \frac{T_2}{T_3}\right) \tag{6a}$$

For p_3/p_2, one can substitute Eq. 7 to get

$$\ln\left[\frac{\gamma \tilde{M}_{N2}^2 + 1}{\gamma \tilde{M}_{N3}^2 + 1}\right] = \frac{L}{RT_2}\left[1 - \frac{T_2}{T_3}\right] \tag{d}$$

Also, Eqs. 1, 7, and 8 can be substituted into the equation of state to give

$$\frac{T_2}{T_3} = \frac{(1-g_3)}{(1-g_2)}\left[\frac{\gamma \tilde{M}_{N3}^2 + 1}{\gamma \tilde{M}_{N2}^2 + 1}\right]\frac{\tilde{M}_{N2}^2}{\tilde{M}_{N3}^2} \tag{e}$$

Lastly, Eq. 9 is still valid with $E_3 \neq 0$ here. We thus have the three equations d, e, and 9 relating the unknowns T_3 g_3 and $\tilde{M}_{N3}$. By combining Eqs. d and e, one can find numerically T_3 and g_3 as functions of $\tilde{M}_{N3}$, hence can plot E_3 vs. $\tilde{M}_{N3}$. The second relation between E_3 and $\tilde{M}_{N3}$ is obtained from Eq. 9, for which a chart is already available.

There are obvious applications for weak oblique waves, namely the shocks produced by slender models in the tunnel. However, the primary aim of the present investigation was to understand the condensation process in a nozzle. Because of the labor involved, no attempt was made therefore to present numerical results* or to find a more convenient calculation procedure for these shocks. However, Grey obtained an approximate computing method which is given in Ref. 17. For very weak waves, one can of course use the Mach wave relation, Eq. 12

In order to plan certain wedge tests, it was important to find

---

* Except those given in Fig. III-8.

the limits of applicability of the complete evaporation shock charts. If we set $g_3 = 0$, we can combine the fundamental equations 1-5 with Eq. 6a to obtain

$$g_2 = \frac{(\Pi_{32}-1) + \frac{(\Pi_{32}-1)}{(RT_2/L)\ln \Pi_{32} - 1} + \frac{2\gamma}{\gamma-1}\frac{(RT_2/L)\ln \Pi_{32}}{(RT_2/L)\ln \Pi_{32} - 1}}{(\Pi_{32}-1) + 2L/RT_2}$$

where Π_{32} has been written for p_3/p_2. This is easily solved numerically and gives the pressure ratio just sufficient to evaporate g_2, with T_2 as parameter. This result, when cross-plotted on the original shock charts, furnishes the conditions under which the flow after the wave will be just saturated.

E. Oblique Shock Calculations for Two-Phase Flow

Once the normal shock case has been solved, oblique shock solutions are obtained in the usual manner by superposition of a tangential velocity component. From geometry and the fact that the tangential velocity component is unchanged across the shock, one obtains immediately

$$\frac{u_{N3}}{u_{N2}} = \frac{\tan(\sigma - \vartheta)}{\tan \sigma} \tag{11}$$

where σ and ϑ are respectively the wave angle and the flow deflection angle with respect to the approaching (undisturbed) flow.

The discussion will be confined to waves with complete evaporation of the condensed phase. Then Eq. 11 together with Eq. 9 and the preceding equations are sufficient to solve any given case. If we assume a flow deflection angle ϑ and a value of E_2, we obtain by Eq. 11 for each pressure ratio p_3/p_2 (or velocity ratio u_3/u_2) a value of the

wave angle, and hence a value of the Mach number $\tilde{M}_2$ ($= \tilde{M}_{N2}/\sin\sigma$). By this method, charts for complete evaporation shocks were constructed. Since these charts were to be used primarily in conjunction with the wedge tests in the tunnel, the computations were carried out only for a very limited number of wedge angles (20, 30, and 40 degrees).

Typical results of these calculations are shown in Figs. III-6 to III-8. Additional results and cross-plots have been presented in Ref. 39. The following general trends are of interest here, at values of $\tilde{M}$ above 5 or 6:

(1) The static pressure ratio across shocks is rather insensitive to various amounts of condensed phase (Cf. Fig. III-6), but is very sensitive to changes in the parameter $\tilde{M}_2$.

(2) The wave angle behaves in precisely the opposite fashion: it is sensitive to changes in the evaporation parameter but very insensitive to changes in $\tilde{M}_2$. In fact, for any wedge angle, a value of E can be found (near -4) for which the wave angle becomes practically independent of $\tilde{M}_2$. (Cf. Figs. III-7a and III-7b.)

Another limiting case of oblique wave, the Mach wave has already been discussed in Section II. We now have all the information necessary for plotting a pressure ratio vs. deflection angle shock polar. It is interesting to note that the curves for complete evaporation shocks run parallel to the ordinary shock polar, i.e., for strong waves $dp/pd\nu$ is not appreciably affected by the evaporation. On the other hand, for infinitesimal waves $dp/pd\nu$ in two-phase flow differs by about 10% from

the value in a perfect gas.

A typical shock polar diagram for two-phase flow is given in Fig. III-8. The partial evaporation line starts at the same slope as the Mach wave relation. It is not parallel to the ordinary shock polar (E = 0). At the pressure ratios required for complete evaporation, the shock lines depart from the partial evaporation line and continue parallel to the ordinary polar. (The maximum values of ν for E $\neq$ 0 have only been estimated and should not be read off this chart.)

It is clear from this chart that the relation of wedge pressure to wedge angle is not sensitive to changes in E and can therefore not be used to determine the state of the fluid in the tunnel. For this, the more sensitive wave angle must be used, preferably in conjunction with the measured pressures.

F. Applications of the Shock Theory

1. The Pitot Tube

Perhaps the most useful result of the shock calculations is the theoretical determination of the pitot pressure. The ratio of the static to the pitot pressure is given by

$$\frac{p_2}{p_0'} = \frac{p_2}{p_3}\,\frac{p_3}{p_0'} = \left[1 - \frac{\gamma-1}{2} M_3^2\right]^{\frac{-\gamma}{\gamma-1}} \left[\frac{1+\gamma M_3^2}{1+\gamma \tilde{M}_2^2}\right] \qquad (12)$$

where M_3 has to be determined from Eq. 9 or Fig. III-1.

Values of p/p_0' have been computed by Eq. 12 for air using values of E from 0 to -10. It was found that these values were within a few per cent of the values given in perfect gas tables if $\tilde{M}_2$ is taken equal

to ordinary Mach number. Conversely, if one measured p/p_o' in a two-phase flow and computed from this the ordinary Rayleigh Mach number as for a perfect gas, this Mach number would be at most about 1% higher than the theoretical value of $\tilde{M}_2$ for the same shock. This will be seen in Fig. III-9 where the ratio

$$r = \frac{\tilde{M}(E)}{M(\text{Rayleigh Equation})}$$

is plotted against p/p_o'. The values of E obtained in a tunnel must lie to the right of the appropriate dashed pressure line on this chart.

It will be seen that, unless extreme accuracy is required, $\tilde{M}$ in two-phase flow can be considered equal to the ordinary Mach number based on p/p_o'. If high accuracy is desired, one can estimate E (from Section II) and use the correction factor given in Fig. III-9.

We can go one step further and substitute for p_2 the theoretical static pressures from the saturated expansion, for a given nozzle area ratio. When this is done, we get a theoretical value of p_o'/p_o based on saturated expansion. The values so obtained for a given area ratio were equal to p_o'/p_o for perfect gas flow, within the accuracy of the calculations, which was about $\pm$ 2%. (This poor accuracy was due to the graphical solution.)

The fact that p_o'/p_o is essentially unchanged by the condensation (for a given area ratio) checks with experimental evidence from several tunnels in which heated and cold runs have been made.* However, experimentally this fact cannot be established accurately because the effective area ratio may change slightly with heating (both due to change in throat size and changes in the boundary layer).

---

* Cf. Ref. 12, page 13.

2. The Value of the Shock Theory

The value of the shock theory lies in the fact that we can now, for any theoretically assumed two-phase flow, calculate two quantities, p and p_o', which can also be measured to good accuracy in the tunnel. This enables us to compare any proposed condensation theory with experimental data. In this comparison, no assumptions have to be made regarding area ratio, uniform flow across the nozzle, or boundary layer thickness, since both measurements can be made at the same point in the free stream.

In the opinion of the writer, it is very important that in any comparison with a proposed theory "pure" experimental points should be used, rather than "pseudo-experimental" points which have been run through a formula which may not apply. It seems best to apply any dubious conversion or correction (which may be necessary for the correlation) to the theory and leave the experimental points unadulterated. In this respect, the many fictitious Mach numbers which have been used are not desirable.

Charts have been prepared with theoretical values of p/p_o' plotted against p_o'/p_o. In this plane any curves based on condensing flow (e.g., equilibrium saturated) have a slope differing appreciably from the perfect gas isentrope. Thus, this method of presenting data is quite sensitive in detecting condensation. An incidental advantage of this method is that on the p/p_o' vs. p_o'/p_o chart, the "dry" isentropes for all stagnation pressures and temperatures coincide.

Extensive comparisons of experimental data with theoretical results have been made on the basis of the above-mentioned chart, both

for air and for nitrogen (Refs. 15, 16, and 17). As an example, the results of Grey and Nagamatsu from the five-inch tunnel are shown in Fig. III-10. It will be seen from the 5 ATM run that the flow followed the isentrope past the saturation point to some highly supersaturated state, then collapsed gradually and continued to expand, roughly along the equilibrium saturation curve. The departure from the saturated expansion toward the end of the nozzle may be due to the fact that a constant L/R has been used for the theoretical curves. Fig. III-11 shows a comparison with typical experimental collapse curves from the 1" x 1" tunnel, for nitrogen (Arthur and Nagamatsu, Ref. 16). In this case, the nozzle is not long enough to establish the nature of the flow after the collapse. In this tunnel the attention was focussed on the collapse region.*

By use of the shock calculations, all the results of the saturated expansion can be plotted against pitot pressure ratio p_o'/p_o or against p/p_o', for comparison with experiments. An interesting result is that the theoretical Mach wave pressure "coefficient" $dp/pd\nu$ when presented against p/p_o' becomes practically independent of the stagnation pressure (for saturated expansion). Only the Mach number where the theory predicts deviation from the isentrope depends, of course, on the pressure level. It will be seen in Fig. III-12 that the calculated values of $\frac{1}{\rho}\frac{d\rho}{d\nu}$ (based on $\overset{o}{M}$) are about 10% lower than the isentropic values, at a given p/p_o'. Therefore, a significant change in the pressure coefficient on slender bodies is to be expected at the onset of condensation in a tunnel.

The above results have not yet been checked experimentally in the neighborhood of the saturation point. However Grey and Nagamatsu (Ref.

---

* See also Fig. V-8.

17) obtained values of $dp/pd\vartheta$ in fair to good agreement with theoretical values, based on saturated expansion. It must be pointed out that reliable experimental values of this important quantity are hard to obtain, since there is a tendency toward flow separation from wedges even at low positive angles of attack.** Also, a good uniform flow without axial pressure gradients is essential for this experiment, and this was not available in the tunnel at the time.*

3. Experimental Determination of $\tilde{M}$, Free Stream Temperature, and Other Flow Parameters

On the basis of the shock calculations, the writer and others suggested several experiments in order to determine the important parameters of the condensing flow experimentally (Cf. Refs. 12 and 39). Most of these have since been carried out.

The first, and most successful, was the determination of the dynamic pressure parameter $\tilde{M}_2$ by two independent methods. One, the pitot and static pressure measurements, was mentioned above. The other fairly accurate method is based on wedge measurements. From Eqs. a (preceding Eq. 7) and 11, the following relation for oblique shock waves is easily derived:

$$\tilde{M}_2^2 = \frac{2\left[\frac{p_3}{p_2} - 1\right]}{\gamma \sin 2\sigma \left[\tan \sigma - \tan(\sigma - \vartheta)\right]} \tag{13}$$

---

* Very recent results of Hansen and Nothwang (Ref. 31) are of great interest in this connection. These have not yet been correlated with results presented here.

** It is therefore probably better to carry out the comparison of theory and experiment for waves of finite strength.

This equation is true with or without condensation since in the derivation the energy equation was not used. By substituting typical values one finds that $\tilde{M}_2$ determined by Eq. 13 is not at all sensitive to errors in the wave angle σ or the wedge angle ν. For instance, a $\frac{1}{2}$ degree error in either σ or ν would change $\tilde{M}_2$ by only about 1%. Grey compared values of $\tilde{M}_2$ from wedge tests with those from p/p_o' and found very good agreement.

It should be emphasized that accurate knowledge of the dynamic pressure parameter is very important if any testing is to be done in the two-phase fluid.

Knowing $\tilde{M}_2$ accurately, one can, in principle, calculate the free stream temperature and g from measurements on oblique shock waves. This has not yet been done successfully because the source flow in the nozzle made the evaluation of wedge results too difficult. However, other methods for the determination of T_2 and g_2 have been developed, notably one by Wegener and Reed (Ref. 12). This method was also used in Refs. 15, 16, and 17.

Finally, the determination of the pertinent "sound" velocity by direct measurement of wave slopes should be mentioned. Coles (Ref. 32) developed a method whereby both the slope and the strength of weak shock waves are obtained accurately with a pitot rake. The wave slope is then corrected theoretically for the wave strength, so that a good estimate of the Mach angle is obtained. The sound velocities so far obtained by this method lie about half way between the theoretical a_o and $\sqrt{\gamma p/\rho}$

IV. THE RATE OF GROWTH OF A DROPLET (OR CRYSTAL) IN A HIGHLY RAREFIED, SUPERSATURATED VAPOR

A. Introductory Remarks

In the present application, it is very difficult to predict whether we are dealing with droplets or crystals. The same difficulty exists in meterological studies of clouds. In several recent papers on this subject, the consensus appears to be that very small water droplets can exist down to about — 40°C. In addition, it is frequently stated in the literature that very small condensed particles quite likely first form as liquid droplets, and freeze into crystals after having grown. It is quite possible however that water may differ in this respect from other substances since water ice melts under external pressure while other substances solidify. Wagner (Ref. 1) states that for air it appears likely that liquid droplets would exist below the triple points of oxygen and nitrogen down to 40° Kelvin. Below that temperature, he believed pure oxygen crystals constituted the most probable state.

In the present report, the question of droplets vs. crystals is left completely open, since the writer is unable to contribute any new arguments on this point. However, for brevity throughout this paper, the word "droplet" is used, with the understanding that this is to designate a small particle of either liquid or solid phase.

The following interpretation of the meaning of these growth calculations is important if we want to avoid serious contradictions. While for very large particles the growth formula holds for each individual particle, for the sizes considered here the calculated growth

can only be considered true as an average for a large number of particles. The distinction is clear when one considers this from the viewpoint of molecular collisions: if a drop is so large that millions of collisions occur on its surface during the characteristic time interval of the problem, the averaging process will hold for this individual drop. On the other hand, when we talk about droplets or nuclei of the order of 10^{-7} cm radius, i.e., less than ten times the "size" of a molecule, there is clearly a possibility of contradiction, and the growth formula should be used with care. Let us for instance assume that we had a group of droplets of equal size and just slightly smaller than the critical radius (at a particular supersaturation). The growth formula would tell us that on the average all must reevaporate. Yet it is known from the germ formation theory that, due to fluctuations there is a finite probability for some of these droplets to grow above critical size and then keep on growing. Now consider a group of perfectly wetted inert foreign condensation nuclei, a little smaller than the critical size. Again, according to the growth formula these cannot start the condensation process. Yet, in analogy to the germ formation theory, there must be a finite probability for some of these nuclei to grow into droplets above critical size. However, the remaining nuclei (assumed solid) will not disappear. Thus eventually, if the supersaturation persists, a large fraction of all the nuclei will form droplets even though the nuclei were presumably too small to do so.

The qualitative discussion above will indicate that the simple joining together of the germ formation theory and the growth formula is not adequate in dealing with problems where very small foreign nuclei may be present. Also the spontaneous germ formation in a mixture of

condensible vapors has apparently not yet been investigated in detail from the viewpoint of inter-molecular forces in the condensed phase. The effect of foreign substances on the collapse of the supersaturated state will not be fully understood until these points can be clarified.

Fortunately it appears that for small nozzles, fair predictions of the collapse phenomenon can be made without complete understanding of the process. This is due to the fact that the supersaturation increases very rapidly along the nozzle. Thus a misjudgement of the supersaturation required to start the collapse causes only a comparatively small error in the predicted space-wise location of the collapse.

Summarizing, the droplet growth calculations of this and the next chapter should be considered valid as an average over a large number of droplets which are appreciably larger than the critical size. In the neighborhood of the critical size, the growth formula must be regarded with utmost suspicion. In addition it must be pointed out again that for the small sizes encountered here, the critical size is not reliably known, and no attempt has been made here to determine it as accurately as possible. Nevertheless, it appears from the work of Reed (Ref. 25) that the Gibbs-Thompson equation with constant surface tension indicates the correct trend even down to very small clusters of molecules.

Droplet growth calculations similar to those of the present chapter have already been made by Oswatitsch for water vapor, also by Lees.* The purpose of the present chapter is to re-examine the growth formula and, where necessary, to include the non-steady terms in the calculations.

---

* Verbal communication.

B. Simplifying Assumptions

The assumptions made in this chapter correspond to those usual for free molecule flow. For the application considered here, the mean free path in the nozzle will be considerably larger than the droplets. (Typical values of the mean free path are shown in Fig. IV-1.) We are therefore in the so-called temperature jump regime. This means that the molecules striking the droplet from the vapor are not appreciably influenced by the molecules which reevaporate from the droplets, since few collisions will take place in the immediate vicinity of the drop. We thus have the following simplified model: the droplet is assumed surrounded by a vapor of constant properties throughout space. The droplet may have a temperature different from that of the vapor. The molecules which are reevaporated have an energy level corresponding to the temperature of the drop but mix with the rest of the vapor only far away from the droplet.

The accommodation coefficient on the surface of the droplets is taken as unity. For pure nitrogen or for air, this may be quite close to the true value.

The velocity distribution throughout the vapor is taken as Maxwellian, except that for the energy transfer across a surface a slight modification is assumed which makes the results agree with the macroscopic condensation theory (Cf. next paragraph).

Here, as throughout this paper, the droplets are assumed to travel through the nozzle at the mean speed of the vapor. This assumption should be realistic everywhere except in the vicinity of shock waves. Order-of-magnitude estimates were made on the basis of several sphere

drag formulas (Cf. Ref. 34, p. 309) of the velocity gradients necessary to make the droplet speed differ from the mean vapor speed by 1%. It was found that for droplets of 10^{-5} cm radius and below, very large gradients would be required for such a deviation.

As in the next Section, foreign nuclei are treated exactly like droplets of the same size. They are assumed spherical, perfectly wetted, but chemically inert, i.e., to have no influence on the vapor pressure or surface tension of the condensing substance. The same assumptions regarding the nuclei have been made by Epstein (Ref. 3).

The vapor pressure of a small droplet (or crystal) is assumed to be given by the Gibbs-Thompson equation

$$\ln \frac{p}{p_s} = \frac{2\sigma}{r' \rho_L R T} \tag{1}$$

In this equation, r', the droplet radius which applies to the surface energy, is taken equal to the droplet radius r based on mass and density. σ is taken as the ordinary macroscopic surface tension and is approximated by the Eötvos formula (Ref. 35, p. 221):

$$\sigma = \frac{K_\varepsilon (T_c - T)}{(M/\rho_L)^{\frac{2}{3}}} = \varkappa (T_c - T) \tag{2}$$

K_ε is by some authors taken as an absolute constant of 2.22, while others choose values of K_ε which best fit available experimental data. The latter approach is used here. Note that $\varkappa$ is not a constant if K_ε is taken as constant. However, $\varkappa/\rho_L$ will be practically constant over wide ranges of temperature.

From Eqs. 1 and 2 above, we obtain the critical droplet radius corresponding to a given saturation ratio as

$$r^+ = \frac{2K}{R\rho_L}\left(\frac{T_c - T}{T}\right)\frac{1}{\ln(P/P_s)} \qquad (3)$$

Values of the surface tension and of K_ε are given in Appendix I.

In the present chapter also, the vapor is treated as a perfect gas.

The surface energy per unit area is taken as a constant, independent of temperature and droplet size.

C. Energy Balance of a Growing Droplet

In order to calculate the mean kinetic energy carried by the condensing molecules, we look first at the macroscopic condensation process. Consider a large vessel with vapor and liquid (or solid) phase at the bottom. The pressure is held constant by a movable piston which adjusts the volume as more vapor is condensed. By definition the heat released in this constant pressure process per unit mass is

$$L(T) = h_V - h_L$$

$$= e_V - e_L + \frac{P}{\rho_V} - \frac{P}{\rho_L}$$

where h and e are the enthalpy and internal energy respectively. p/ρ_L is usually negligible compared with the other terms, since $\rho_L \gg \rho_V$

Now in the Maxwellian distribution, the mass of the vapor molecules striking a unit area per second is

$$\Gamma_V = \frac{\rho_V}{\sqrt{2\pi R T_V}} \qquad gm/sec \qquad (4)$$

The kinetic energy carried by these molecules striking the surface would

be*

$$\Gamma_v \left(C_v + \tfrac{1}{2}R\right) T_v \qquad \text{ergs/cm}^2\text{sec} \tag{a}$$

However, if there is a steady rate of condensation, there is a very slow mass velocity of the whole vapor toward the liquid surface. This raises the mean energy of all the incoming molecules by an infinitesimal amount. When this is added up over all the collisions which take place at the vapor surface, it can be shown** that the resultant effect is the same as if all the net amount of vapor which remained condensed had carried kinetic energy at the rate of $(C_v + R)T$ per unit mass, or

$$\left(\Gamma_v - \Gamma_L\right)\left(C_v + \tfrac{1}{2}R + \tfrac{1}{2}R\right)T \qquad \text{erg/cm}^2\text{ sec.}$$

where Γ_L is the amount which reevaporates per second. The missing $\frac{1}{2}R$ of the macroscopic latent heat can thus be accounted for by the mass motion of the vapor toward the liquid surface during condensation.

It is difficult to decide what the correct energy release should be for the free molecule condensation at hand. In a Maxwellian distribution, the mean incoming energy would again be given by (a) above, but if there is a net flow of vapor toward the drop it must be slightly larger. Fortunately the assumption made here is not too serious since this uncertainty is no larger than uncertainties in either the latent heat or the accommodation coefficient. It turns out that the equations simplify somewhat (and are in agreement with the macroscopic case) if

---

* See for instance, Kennard (Ref. 34), p. 64.

** Dr. F. Gilmore assisted the writer in clarifying this point.

the incoming energy per unit area and time is taken as

$$\Gamma_V (C_v + R) T_V = \Gamma_V C_p T_V \qquad (b)$$

As is usual in condensation theory, the rate of evaporation is calculated from a hypothetical vapor which would be in equilibrium with the condensed phase. Thus, if the drop has a temperature T_D and vapor pressure p_D, the rate of reevaporation would be given by Γ_D , and the kinetic energy of the emitted molecules would be

$$\Gamma_D C_p T_D \qquad \text{ergs/cm}^2 \text{ sec.}$$

For very small droplets, we must consider both the bulk internal energy of the liquid and the surface energy. Frenkel (Ref. 36) states that the total surface energy per unit area, w, may be taken as a constant independent of temperature and size of the droplet. Thus

$$w \doteq \mathcal{K} T_c$$

The energy stored in the drop is then

$$\frac{4}{3}\pi r^3 \rho_L e_L + 4\pi r^2 w.$$

Thus the energy balance for the droplet becomes

$$4\pi r^2 C_p \left[\Gamma_V T_V - \Gamma_D T_D\right] = \frac{d}{dt}\left[\frac{4}{3}\pi r^3 \rho_L e_L + 4\pi r^2 w\right] \qquad (5)$$

where the bulk internal energy of the condensed phase, e_L, is given by

$$e_L(T_D) \doteq h_L(T_D) = C_p T_D - L(T_D) \qquad (6)$$

The right-hand side of Eq. 5, the rate of change of energy in the drop, consists of two terms, one due to rate of change of size and the other due to rate of change of temperature:

$$\left[4\pi r^2 \rho_L e_L + 8\pi r w\right]\frac{dr}{dt} + \frac{4}{3}\pi r^3 \frac{d}{dT_D}(\rho_L e_L)\frac{dT_D}{dt} \quad * \qquad (c)$$

The rate of change of droplet radius is given by the net rate of condensation on the surface:

$$\frac{dr}{dt} = \frac{\Gamma_V - \Gamma_D}{\rho_L} \qquad (7)$$

An interesting side remark may be made about the quantity $\rho_L e_L$ which is the internal energy per unit volume. It was found that both for air and for nitrogen, this quantity is very close to a linear function of the temperature. Thus

$$\frac{d}{dT_D}(\rho_L e_L) = \lambda \qquad (8)$$

where λ is a constant for the present application, to good accuracy.

After substituting Eqs. 7 and 8 and rearranging, the energy balance may be put into the form

$$C_p \Gamma_V \left[T_V - T_D\right] + \left[L - \frac{2w}{r\rho_L}\right]\left[\Gamma_V - \Gamma_D\right] = \frac{r}{3}\lambda \frac{dT_D}{dt} \qquad (9)$$

where by the Gibbs Thompson equation

$$\Gamma_D = \frac{p_s(T_D)}{\sqrt{2\pi R T_D}} \exp\left(\frac{2\sigma}{r\rho_L R T_D}\right) \qquad (10)$$

For a complete non-steady solution, Eq. 9 would have to be integrated step-by-step simultaneously with Eq. 7. Fortunately it is found that a good approximation to the non-steady solution may be found from the quasi-steady solution.

---

* Note that the product $\rho_L e_L$ has been assumed independent of the pressure and the droplet size.

It will be seen that the terms of Eq. 9 are of three different orders of magnitude in r: the main term has been written independent of r. The term $2w/r\rho_L$ is the "correction to the latent heat" due to the surface energy. This term is usually neglected. However, for $r = 10^{-7}$ cm, it amounts to about 20% of the latent heat (for nitrogen). This term has the tendency to increase the growth rates of the smallest drops, thereby bringing them closer to the growth rates of the 10^{-6} and 10^{-5} cm drops. The effect of the correction term on T_D is very small.

The non-steady term $\frac{r}{3}\lambda\frac{dT_D}{dt}$ is also usually neglected. It clearly becomes more important for large droplets.

D. The Quasi-Steady Theory

Let us assume for the moment that the droplet radius is held fixed. Then for each temperature and pressure of the vapor, there exists one droplet temperature for which the left side of Eq. 9 vanishes. This will be called the "quasi-steady equilibrium temperature", T_E. (Quasi-steady here means that the droplet temperature and growth ratedepends only on local conditions at that point* and on the drop size.) Thus, by Eq. 9, if T_D becomes equal to $T_E(T_v\ p_v\ r)$ (which is constant by hypothesis)

$$\frac{dT_D}{dt} = 0$$

This equilibrium state is found to be stable: we obtain from Eq. 9:

$$\frac{dT_D}{dt} > 0 \text{ when } T_D < T_E$$

$$\frac{dT_D}{dt} < 0 \text{ when } T_D > T_E$$

---

* i.e., on p_v and T_v, but not on their derivatives.

Note that T_E depends on r primarily through the vapor pressure correction in Γ_D (Cf. Eq. 10).

The question is now: how fast does a droplet approach this equilibrium state, if the vapor properties are held constant.* To calculate this, we set the initial temperature of the droplet (or nucleus) equal to the vapor temperature, and obtain dT_D/dt from Eq. 9. It is reasonable to assume for this estimate that dT_D/dt will decrease linearly to zero as T_D approaches T_E. Thus setting

$$\frac{T_D - T_E}{T_V - T_E} = \vartheta, \quad \text{and} \quad \frac{dT_D}{dt} = (T_V - T_E)\frac{d\vartheta}{dt} \tag{d}$$

we get by the above assumption

$$\frac{dT_D}{dt} = \vartheta f(r) \tag{e}$$

f(r) is the initial adjustment rate, found from Eq. 9 when $T_D = T_V$. We thus have from (d) and (e)

$$(T_V - T_E)\frac{d\vartheta}{dt} = f(r)\vartheta \tag{g}$$

with the initial condition: $\vartheta = 1$ when $t = 0$. We hold f(r) constant during the integration. It can be shown that r changes very little during the time of adjustment, less than 10% for a typical case. Then (g) integrates to

$$t = -\frac{T_E - T_V}{f(r)} \ln \vartheta \tag{h}$$

We will designate as "adjustment time" the time required for the droplet

---

* The condition of constant vapor properties may be called the "cloud chamber" case.

to reduce its perturbation from equilibrium to 1/10 of the original value, that is $t_{10\%}$ corresponds to the time required to reach $\vartheta = .1$. For a typical case with nitrogen at 38°K (p_o = 8 atm, T_o = 290°K), we obtain the following values for the adjustment time:

r cm	10^{-7}	3.0×10^{-7}	10^{-6}	3×10^{-6}	10^{-5}
$t_{10\%}$ secs.	3.1×10^{-8}	1.2×10^{-7}	4.2×10^{-7}	1.4×10^{-6}	4.3×10^{-6}

Roughly then, the adjustment time for this case is $\underline{.4 \times r}$ seconds (r in cm).

This must be compared with the transit time of the droplet through the nozzle, which is of the order $\underline{2 \times 10^{-5} \text{ sec/cm}}$. Thus, even a droplet as large as 10^{-4} cm radius would travel only 2 millimeter before being practically adjusted to the equilibrium temperature.

The general approach for justifying the quasi-steady growth formula now goes as follows: we solve the energy balance with the term dT_D/dt held zero, thus finding a value of T_E and a quasi-steady growth rate. This would be exact if both r and the vapor properties remained constant. Now by hypothesis $T_D \approx T_E$. We then calculate dT_E/dt and see whether or not this term would make an appreciable difference in the energy balance, Eq. 9.

To shorten the writing, we now consider a flow through a nozzle, so that p_v and T_v are functions of a single variable x. Then

$$T_E = T_E(x,r)$$

$$\frac{dT_D}{dt} \approx \frac{dT_E}{dt} = \left.\frac{\partial T_E}{\partial r}\right|_x \frac{dr}{dt} + \left.\frac{\partial T_E}{\partial x}\right|_r \frac{dx}{dt} \tag{11}$$

The first term on the right-hand side of Eq. 11 enters into the cloud chamber case also, while the last term is of course zero there. It is found that the term containing $\partial T_E / \partial r$ is very much smaller than the dominating terms of the energy balance. This term may therefore safely be neglected.

It appears then that for the "cloud chamber" case the droplet (or nucleus) will adjust itself extremely rapidly to the equilibrium temperature T_E and will remain there. One exception to this must be mentioned: if either in a nozzle or a cloud chamber the foreign nuclei were initially too warm, the adjustment times calculated above would not be valid, since the process by which the adjustment occurred was that of condensation or evaporation. For a particle which has nothing to evaporate, the ordinary free molecule heat transfer equation must be used. Then the adjustment will be much slower. The case just mentioned would apply to very large nuclei in a nozzle with an extreme temperature gradient. However, we are not concerned with such nuclei in the present case since the total mass of the impurities is assumed small.

It has now been shown that for the sizes of practical importance, both droplets and nuclei will quickly reach the quasi-steady equilibrium temperature. It is also evident from the above adjustment times that the droplets, unless they are rather large, will be able to follow very rapidly any changes in T_E along the nozzle. To justify the quasi-steady theory, it remains to be determined by how much the growth rates are affected when a certain rate of change of temperature is imposed upon the droplets. This non-steady effect on the growth rate is evaluated in the next paragraph. First we need the steady solution.

For the nozzle case, the energy balance now reads

$$C_p \Gamma_V \left[T_V - T_D\right] + \left[L - \frac{2w}{r\rho_L}\right]\left[\Gamma_V - \Gamma_D\right] = \frac{r}{3}\lambda \frac{\partial T_D}{\partial x}\bigg|_r \frac{dx}{dt} \qquad (12)$$

If the droplet passes through a region of constant vapor properties, $\partial T_D/\partial x$ vanishes and T_D again becomes T_E. To solve Eq. 12 for the quasi-steady case, it is re-written in the form

$$\Gamma_E = \Gamma_V \left[1 - \frac{C_p}{L}\frac{(T_E - T_V)}{\left(1 - \frac{2w}{r\rho_L L}\right)}\right] \qquad (13)$$

The left-hand side depends only on r and T_E, not on the vapor properties. The right hand side of Eq. 13 depends on T_E and the vapor properties but changes only slightly with r. Solutions are most easily obtained graphically. A typical chart of this type is shown in Fig. IV-3. Values of T_E for which Eq. 13 is satisfied are read off the chart. The quasi-steady growth rate is then given by

$$\frac{dr}{dt}\bigg|_{QS} = \frac{\Gamma_E - \Gamma_V}{\rho_L} = \frac{C_p}{L}\frac{\Gamma_V}{\rho_L}\frac{(T_E - T_V)}{\left(1 - \frac{2w}{r\rho_L L}\right)} \qquad (14)$$

An interesting result of the quasi-steady equations is immediately clear from Eq. 13. In this equation, the term $(C_p/L)(T_E - T_V)$ is always $\ll 1$. For nitrogen, $C_p/L \approx 1/200$. $T_E - T_V$ can hardly be much larger than 20°K, because the degree of supersaturation would become "astronomical", and spontaneous self-nucleation would presumably take over. Thus by Eq. 13

$$\frac{\Gamma_E}{\Gamma_V} \approx 1$$

that is, the quasi-steady equilibrium temperature adjusts itself in such a manner that the rate of evaporation nearly equals the rate of con-

densation. If we assumed the droplet temperature equal to that of the vapor, Γ_D would be small compared with Γ_V, and we would overestimate the growth rate $(\Gamma_V - \Gamma_D)/\rho_L$ by a factor of the order of ten.

The above remark holds only for condensation in a single vapor. If a non-condensible carrier gas is present which transfers heat from the droplet (such as the case of moisture in air), conditions can be quite different. In any case, the equations of this chapter are valid only for a pure vapor.

E. Iteration Solution of the Non-Steady Case

The solution of the complete equation, 12, simultaneously with Eq. 7 would still be a formidable job because of the complicated dependence of Γ_D on T_D and r. However, it turns out that a simple iteration converges very rapidly and gives a close approximation to the non-steady solution. Again we write Eq. 12 in the form

$$\Gamma_D = \Gamma_V \left[1 - \frac{C_p(T_D - T_V)}{L\left(1 - \frac{2W}{r\rho_L L}\right)} \right] - \frac{r}{3} \frac{dT_D}{dt} \frac{\lambda}{L\left(1 - \frac{2W}{r\rho_L L}\right)} \qquad (12a)$$

After a quasi-steady solution has been obtained, we calculate dT_E/dt, substitute this for dT_D/dt, and solve again, to get a closer approximation to the true non-steady T_D. It now turns out that this new value, say $T_D^{(1)}$, differs only slightly from T_E. This is due to the fact that Γ_D is a steep exponential function of T_D while the right-hand side is linear, with the small slope C_p/L. This is seen clearly in Fig. IV-3. Thus the change in the right-hand side due to the non-steady term is almost completely absorbed by Γ_D. It is therefore unnecessary to

carry the iteration beyond the first step. This means that the non-steady term may be simply added to Γ_D . A good approximation to the non-steady growth rate is then given by

$$\frac{dr}{dt} = \frac{\Gamma_V}{\rho_L} \frac{C_p}{L} \frac{(T_E - T_V)}{\left(1 - \frac{2w}{r\rho_L L}\right)} + \frac{r}{3} \frac{\lambda}{\rho_L L} \frac{dT_E}{dt} \qquad (15)$$

Note that the last term in this equation is usually negative (expansion). In this equation the surface energy correction term for the latent heat, $2w/r\rho_L L$, can be neglected compared with unity, because the non-steady term is only of importance for radii above 10^{-6} cm.

To give an indication of the effect of the non-steady term on the growth rate, a typical case will be given. For nitrogen at p_o = 20 atm, T_o = 300°K, and Mach number 6 (T_V = 36°K), $\frac{\partial T_E}{\partial x}$ would have to have the following values to cause a 10% error in the growth rate:

r_{cm}	10^{-7}	3×10^{-7}	10^{-6}	10^{-5}	10^{-4}
$\frac{\partial T_E}{\partial x}$ °K/cm for 10% error	37	38	15	1.6	.16

The actual gradient in the nozzle (5" x 5" tunnel) at this point would be $\approx$ 1.2°K/cm. Thus only droplets above 10^{-5} cm would be appreciably affected.

Because the iteration converges so fast, we have thus a simple way of checking the validity of the quasi-steady calculation in any particular case. The criterion of validity is

$$\frac{r}{3}\,\frac{\lambda}{\rho_L L}\,\frac{\partial T_E}{\partial x}\,\frac{dx}{dt} \ll \left.\frac{dr}{dt}\right|_{qs}$$

or

$$\frac{r}{3}\,\frac{\lambda}{\rho_L L}\,\frac{\partial T_E}{\partial x} \ll \left.\frac{dr}{dx}\right|_{qs} \tag{16}$$

In writing this, the fact that

$$\frac{dT_E}{dt} \approx \frac{\partial T_E}{\partial x}\,\Big|_r\,\frac{dx}{dt}$$

was used again, as discussed above. Equations 15 and 16 show

(1) that the non-steady effect increases with radius (linearly above 10^{-5} cm),

(2) that this effect is about inversely proportional to the pressure, since dr/dt is proportional to p_v,

(3) that the non-steady effect depends on the gradient of T_E in the nozzle, not of T_V as has sometimes been assumed. Fortunately $\frac{\partial T_E}{\partial x} \ll \frac{\partial T_V}{\partial x}$, roughly by a factor of ten (Cf. Figs. IV-4b and IV-5b).

F. The Zero-Growth Radius

It is now of interest to find the droplet size which has just zero growth due to the rate of change of T_E. To find this, we set $\Gamma_V - \Gamma_D = 0$ in Eq. 12 and solve. Using again T_E for T_D (which is justified here also) we get the approximate relation for the zero-growth radius

$$r_{zg} \doteq \frac{3}{\lambda}\,\frac{C_p \Gamma_v}{\frac{dx}{dt}}\,\frac{T_V - T_E}{\frac{\partial T_E}{\partial x}} \tag{17}$$

For given stagnation conditions, this can also be expressed in terms of the Mach number and dM/dx. Again r_{zg} is proportional to the pressure p_v.

There is thus for any point in a nozzle an upper as well as a lower limit on the size of droplet which is able to grow. The neighborhood of the upper "critical" radius, r_{zg}, is a stable region which the growing droplets will usually approach asymptotically. Nevertheless it is in principle quite conceivable to have in a nozzle a sudden expansion region where the zero growth radius may (locally) drop below the average droplet size. Under those conditions, the droplets larger than the local r_{zg} would have to reevaporate, even though the saturation ratio might increase at that point.

A similar, seemingly contradictory case arises when droplets suddenly enter a region of increasing T_E, in passing through a pressure wave. There the droplets will for an instant grow (even though the region may be undersaturated) before they heat up and evaporate. Qualitatively this can also be seen from Eq. 15 which shows that the growth rate can be positive for $T_V > T_E$ provided $r \frac{\partial T_E}{\partial x} \frac{dx}{dt}$ is positive and sufficiently large.

It must be emphasized however that the equations do not quantitatively apply to the case of droplets passing through shock waves, because the assumption of equal droplet and vapor speed looses validity there.

G. Results and Applications of the Growth Formula -- Case where Vapor Properties Are Known in Advance

In Figs. IV-3a to e, the results of the growth calculations are shown for air at 1 atm. stagnation pressure and atmospheric stagnation temperature. In Figs. IV-4a to e, similar results are given for air at p_o = 20 atm. In Figs. IV-5a to d, similar results are shown for nitrogen at p_o = 20 atm.

Those of the curves which are plotted against Mach numbers are valid for any nozzle. The others are valid only for the specific nozzle of the 5" x 5" tunnel for which they were calculated, though general trends will carry over to other nozzles.

On the two sets of charts for air, the non-steady correction term is shown. This is to be subtracted from the quasi-steady growth rates. In the preparation of the isocline integration charts 3e, 4e, and 5d, the non-steady correction has been included.

A very interesting (and quite unexpected) result is found by comparing Figs. IV-3a and IV-4a with the corresponding temperatures for saturated expansion (Fig. II-3). It will be seen that the droplet temperatures for 10^{-5} cm. radius are nearly identical with those for saturated flow.

The results of this paragraph are valid only for the case where there are very few droplets present so that the vapor is not influenced by them. The vapor pressure and temperature have been assumed to follow the perfect gas isentrope. However, the above-mentioned "coincidence" of the temperature curves seems to indicate that the droplets above, say, 5×10^{-6} cm radius assume at a point in the nozzle essentially the same temperature T_E regardless of how many other droplets there are present in the flow.

Fig. IV-3e shows that at 1 atm stagnation pressure, the droplets will grow very slowly in the nozzle. A droplet starting at 10^{-7} cm would hardly reach 3 times that size at the end of the nozzle.

For 20 atm. stagnation pressure, the growth rates are much increased. Any droplets which can grow at all will very quickly reach 3×10^{-6} cm and may get to 10^{-5} by the end of the nozzle.

After integrating the radii along the nozzle, one can estimate the number of nuclei required to condense (say) 1% of the air at the end of the nozzle. As an example, let us take (spherical) nuclei of 10^{-7} cm radius. At 20 atmospheres stagnation pressure, these will grow to about 5×10^{-6} cm radius at the end of the nozzle, while at P_o = 1 atm they may reach about 2.2×10^{-7} cm radius.

The number of nuclei per unit mass of air, ν , required to condense one per cent of the air at the end of the nozzle is given below for the two cases

P_o	ν, for g = .01	ϵ (for CO_2)
1 atm	$\approx 2 \times 10^{17}$	1.5×10^{-3}
20 atm	$\approx 2 \times 10^{13}$	1.5×10^{-7}

In the last column, the fraction by weight, ϵ , of carbon dioxide is given corresponding to the mass of the nuclei.

The rough figures above are rather hypothetical. First, the nucleus sizes may not be the same at different pressure levels, and would certainly not be the same for widely differing values of impurity concentration. Second, the saturation ratios in the nozzle would reach unreasonably high values. Nevertheless, such calculations indicate

that from the viewpoint of air droplet growth, very small fractions of CO_2 (or water) would suffice as nucleants.

The growth rates along the isentrope can be used for semi-empirical estimates if the onset of condensation is known experimentally. Arthur (Ref. 26) matched the early part of an experimental collapse curve by choosing numbers and sizes of nuclei compatible with the total impurity present. The result of this matching is in fair agreement with results of the next section. One difficulty in this approach is that the onset of the condensation is hard to determine from experiments with any accuracy. It seems therefore better to find a method of calculating the whole collapse curve. The slope of this can then be compared with experiment. It turns out that this slope must be quite sensitive to the number of nuclei present. This is discussed in Section V.

V. A SIMPLIFIED THEORY OF THE COLLAPSE OF THE SUPERSATURATED STATE

A. Objectives

The collapse of the supersaturated state in a nozzle is basically a non-linear phenomenon: the local rate of growth of the droplets depends on the pressure and temperature of the vapor (and possibly their rate of change) as well as on the size of the drop. But all of the above quantities depend in turn on the integrated rate of growth up to this point, and on the number of droplets present.

Given the number of droplets or nuclei present at the beginning of the collapse, it is possible, by means of the growth formula from the previous section, to set up a step-by-step computation method for the collapse in a nozzle. At each step one computes the amount of vapor condensed, the resulting change in pressure, temperature and speed in the nozzle. One then obtains a new equilibrium temperature and growth rate. Several computations of this type have in fact, been carried out by Oswatitsch (Ref. 6) for water vapor.

The outline above will reveal that such a computation is extremely tedious. What is worse, the information obtained by it is purely numerical: thus, it applies to only one nucleus size, number and nozzle flow condition. The manner in which the result depends on all of these parameters is, of course, not given by the stepwise integration.

An attempt is therefore made here to obtain a simple theory which would (1) retain the dependence on the important parameters, and (2) reduce the labor so that many cases can be solved and compared with experimental data.

B. Assumptions Involved

The clue for finding useful simplifying assumptions is given by the instantaneous collapse calculation, described in Section II-B. It was found there that even for this most extreme case of an irreversible condensation process, the final temperature, pressure, and g were not much different from the values obtained in a reversible equilibrium (i.e., "saturated") expansion and condensation process. Moreover, it was found that during the instantaneous collapse p_v and T_V vary practically linearly with g, the amount of condensed phase. It is therefore clear that at any point in the nozzle the flow variables (p_v T_V u, etc.) depend primarily on the amount of condensation which has taken place, and only very slightly on the manner in which the condensation has occurred. It will therefore be assumed that at each point in the nozzle p_v T_V and u are linear functions of g only, lying between the saturation curve and the isentrope.

It has been shown also by computation that along one instantaneous collapse curve, the growth rate dr/dt is a linear function of g, to very good accuracy.

A new variable η is therefore introduced, defined by

$$\eta = g/g_{sat} \tag{1}$$

which is zero* on the isentrope and unity (or close to unity) after the collapse. There is some question as to the best values of g_{sat} to use.

---

* It turns out convenient to include the volume of the nuclei in g. Then η along the isentrope differs slightly from zero (Cf. Section V-C below).

In the first calculations, the line $\eta = 1$ was taken along the saturated (i.e., equilibrium) expansion. However, later comparison with experiments makes it seem more reasonable to use the condensation shock curve, i.e., the locus of the final states of instantaneous collapse calculations (Cf. Fig. V-8 and Table I). In any case, the choice of the theoretical $\eta = 1$ line does not affect our basic understanding of the collapse process but merely affects the agreement between experiment and theory at the end of the collapse, which seems not too important here.

Since the pitot pressure was not greatly affected by the condensation process (both theoretically and experimentally), it is assumed as before that the pitot pressure may be used throughout the collapse to give the "effective area ratio" for the streamline considered. This assumption is not needed for the theory itself but is used in comparing it with experimental data, in order to locate the x coordinate of the theoretical calculations with respect to the actual nozzle. This is done by the use of a faired experimental pitot pressure vs. x curve from run 23-1 of Ref. 16.

For further simplifications, we must now look at the growth rate curves (Cf. Fig. V-1. Also Figs. IV-4c, IV-5c, and IV-6b.) While the growth "rate" dr/dx depends on the droplet radius, we know that the drops grow quite rapidly to about 10^{-6} cm, from where on the growth rate becomes nearly independent of radius. A typical growth rate curve for an actual droplet in the nozzle is sketched in Fig. V-1, where the dotted line represents a droplet starting at 10^{-7} cm radius. Its growth curve is quite similar to the 10^{-6} cm curve but the starting point is displaced a distance δ by virtue of its smaller initial size.

For our simplified theory we will therefore use a growth curve for constant r and adjust only the displacement δ by the Thompson formula to fit the nucleus size. For the present calculation, the growth curve for $r = 10^{-6}$ cm is used.

Some further and rather important assumptions concern the sizes, shapes, and numbers of the nuclei. First, all nuclei are assumed to be of equal size and of spherical shape. While in reality there is likely to be a distribution of sizes and possible shapes, it would at present be extremely hard to predict this distribution. We must thus be content to consider all these nuclei replaced by an equal mass of impurity divided into a number of spherical particles; their size must be considered as an "equivalent mean" size corresponding to the actual distribution of sizes and shapes.

It is further assumed that these nuclei be perfectly wetted, so that they begin to grow (on average) at the same supersaturation as a condensation germ of the same size.* Moreover, it is assumed that the nuclei are inert, i.e., do not go into solution and do not affect the vapor pressure or surface tension of the condensing substance (nitrogen).

During the collapse process the number of nuclei (or droplets) per unit mass of vapor present is assumed constant. It must be pointed out that, in spite of this restriction, the present theory could also be used for cases where spontaneous self-nucleation is important. The reason is that any condensation germs formed after the beginning of the

---

* These assumptions are discussed in Sections I and IV.

collapse will contribute virtually nothing to the collapse because they are too small. Also the self-nucleation process will slow down as soon as the supersaturation decreases. In fact, it must be expected that toward the end of the collapse, where the supersaturation becomes low, the smallest droplets will reevaporate again in favor of the larger ones. It is thus to be expected that only the nuclei or germs present in the very early stages of the collapse will be important later. Oswatitsch (Ref. 7) already has demonstrated this in a rough calculation for the moisture case. He calculated the contribution to the final collapse by condensation germs formed at various points upstream. He demonstrated that the germs formed at the point where the collapse is detected, even though large in number, have little effect on the collapse compared with those formed earlier.

Finally, the computing procedures are much simplified if the percentage (by weight) of the nucleus forming impurities is small.

Before summarizing the assumptions, it is worthwhile to show the meaning of the simplifications which have been introduced. For this consider the pressure ratio chart, Fig. V-8. (p = static, p_o' = pitot pressure, x = axial distance along the nozzle) The pressure ratio vs. distance plane has been chosen for several reasons. One is that it permits direct comparison with experiment, since both ordinate and abscissa can be measured as well as calculated quantities. The reason for choosing x here rather than the more convenient p_o'/p_o is that x represents the time scale of the phenomenon (velocity being practically constant). The assumptions make the pressure and the growth rate point functions of η and x, independent of the flow history up to this

point. Moreover, for any value of η the growth rate can be obtained from the known growth rate on the isentrope for the same x. It should be pointed out again that the value $g_{sat}(x)$ used in η can be calculated by one of two limiting thermodynamic processes, the (equilibrium) saturated expansion or the locus of instantaneous collapse end points. Either of these appears satisfactory for the purpose at hand.

The assumptions are summarized in brief form as follows:

(1) All nuclei or condensation germs are of equal size, spherical shape and inert material, but perfectly wetted.

(2) During the collapse, all droplets (or crystals) are of equal size (at one point), and their total number (per unit mass of vapor) remains constant.

(3) Growth curves for all drop sizes are approximated by the curve for $r = 10^{-6}$ cm, with proper displacement to match starting point.

(4) p_v are T_V are functions only of η and x, p_v being a linear function of η.

(5) dr/dx for $r = 10^{-6}$ cm is a linear function of η, with a slight modification to match the boundary condition at $\eta = 1$ (Cf. next paragraph)

(6) The total mass of the nuclei per unit mass of vapor is small (i.e., less than 1/10%).

(7) Pitot pressure p_o' is a function of x only, unaffected by the condensation.*

---

* This is required only for the comparison of theory and experiment. For the theory alone, we could dispense with p_o' altogether and plot p/p_o vs. area ratio or x.

C. The Equations and Initial Conditions

Assumptions (4) and (7) together give us a linearly spaced grid of constant η lines in the p/p_o' vs. x plane (or in the p/p_o vs. x plane).

$$\frac{p}{p_o'}(\eta,x) = (1-\eta)\left.\frac{p}{p_o'}\right|_{is} + \eta\left.\frac{p}{p_o'}\right|_{sat} \qquad (1)$$

This grid puts the theoretical results into a form for convenient comparison with experiment.

The variation of dr/dx (η , x, 10^{-6}) is given by assumption (5). If we took the growth "rate"* strictly as a linear function of η , decreasing to zero at the saturation line, we would get at any point (along an actual collapse)

$$\frac{dr}{dx}(\eta,x) = (1-\eta)\left.\frac{dr}{dx}\right|_{is}$$

or

$$\frac{dg}{dx} = (1-\eta)\,4\pi r^2 \nu \rho_L \left.\frac{dr}{dx}\right|_{is} \qquad (a)$$

where ν is the number of droplets (or nuclei) per unit mass of air or nitrogen in the nozzle, and ρ_L is the density of the condensed phase.

It is clear however, that dg/dx is not quite zero after the collapse if there is further expansion in the nozzle. To satisfy the boundary condition at $\eta = 1$ and at the same time keep the mathematics simple, it is best to add to the above Eq.(a)a term $\eta \frac{dg_s}{dx}$. It must be appreciated that dg_s/dx is very small compared with the condensation rates during the collapse.

---

* Both dr/dt and dr/dx are here referred to as growth rates. One is proportional to the other since the velocity is practically constant through the region of interest.

Thus, the assumed form of the condensation rate (along one collapse) becomes

$$\frac{dg}{dx} = \eta \frac{dg_s}{dx} + (1-\eta) 4\pi \nu \rho_L r^2 \left.\frac{dr}{dx}\right|_{is} \tag{2}$$

or

$$\frac{dg}{g} = \frac{dg_s}{g_s} + \frac{3}{r}(1-\eta)\left.\frac{dr}{dx}\right|_{is} dx \tag{3}$$

Now, since the fraction which is in condensed form, g, is given by*

$$g = \eta g_s = \frac{4}{3}\pi \nu \rho_L r^3,$$

$$\frac{1}{r} = \frac{1}{\eta^{\frac{1}{3}}}\left(\frac{4\pi \nu \rho_L}{3 g_s}\right)^{\frac{1}{3}}$$

We then get (along one collapse)

$$\frac{dg}{g} = \frac{dg_s}{g_s} + \frac{1-\eta}{\eta^{\frac{1}{3}}} 3C_\nu \frac{1}{g_s^{\frac{1}{3}}} \left.\frac{dr}{dx}\right|_{is} dx \tag{4}$$

where

$$C_\nu = \left(\frac{4\pi \nu \rho_L}{3}\right)^{\frac{1}{3}} \qquad cm^{-1} \tag{5}$$

However, from the definition of η we get by logarithmic differentiation a relation which is valid throughout the supersaturated region:

$$\frac{dg}{g} = \frac{dg_s}{g_s} + \frac{d\eta}{\eta} \tag{6}$$

When this is subtracted from Eq. 4 above we obtain

---

* g here includes the volume of the nuclei.

$$\frac{\eta^{-\frac{2}{3}}}{1-\eta}\,d\eta = 3C_\nu\left[\left.\frac{dr}{dx}\right|_{is} \Big/ g_s^{\frac{1}{3}}\right] dx \qquad (7)$$

This is the differential equation giving η as a function of $\dot{x}$ for one particular collapse.

It is noteworthy that only one single parameter, $C_\nu \alpha \nu^{\frac{1}{3}}$, enters into the differential equation of the collapse curves, under the simplifying assumptions we have made. A second parameter, the nucleus or germ size, enters the problem through the initial conditions (below). It is also very fortunate that in the above equation it was possible to separate the variables, which greatly simplified the computation procedure. This simplification was made possible by the introduction of the term $\eta \frac{dg_s}{dx}$ in Eq. 2 above. If we had taken dr/dx exactly as a linear function of η, we would have obtained instead of dg_s/gs in Eq. 4 a term $3\eta^{\frac{2}{3}}dg_s/gs$. The difference between the strictly linear dr/dx and the approximation used here is quite small except in the immediate vicinity of the $\eta = 1$ line. The collapse curve obtained here approaches the saturation line more slowly than it would have without the additional approximation. If the collapse ends in a region of the nozzle where there is parallel flow, dg_s would be zero there and the additional approximation is unnecessary. In any case, in the light of the general aim of the present investigation great accuracy over the final stages of the collapse appears unimportant.

The initial condition for Eq. 7 is

$$\eta = \eta_o \qquad \text{when } x = x^+$$

At x^+ the supersaturation is such that condensation can just begin, i.e., with the assumption (1) the nuclei correspond to droplets of critical size, r^+. η_o corresponds to the radius of the nuclei, i.e.,

$$\eta_o = \frac{g_o}{g_s(x^+)} = \frac{\varepsilon}{g_s}\frac{\rho_L}{\rho_{NUC}}$$

where

$$g_o = \varepsilon \frac{\rho_L}{\rho_{NUC}}$$

is the equivalent mass the nuclei would have if they consisted of the same substance as the primary (condensing) vapor. ε is the mass of the nucleant (impurity) per unit mass of vapor.

Now, in practice for the supersaturation to be appreciable, the total mass of the nucleus forming impurities must be small, i.e., $\varepsilon/g_s \ll 1$, or $\eta_o \ll 1$. This fact will be used below for further approximations.

Eq. 7 can now be integrated without difficulty. The left-hand term is integrable in closed form and results in $f(\eta) - f(\eta_o)$ where

$$f(\eta) = \int_o^\eta \frac{y^{-\frac{2}{3}}}{1-y}\,dy$$

$$= \frac{1}{2}\ln\frac{1+\eta^{\frac{1}{3}}+\eta^{\frac{2}{3}}}{(1-\eta^{1/3})^2} + \sqrt{3}\tan^{-1}\frac{2\eta^{\frac{1}{3}}+1}{\sqrt{3}} - \sqrt{3}\tan^{-1}\frac{1}{\sqrt{3}} \qquad (8)$$

A plot of $f(\eta)$ is given in Fig. V-2.

The right-hand side of Eq. 7 results in

$$C_v I(x) = C_v 3\int_{x^+}^{x}\left[\left.\frac{dr}{dx}\right|_{is}/g^{\frac{1}{3}}\right]dx \qquad (9)$$

The integral I(x) is best evaluated numerically. In the present

calculation this was done with a planimeter. Within the present approximation, this numerical integration needs to be done only once for a given nozzle and stagnation pressure. The collapse curves η vs. x are now obtained from

$$f(\eta) - f(\eta_o) = C_\nu I(x) \tag{10}$$

Now, over most of the collapse $f(\eta_o)$ is small compared to $f(\eta)$ since $\eta_o \ll 1$. For instance, for the case where 1/10% CO_2 (by weight) is added to pure nitrogen (i.e., $\mathcal{E} = 10^{-3}$), $\eta_o \doteq .01$ and $f(\eta_o) \approx .65$. In most cases much less impurity is to be expected in a tunnel, so that $f(\eta_o)$ is usually much smaller.

Therefore, as a first approximation, valid for small amounts of impurity (say $\mathcal{E} = 10^{-4}$ or less), we neglect the term $f(\eta_o)$ in Eq. 10. This greatly simplifies the preliminary numerical work since we do not have to decide on values of in advance. The solution of the equation

$$f(\eta) = C_\nu I(x) \tag{10a}$$

then gives a one parameter family of collapse curves in the η vs. x plane.

A typical family of such collapse curves is shown in Fig. V-3a. This was calculated for the 1" x 1" nitrogen tunnel (Refs. 15 and 16). The curves given correspond to a stagnation pressure of 8.3 atm. and stagnation temperature of 290°K. All curves of the family start at $x = x^+$ where, according to the Thompson formula, the critical radius is 10^{-6} cm.

The curves are valid for $\eta_o = 0$. For small but not negligible

values of $f(\eta_o)$ the curves are shifted somewhat toward lower values of x. In Fig. V-3b, a set of collapse curves is shown in which $f(\eta_o)$ was not neglected. These curves correspond to η_o of .01 or about 1/10% impurity by weight, the largest value considered here. Even though for this extreme case the η vs. x curves appear appreciably changed, the final results of the theoretical collapse estimate are not too seriously affected by this (Cf. E and F below).

The collapse curves approach $\eta = 1$ asymptotically as to be expected. The steepness of the curves turns out very sensitive to C_ν (or $\nu^{\frac{1}{3}}$).

It is clear that the theoretical collapse curves can also be transferred into the pressure vs. x plane, by the use of the grid of constant η lines.

D. Dependence of the Collapse on Nucleus Size

We now have a family of collapse curves which apply to droplets of 10^{-6} cm radius or larger.* According to assumption (3) the same collapse curves will also be used for smaller droplets except that the starting points of these curves will be shifted to a new value of x^+, in accordance with the Thompson formula (Cf. Fig. V-5). To be specific: if the critical drop radius $r^+ = 10^{-7}$ cm occurred in our nozzle at x = 4.5 cm, and $r^+ = 10^{-6}$ cm occurred at x = 2.9 cm, we would for nuclei of 10^{-7} cm simply shift all the collapse curves by $x^+ = 1.6$ cm. At first, this method may seem like an extremely crude approximation, because the

---

* The growth rates change very little above 10^{-6} cm except that in some nozzles the non-steady correction term can become important.

maximum growth rates for the two drop sizes can differ by a factor of 2 or more. However, fortunately we are looking in the collapse calculation for an integrated effect, and since the droplets must over a large part of their travel be near or above 10^{-6} cm radius, the error introduced by assumption (3) is not quite as serious as might be expected.

It should be pointed out, however, that for very much lower pressures than those considered here together with very small nuclei a more refined approach will be necessary. In practice this may occur in heated tunnels where the condensation is delayed so that the collapse will occur at much lower temperatures and pressures (for the same stagnation pressure).

We now have the following result: within the simplifying assumptions made here, the collapse curves for all nucleus sizes are similar in the η vs. x plane, as long as the number of nuclei, the nozzle geometry and stagnation conditions are held constant. However, when the curves are presented in the pressure vs. distance plane, they are distorted and look somewhat idfferent for different sizes.

E. Most Effective Nucleus Size, Earliest Possible Collapse

By the method discussed above, or by a more accurate calculation, one could make a theoretical prediction of the collapse phenomenon in a nozzle <u>if</u> the number and size of the nuclei were <u>given</u>. However, at present reliable information on the potential nuclei would be very hard to obtain, either experimentally* or theoretically.

---

* An attempt to determine particle numbers and sizes has been made by Durbin (Ref. 40). However, for the small nuclei considered here, $O(10^{-7}$ cm), this involves great difficulties.

We can, however, obtain some estimate of the collapse position in the nozzle by further theoretical speculation. Let us assume that the total mass of the nuclei is fixed, say $\varepsilon = 10^{-4}$. By assuming different nucleus sizes, we get different values of C_ν (Cf. Fig. V-4) and different collapse curves. For small nucleus radii, the collapse will be delayed far down the nozzle, but the collapse curve will be steep, since C_ν is large. For larger nuclei (same total mass) the collapse will start nearer the saturation point but will be much shallower (small C_ν). We can thus calculate from the η vs. x chart at what point in the nozzle we would reach, say $\eta = .5$ or $\eta = .8$ with different sizes of nuclei. This has been carried out for the nitrogen nozzle mentioned previously. The results are shown in Fig. V-6.

One can now define a "most effective" nucleus size, for each amount of nucleus forming impurities. It will be seen that this nucleus size depends slightly on the criterion chosen (here $\eta = .5$ or $\eta = .8$). If we take the half-way point on the collapse ($\eta = .5$) as criterion, we favor slightly larger nuclei. However, the difference in the nucleus size (10 to 15%) is too small to be significant within the accuracy to be expected from this very approximate theory. The most effective nucleus sizes are plotted against ε in Fig. V-7.

Corresponding to the "most effective" nucleus sizes, we get thus a theoretical estimate of the "earliest possible" collapse. The places in the nozzle where $\eta = .5$ (or $\eta = .8$) can first be reached (according to this simple calculation) can be read off directly in Fig. V-6.

It should be mentioned that for $\varepsilon = 10^{-5}$, the lowest concentration considered, the supersaturations in the nozzle are very high at the onset of collapse. Under these conditions, the simple growth calculation

made here may become meaningless. Rather, one should probably consider a process similar to the germ formation of Volmer where, due to fluctuations, some droplets grow in spite of being smaller than critical size.

For the highest concentration considered, $\varepsilon = 10^{-3}$, the calculations were carried out both with the correct η_o and with $\eta_o = 0$. Where $f(\eta_o)$ was retained, the curves are designated as "corrected". In Fig. V-8, only the corrected curve is given (for $\varepsilon = 10^{-3}$).

The numerical results of the earliest possible collapse estimate are summarized in Table II. It will be seen that for the $\eta = .8$ criterion, the most effective radii run from .57 to $1.14 \cdot 10^{-7}$ cm, and the numbers ν from .82 to $7.7 \cdot 10^{16}$. Slightly lower numbers and larger radii were found for the $\eta = .5$ criterion. The column marked collapse point, x**, refers to the point in the nozzle where the $\eta = .5$ or $\eta = .8$ line is reached.

For the theoretical estimate, the onset of the collapse may be defined as the point (i.e., x^+) where the droplets just begin to grow. It is also of interest to calculate the points along the collapse where η has reached some small but finite value which could be detected by experiment. For this $\eta = .05$ was arbitrarily chosen although this is probably smaller than can be detected within the experimental scatter. The calculated saturation ratios in the 1" x 1" tunnel at the departure point ($x = x^+$) and at the points where $\eta = .05$ are given in Fig. V-9.

F. Comparison of Results with Experiments

Comparison has been made with experimental data obtained in the 1" x 1" nitrogen tunnel, described in Refs. 15 and 16. The runs used

here are given in the latter reference. The theoretical calculations are based on nitrogen at stagnation pressure of 8.3 atm. and stagnation temperature of 290°K.

In Fig. V-6, static to pitot pressure ratios are plotted against axial distance. All theoretical curves were first calculated with the theoretical pitot pressure ratio (p_o'/p_o) as abscissa. This abscissa was then correlated with respect to the axial distance x in the nozzle by the use of experimental pitot pressures faired from Run 23-1. Since experimental pitot pressures from run to run in this tunnel varied up to about 8% due to the effect of added impurities,* this constitutes an uncertainty in the correlation between theoretical and experimental results. The corresponding maximum error due to this is about one cm in the proper location of the theoretical curves with respect to the physical nozzle and the experimental points.

In the computations leading to Fig. V-8, the (equilibrium) saturated expansion has been taken as the $\eta = 1$ line. Actually it was found later that the locus of instantaneous collapse end points would have been a better choice, since the pressure after collapse appear to approach that line more closely.

The experimental points shown include three runs with commercial grade nitrogen. The exact amounts of impurities for runs 27 and 34 are not known. For the gas of run 27, a mass spectrometer analysis indicated "less than .004% CO_2 by volume", (i.e., $\varepsilon < .0063\%$ by weight).

---

* The experimental scatter (due to waves, etc.) for any given composition was much smaller, about 2% or 3%.

For run 23 a chemical analysis indicated about .0033 per cent CO_2 by weight, and about half that amount of water vapor. For the other runs, the total amounts of impurities are given. The methods used and the probable accuracy are discussed in Ref. 16.

The theoretical estimates of the earliest possible collapse (due to foreign impurities) are shown for CO_2 in weight fractions ϵ of 10^{-3}, 10^{-4}, and 10^{-5}, respectively.

Possible agreement of the theoretical estimate with any one experiment must be considered as fortuitous. It is, of course, by no means to be expected that in a true physical case, all the simplifying assumptions made would be satisfied, in particular, that all nuclei would be in the vicinity of the most effective size.

However, the theoretical estimate does seem to predict quite well the general trend of delayed collapse with reduced impurities. This general agreement seems to indicate that the nuclei due to impurities do become smaller as the concentration is decreased, roughly in the same manner as the calculated "most effective" sizes. The rough prediction or explanation of general trends is the most that should be expected from the simplified theoretical calculations.

In Fig. V-9, the saturation ratios at the departure points are given for the theoretical estimate. Also shown is the line where the theoretical curves reach $\eta = .05$. The experimental points, due to Arthur, represent the departure from the isentrope on the p/p_o' vs. p_o'/p_o charts. The two points of lowest impurity should probably be plotted higher up since both moisture and carbon dioxide were present in these runs (about .002% by volume for each). In this representation

too, the theoretical (earliest collapse) estimate seems to give about the right trend. Above 1/10% impurity by weight ($\varepsilon = 10^{-3}$), the theoretical estimate can hardly be considered valid. Fortunately, well dried wind tunnel air will not contain such high concentrations of impurities.

G. Preliminary Thoughts on Scale Effects

Let us consider two geometrically similar nozzles* under the same stagnation conditions. At corresponding stations in both nozzles the flow properties(p_v T_v u, etc.) will be the same up to the condensation region (neglecting viscous effects). We want to investigate the difference between the collapse positions and shapes in the two nozzles.

Consider this first from the view point of the simplified analysis in which all nuclei are assumed of equal size (in one nozzle at one ε). The collapse was given by

$$f(\eta) - f(\eta_0) = C_v\, 3 \int_{x^+}^{x} \frac{\left(\frac{dr}{dt}\right)_{is} \frac{1}{u}}{g_s^{1/3}}\, dx$$

In the right-hand term, the integrand consists entirely of thermodynamic quantities which are not influenced by the scale.** To make the integral dimensionless we only need to change the geometric variable x. We

---

* In the following discussion, whenever comparison between two nozzles enters, it will be understood that they are geometrically similar.

** An exception is the growth cut-off for large droplets due to temperature gradient, which will not be important here (Cf. Section IV).

introduce a new variable

$$\xi = x/x_s$$

where x_s is the location of the saturation point. For all geometrically similar nozzles at the same stagnation conditions, the flow variables are then unique functions of ξ. Thus we have

$$f(\eta) - f(\eta_0) = (C_\nu x_s) 3 \int_{\xi^+}^{\xi} \frac{\left.\frac{dr}{dt}\right|_{is} \frac{1}{u}}{g_s^{\frac{1}{3}}} d\xi = (C_\nu x_s) I(\xi) \qquad (11)$$

where $I(\xi)$ again has the same value in all nozzles at corresponding points.

The last equation shows that for fixed nucleus size, we would get similar collapse curves in two nozzles if the product $C_\nu x_o$ remained unchanged, that is, if the larger nozzle had proportionately fewer nuclei per unit mass of vapor. Alternately, for a fixed number of nuclei we would get in the larger nozzle a relatively steeper collapse (i.e., in this case the absolute distance over which the collapse occurs would be roughly the same in both nozzles).

The scale effect must depend mostly on the manner in which the nucleus sizes and numbers are affected by the nozzle size. Since nothing reliable is known about this, the speculation is not persued further here. It appears, however, that from experiments with two similar nozzles of different sizes, one could draw reasonably reliable conclusions regarding the nucleus size distribution.

The writer has not yet compared data from nozzles of different scale. In fact, very few such data are available for comparison. One attempt of such a comparison was made at GALCIT by passing air from the Five-Inch Hypersonic Tunnel through the One-Inch Nitrogen Tunnel. The results, which are discussed in more detail in Ref. 26, indicate no appreciable difference between the values of the supersaturation reached in the two nozzles.

The effect of changing stagnation pressure on the collapse may be called a "quasi-scale effect". It was pointed out that $dr/dx\big|_{is}$ is roughly proportional to the pressure, and the same will be true for $I(\xi)$ at corresponding points. Thus, if the nucleus size distribution remained unaffected by pressure, the collapse would be steeper under increased pressure (other factors remaining constant).

Further experiments at various pressures and analysis of already existing data may clarify the nucleus size distribution somewhat. To date there are primarily the results of Hill (Ref. 41) which indicate little change in the supersaturation reached over a very wide range of pressures. Tentative results of Arthur show a comparative insensitivity of supersaturation to stagnation pressure (Ref. 26).

VI. CONCLUSIONS

1. The effect of condensation on the flow in hypersonic tunnels is bracketed by two simple limiting thermodynamic processes, equilibrium saturated expansion and instantaneous condensation. Both processes give similar end conditions.

2. The condensation of air (or nitrogen) in a hypersonic nozzle affects primarily the free stream pressure and temperature, while velocity, density and dynamic pressure remain practically unchanged.

3. The effect of the condensation on the pressure and temperature is roughly proportional to the fraction of vapor condensed, but the sound speed may be expected to change (by about 10%) at the very onset of condensation.

4. At least two parameters must take the place of the ordinary Mach number for the case of the two-phase fluid. One of these, the dynamic pressure parameter $\tilde{M}$ is well established and can be determined accurately by several experimental methods (Refs. 17 and 38). Its value is close to the Mach number calculated from pitot and static pressures by the Rayleigh equation for a perfect gas.

5. The speed and the pressure coefficient of infinitesimal waves in the two-phase fluid are not yet definitely established. A simple limiting sound speed for low frequency waves, $\overset{\circ}{a}$, appears to approximate some experimental results (Refs. 17 and 32). The theoretical Mach wave relation for saturated flow based on $\overset{\circ}{a}$ depends (for a fixed stagnation temperature) practically only on $\tilde{M}$ (Fig. III-12).

6. For all discontinuities with phase transition in a vapor, a simple invariant $\Phi(\tilde{M}_N, E)$ is found to exist (Cf. Eq. III-9) within the assumptions of Section III.

7. Evaporation increases slightly the pressure ratio of shock waves, for a given normal component $\tilde{M}_{N2}$ of the dynamic pressure parameter. For a given wedge angle and free stream $\tilde{M}$ evaporation decreases the wave angle appreciably and the pressure ratio slightly (Figs. III-6 to III-8). There exists a value of the evaporation parameter E for which the wave angle on a given wedge becomes practically independent of $\tilde{M}$.

8. By the use of the normal shock results for two-phase fluid, it is possible to directly compare theoretically computed pressures with experimental measurements, without further assumptions concerning wall friction and uniform flow (Cf. Figs. III-10 and III-11). By this method the saturated expansion theory is shown to be a fair approximation to the flow after the collapse.

9. A good approximation to the non-steady free molecule droplet growth rate is obtainable from the quasi-steady solution by a simple iteration. From this, limits of validity of the quasi-steady drop growth theory and the upper limiting (zero growth) drop size are defined.

10. Isolated droplets above 10^{-6} cm radius growing in supersaturated air or nitrogen are found to assume a temperature close to that calculated for saturated expansion in the same nozzle (page 64).

11. By integration of the drop growth along a typical nozzle, it is shown that (a) for stagnation pressures above 10 atm, very small traces of CO_2 or water could supply sufficient nuclei for appreciable condensation, and (b) for stagnation pressures below one atm, foreign nuclei become much less effective.

12. The dependence of the collapse of the supersaturated state on the numbers and sizes of nuclei present is obtained by an approximate integration procedure, valid for low impurity concentrations. From this

the most effective nucleus size for any impurity concentration and the earliest possible collapse in a given nozzle can be calculated. This theoretical estimate predicts to fair accuracy the effect of CO_2 on the collapse in the 1" x 1" nitrogen tunnel and on the minimum supersaturation before collapse (Figs. V-8 and V-9).

13. It has now been shown convincingly that the attainable supersaturation of air or nitrogen in hypersonic nozzles depends on foreign nuclei (or at least on the presence of impurities). However, the self-nucleation process of these impurities is not yet understood well enough to predict nucleus numbers and sizes for given impurity concentrations. Also the effectiveness of different substances as nuclei is not yet fully known. Therefore, no reliable predictions of the actual collapse positions in much larger (or much smaller) nozzles than the one studied here can be made. Nevertheless, the method given for estimating the "earliest possible" collapse should be valid over a wide range of nozzle sizes and pressures.

REFERENCES

1. Wagner, Carl: "Calculations on the Possibility of Obtaining Higher Mach Numbers in Wind Tunnel Tests". WVA Archive A-3, (1942).

2. Grunewald: "Wind Tunnel Mach Numbers Attainable under Consideration of Supersaturation Phenomena of Air". WVA Archive 204, Kochel (1945).

*3. Epstein, P. S.: "Condensation Through Expansion" and "Rapidity of Condensation on Foreign Nuclei". Reports No. 2 and 3 of a group of reports written for the U. S. Army Ordnance (unpublished), (about 1943).

4. Puckett, A. E. and Schamberg, R.: "Hypersonic Wind Tunnel Progress Report No. 5", Contract No. W-04-200-Ord-1463, Ord., Dept. Army, and GALCIT, (August 8, 1946).

5. Charyk, J. and Lees, L.: "Condensation of the Components of Air in Supersonic Wind Tunnels". Report 127, Aero. Eng. Lab., Princeton University, (March 1, 1948).

6. Oswatitsch, K.: "Condensation Phenomena in Supersonic Nozzles". ZAMM, Vol. 22, No. 1, pp. 1-14, (February, 1942). Also Translation RTP 1905.

7. Oswatitsch, K.: "Fog Formation in a Wind Tunnel and Its Influence on Model Tests". Jahrbuch der Luftfahrtforshung, p. 692, (1941). Also Translation R. and T. No. 459 and MAPVG 248.

8. Head, Richard M.: "Investigations of Spontaneous Condensation Phenomena". Ph.D. Thesis at the California Institute of Technology, (1949).

9. Wegener, P. and Smelt, R.: "Summary of N.O.L. Research on Liquification Phenomena in Hypersonic Wind Tunnels". Naval Ordnance Laboratory Memorandum No. 10772. (Feb. 15, 1950).

10. Bogdonoff, S. M. and Lees, L.: "Study of the Condensation of the Components of Air in Supersonic Wind Tunnels. Part I: Absence of Condensation and Tentative Explanation". Report No. 146, Contract AF 33-(038)-250, Air Materiel Command, USAF, and Aero. Eng. Lab., Princeton University, (May 25, 1949).

11. Becker, J. V.: "Results of Recent Hypersonic and Unsteady Flow Research at the Langley Aeronautical Laboratory". Journal of Applied Physics, Vol. 21, No. 7, pp. 619-628, (July, 1950).

12. Wegener, P. P.; Stollenwerk, E.; Reed, S.; and Lundquist, G.: "NOL Hyperballistics Tunnel No. 4, Result I: Air Liquefaction". NAVORD 1742, (January 4, 1951).

---

* Cf. Footnote on page 92.

13. Stever, H. G.: "A Modification of the Theory of Kinetics of Condensation and Its Application to Air Condensation in Hypersonic Wind Tunnels". Contributed paper, Division of Fluid Mechanics, American Physical Society Meeting, Charlottesville, Va., (December 28, 29, 30, 1949).

Stever, H. G. and Rathbun, K. C.: "Theoretical and Experimental Investigation of Condensation of Air in Hypersonic Wind Tunnels". NACA TN 2559, (November, 1951).

14. Tsien, H. S.: "Wind Tunnel Testing Problems in Superaerodynamics". Journal of the Aeronautical Sciences, Vol. 15, No. 10, p. 573, (October, 1948).

15. Nagamatsu, H. T. and Willmarth, W. W.: "Condensation of Nitrogen in a Hypersonic Nozzle". Memorandum No. 6, Contract No. DA-04-495-Ord-19, Army Ordnance Department, California Institute of Technology, (January 15, 1952).

16. Arthur, P. D. and Nagamatsu, H. T.: "Effects of Impurities on the Supersaturation of Nitrogen in a Hypersonic Nozzle". Hypersonic Wind Tunnel Memorandum No. 7, Guggenheim Aeronautical Laboratory, California Institute of Technology, (February 15, 1952).

17. Grey, J. and Nagamatsu, H.: "The Effects of Air Condensation on Properties of Flow and Their Measurement in Hypersonic Wind Tunnels". Hypersonic Wind Tunnel Memorandum No 8, Guggenheim Aeronautical Laboratory, California Institute of Technology, (June 15, 1952).

18. Volmer, Max: "Kinetic der Phasenbildung". Verlag von Theodor Steinkopff, Dresden and Leipzig, (1939).

19. Charyk, J. V.: "Condensation Phenomena in Supersonic Flows". Ph.D. Thesis, California Institute of Technology, (August, 1946).

20. Kantrowitz, A.: "Nucleation in Very Rapid Vapor Expansions". Journal of Chemical Physics, Vol. 19, No. 9, 1097-1100, (September, 1951).

21. Probstein: "Time Lag in Self-Nucleation of Supersaturated Vapor". Report No. 168, Princeton University, (November 27, 1950).

22. Gilmore, F.: "The Dynamics of Condensation and Vaporization". Ph.D. Thesis, California Institute of Technology, (1951).

23. Buff, F. P. and Kirkwood, J.: Journal of Chemical Physics, 18, 991, (1950).

24. Buff, F. P.: "The Spherical Interface. I. Thermodynamics". Journal of Chemical Physics, Vol. 19, No. 12, p. 1591, (December, 1951).

25. Reed, S.: "On the Early Stages of Condensation". J. Chem. Phys. (February, 1952).

26. Arthur, P. D.: "The Effect of Impurities on the Supersaturation of Nitrogen in a Hypersonic Wind Tunnel". Ph.D. Thesis, California Institute of Technology, (1952).

27. Buhler, R. D.: "Recent Results on the Condensation Investigation". Hypersonic Wind Tunnel Memorandum No. 1, Guggenheim Aeronautical Laboratory, California Institute of Technology, (July 9, 1950).

28. Epstein, P. S.: "Absorption of Sound in Suspensions". Seminar presented at the California Institute of Technology, (November, 1951).

29. Heybey: "Analytical Treatment of Normal Condensation Shocks". Kochel Report No. 66/72. Available as NACA TM 1174.

30. Samaras, D. G.: "Gas Dynamic Treatment of Exothermic and Endothermic Discontinuities". Canadian Journal of Research, Vol. 26, Sec. A, No. 1, (January, 1948).

**31. Hansen, C. F. and Nothwang, G. J.: "Condensation of Air in Supersonic Wind Tunnels and Its Effects on Flow about Models". NACA TN 2690 (April, 1952).

32. Coles, D. and Nagamatsu, H. T.: "Experimental Techniques and Preliminary Test Data from the GALCIT 5" Hypersonic Wind Tunnel". Hypersonic Wind Tunnel Memorandum in preparation, Guggenheim Aeronautical Laboratory, California Institute of Technology.

33. Faro, I. D.; Small, R. T.; and Hill, F. K.: "Hypersonic Flow at a Mach Number of 10". Journal of Applied Physics, Vol. 22, No. 2, p. 220, (February, 1951).

34. Kennard, E. H.: "Kinetic Theory of Gases". McGraw-Hill, (1938).

35. Epstein, P. S.: "Textbook of Thermodynamics". John Wiley and Sons, New York, (1937).

36. Frenkel, J.: "Kinetic Theory of Liquids". Clarendon Press, Oxford, (1946).

**37. Ross, F. W.: "The Propagation in a Compressible Fluid of Finite Oblique Disturbances with Energy Exchange and Change of State". Journal of Applied Physics, Vol. 22, No. 12, p. 1414, (December, 1951).

38. Buhler, R. D.: "Methods for Determining the Mach Number in Hypersonic Wind Tunnels". Hypersonic Wind Tunnel Memorandum No. 2, Guggenheim Aeronautical Laboratory, California Institute of Technology, (August 21, 1950).

** Cf. Footnote on page 92.

39. Buhler, R. D.; Jackson, P. H.; and Nagamatsu, H. T.: "Oblique Shock Waves with Evaporation; Method of Calculating Free Stream Temperature and Amount of Condensation from Wedge Tests; Remarks on the Pressure Coefficient in Hypersonic Tunnels". Hypersonic Wind Tunnel Memorandum No. 3, Guggenheim Aeronautical Laboratory, California Institute of Technology, (April 10, 1951).

40. Durbin, E. J.: "Optical Methods Involving Light-Scattering for Measuring Size and Concentration of Condensation Particles in Supercooled Hypersonic Flow". NACA TN 2441, (August, 1951).

41. Faro, I. D.; Small, T. R.; and Hill, F. K.: "Supersaturation of Nitrogen in a Hypersonic Wind Tunnel". Journal of Applied Physics, Vol. 23, No. 1, p. 40, (January, 1952).

42. Aoyama, Shin'ich and Kanda, Eizo: "The Vapor Tensions of Oxygen and Nitrogen in the Solid State". Science Reps., Tohoku Imp. Univ. Sendai, Vol. 24, pp. 107-115, (1935).

43. Claitor, L. C. and Crawford, D. B.: "Thermodynamic Properties of Oxygen, Nitrogen, and Air at Low Temperatures". Transactions of the ASME, Vol. 71, No. 8, p. 885, (November, 1949).

44. The NBS-NACA Tables of Thermal Properties of Gases. United States Department of Commerce.

45. Dodge, B. F. and Dunbar, A. K.: "An Investigation of the Co-existing Liquid and Vapor Phases of Solutions of Oxygen and Nitrogen". J. Am. Chem. Soc. 49, pp. 591-610, (1927).

---

* A copy of this remarkable manuscript was received by the writer shortly before completion of this paper. A thorough comparison of the results has therefore not yet been made.

** Copies of these papers were received too late to include their discussion here.

APPENDIX I

PHYSICAL PROPERTIES OF OXYGEN, NITROGEN, AND AIR

No experimental data on air below $\sim 80^{\circ}K$ appear to be available at this time. Therefore, the computed vapor pressure curve of Wagner (Ref. 1) was used for the air calculations. This is based on the extrapolation formulas of Dodge and Davis and on the results of Aoyama and Kanda (Ref. 42). With an additional assumption on the vapor pressure of a mixture of liquid oxygen and nitrogen, Wagner calculates both the composition and the vapor pressures of the droplets which are in equilibrium with air. The resulting vapor pressure curve is shown in Fig. A-1.

For most of the calculations, i.e., for all of Sections II and III, constant values of L had to be used. For this purpose, Wagner's curve was matched with the integrated Clapeyron-Clausius equation at 47.5 and $75^{\circ}K$. The corresponding value of L/R is $823.64^{\circ}K$. Except for the change in droplet composition implied by Wagner's curve, air was considered throughout this paper like a single substance.

For the density of the condensed phase, ρ_L an interpolation was made between the oxygen and nitrogen curves. The interpolation is based on the calculated compositions of Wagner and approaches the pure oxygen below $\sim 40^{\circ}K$ (Cf. Fig. A-2).

The surface tension values used in the drop growth calculations are shown in Fig. A-3.

For the pure nitrogen calculations, the suggested vapor pressure curve of Ref. 42 was used, in order to make the results consistent with

those of Arthur (Ref. 26). The "suggested" curve of Aoyama and Kanda does not differ greatly from the extrapolation equation given in Ref. 44.

In connection with the droplet growth calculations, variable latent heats were used. The values taken apply to the liquid phase of nitrogen and of air. Extrapolation formulas given by Claitor and Crawford (Ref. 43) were used, which are based on the results of Dodge and Dunbar (Ref. 45).

TABLE I

COMPARISON OF "DRY" ISENTROPIC, EQUILIBRIUM SATURATED EXPANSION, AND INSTANTANEOUS COLLAPSE RESULTS

At Given Area Ratios, for the 1" x 1" Nitrogen Tunnel

Area Ratio	Condensation Free Isentropic Flow				Equilibrium Saturated Expansion*				Condensation Shock*		
A/A*	p/p_o	T °K	p_o'/p_o	x Run 23-1 Inches	p/p_o	T °K	p_o'/p_o	g	p/p_o	T °K	g
	T_o = 290°K				T_o = 290°K L/R = 844.87°K p_o = 8.30 atm T_s = 56.7°K				T_o = 290°K T_s = 56.7°K p_o = 8.30 atm. L/R = 844.87°K		
24.1	.00199	49.1	.0639	1.52	.00213	55.0	.0641	.023	.00219	55.1	.019
30.7	.00140	44.4	.0506	2.04	.00160	54.0	.0507	.036	.00166	54.1	.030
39.6	.000970	39.9	.0395	2.68	.00119	53.0	.0397	.050	.00125	53.2	.042
51.6	.000660	35.8	.0305	3.60	.000877	52.0	.0307	.064	.000919	52.2	.051
68.1	.000443	31.9	.0233	4.94	.000637	51.0	.0235	.077	.000677	51.2	.061
90.8	.000294	28.4	.0176	--	.000457	50.0	.0177	.091	.000490	50.2	.066

* Based on Vapor Pressures of Aoyama and Kanda (Refs. 16 and 42).

TABLE II

RESULTS OF THEORETICAL COLLAPSE ESTIMATES

For CO_2 Nuclei in Nitrogen, 1" x 1" Nozzle

P_o = 8.33 atm., T_o = 290°K

Impurity, By Weight ε		$\varepsilon = 10^{-5}$		$\varepsilon = 10^{-4}$		$\varepsilon = 10^{-3}$ Uncorrected		$\varepsilon = 10^{-3}$ Corrected	
Criterion Used		η =.5	η =.8	η =.5	η =.8	η =.5	η =.8	η =.5	η =.8
Most Effective Radius	r_o**.10^7 cm	.66	.57	.89	.78	1.2	1.06	1.38	1.14
Collapse Point	x** η =.5 cm η =.8	12.1 --	-- 14.9	8.54 --	-- 9.90	6.70 --	-- 7.47	6.18 --	-- 7.04
Departure Point	x^+ cm	6.2	7.3	4.9	5.3	4.1	4.4	3.8	4.2
	$C_\nu \cdot 10^{-5}$	2.70	3.15	4.35	5.0	7.0	7.8	4.75	6.6
Number of Nuclei per Unit Mass of Vapor	$\nu_{gm^{-1}} \cdot 10^{-16}$	.54	.82	2.2	3.3	9.1	12.6	2.9	7.7

SATURATION POINT CHART

FOR ISENTROPIC EXPANSION OF AIR BASED ON $\gamma = 1.40$ AND THE VAPOR PRESSURES CALCULATED BY CARL WAGNER

P_s (ATM.)

20 — 10 — 5 — 1 — 10^{-1} — 10^{-2} — 10^{-3} — 10^{-4} — 10^{-5} — 10^{-6}

T_v (°K.)

120 110 100 90 80 70 60 50 40 30 20 10 0

P_o = 200 ATM.
P_o = 100 ATM.
P_o = 50 ATM.
P_o = 20 ATM.
P_o = 10 ATM.
P_o = 5 ATM.
P_o = 2 ATM.
P_o = 1 ATM.
P_o = 0.5 ATM.
P_o = 0.2 ATM.
P_o = 0.1 ATM.

M = 0
M = 1
M = 2
M = 3
M = 4
M = 5
M = 6
M = 7
M = 8
M = 9
M = 10

0 100 200 300 400 500 600 700 800

T_o (°K.)

FIG II-1

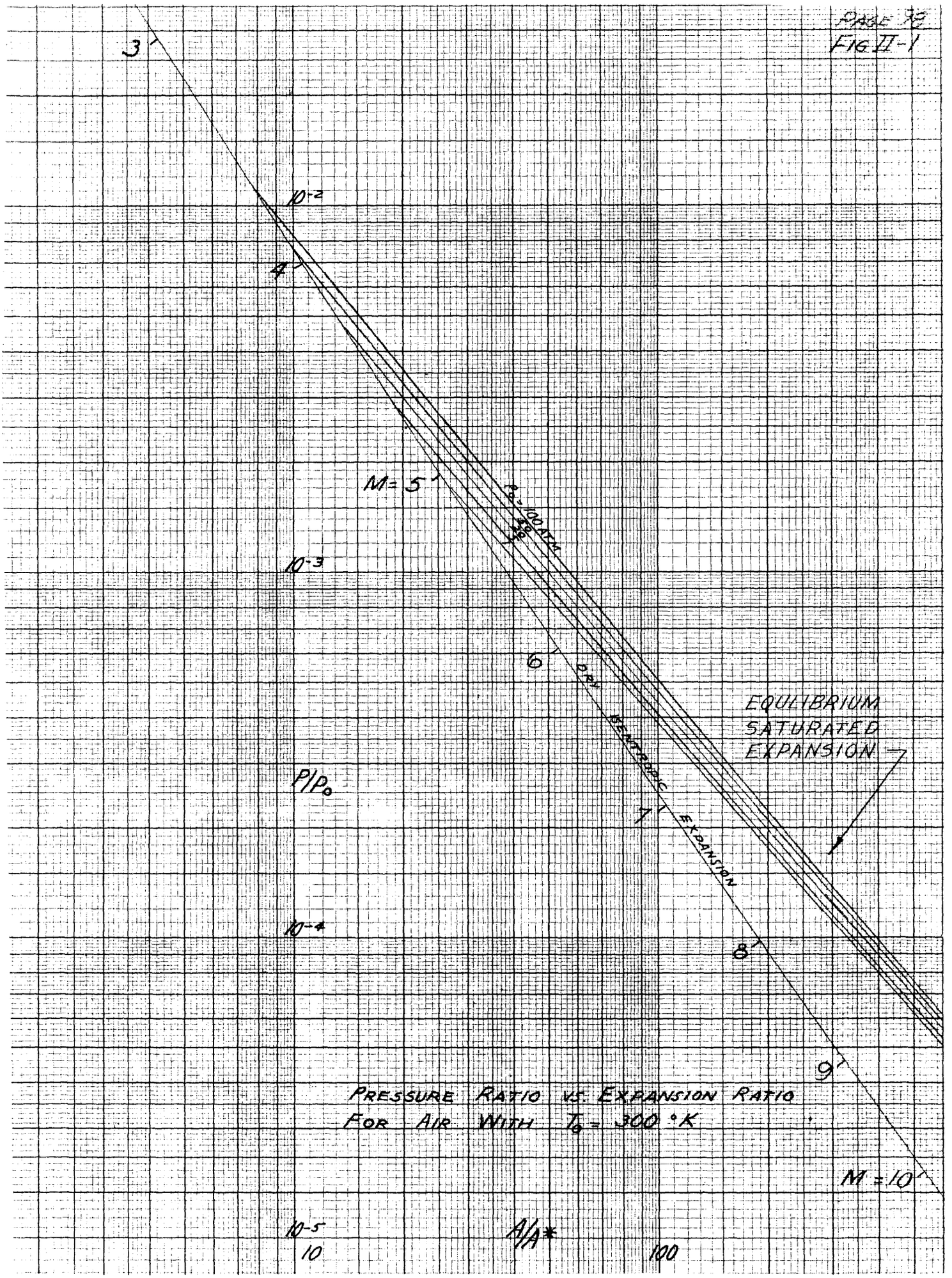

PRESSURE RATIO VS. EXPANSION RATIO
FOR AIR WITH T_0 = 300 °K

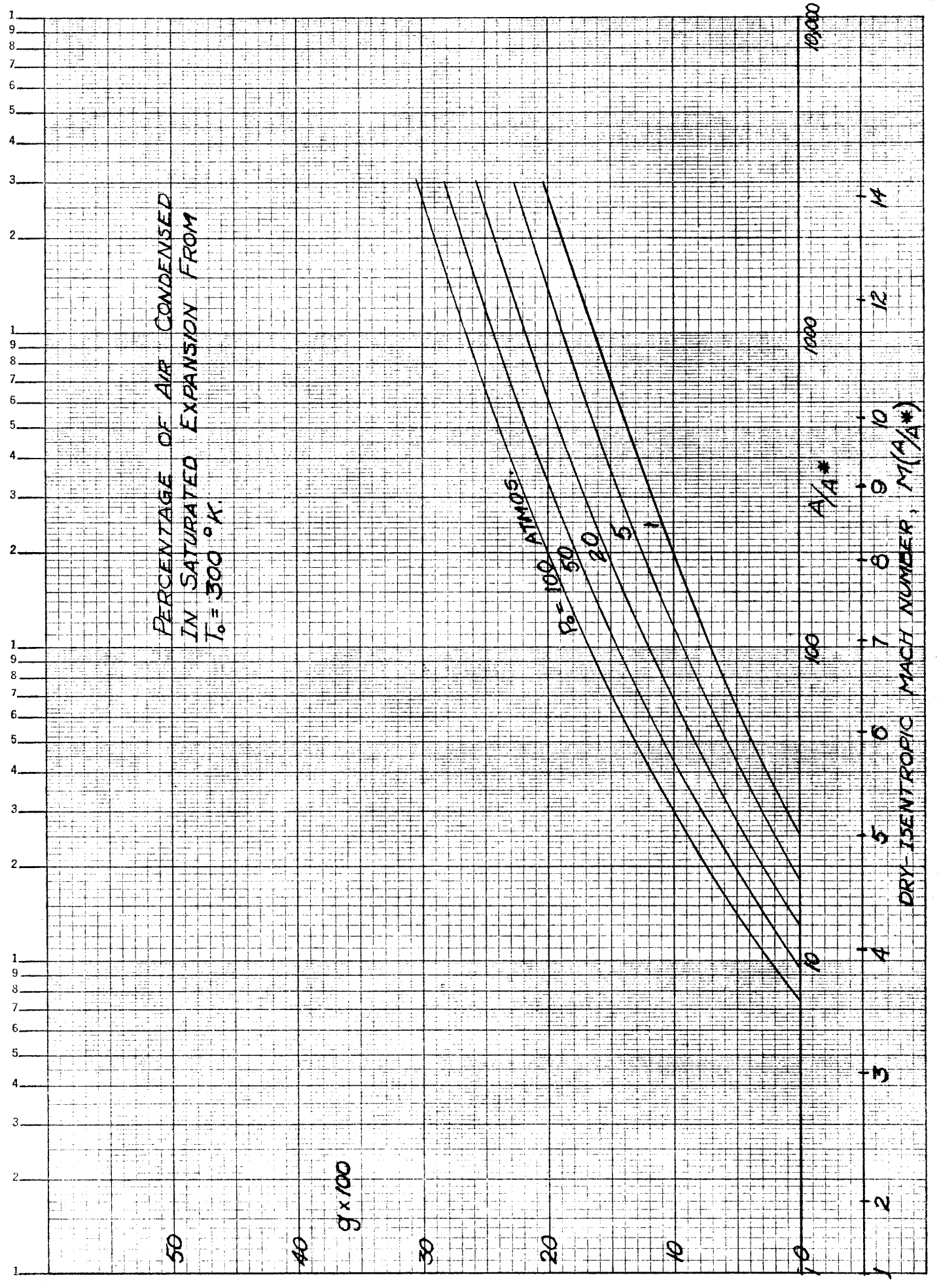
PERCENTAGE OF AIR CONDENSED IN SATURATED EXPANSION FROM T_o = 300 °K.
p_o = 100 ATMOS.
50
20
5
1
g x 100
50
40
30
20
10
0
A/A*
10,000
1000
100
10
DRY-ISENTROPIC MACH NUMBER, M(A/A*)
14
12
10
9
8
7
6
5
4
3
2
1

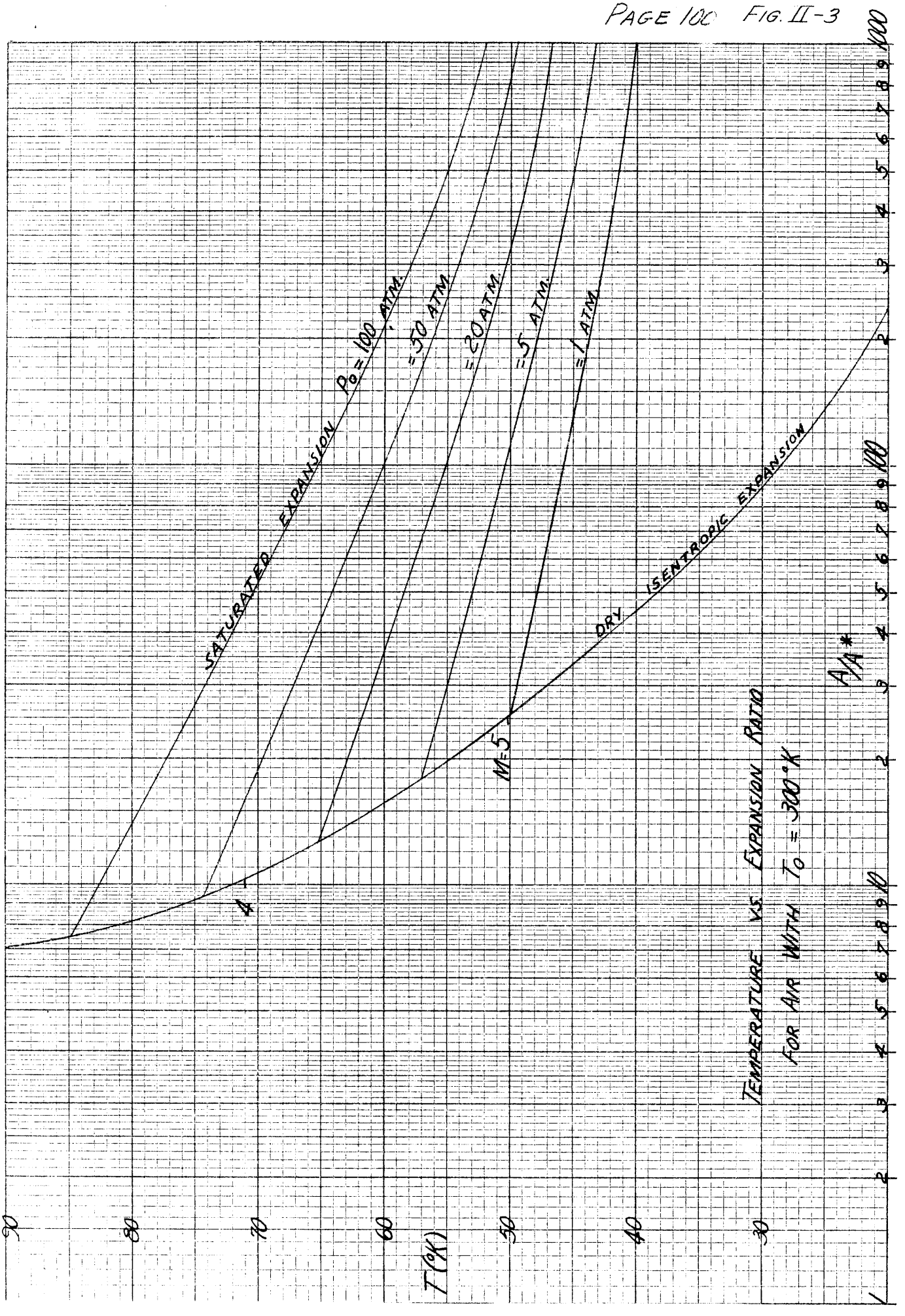
SATURATED EXPANSION P_0 = 100 ATM.
= 50 ATM.
= 20 ATM.
= 5 ATM.
= 1 ATM.
DRY ISENTROPIC EXPANSION
M=5
4
T(°K)
A/A*
TEMPERATURE VS EXPANSION RATIO
FOR AIR WITH T_0 = 300 °K

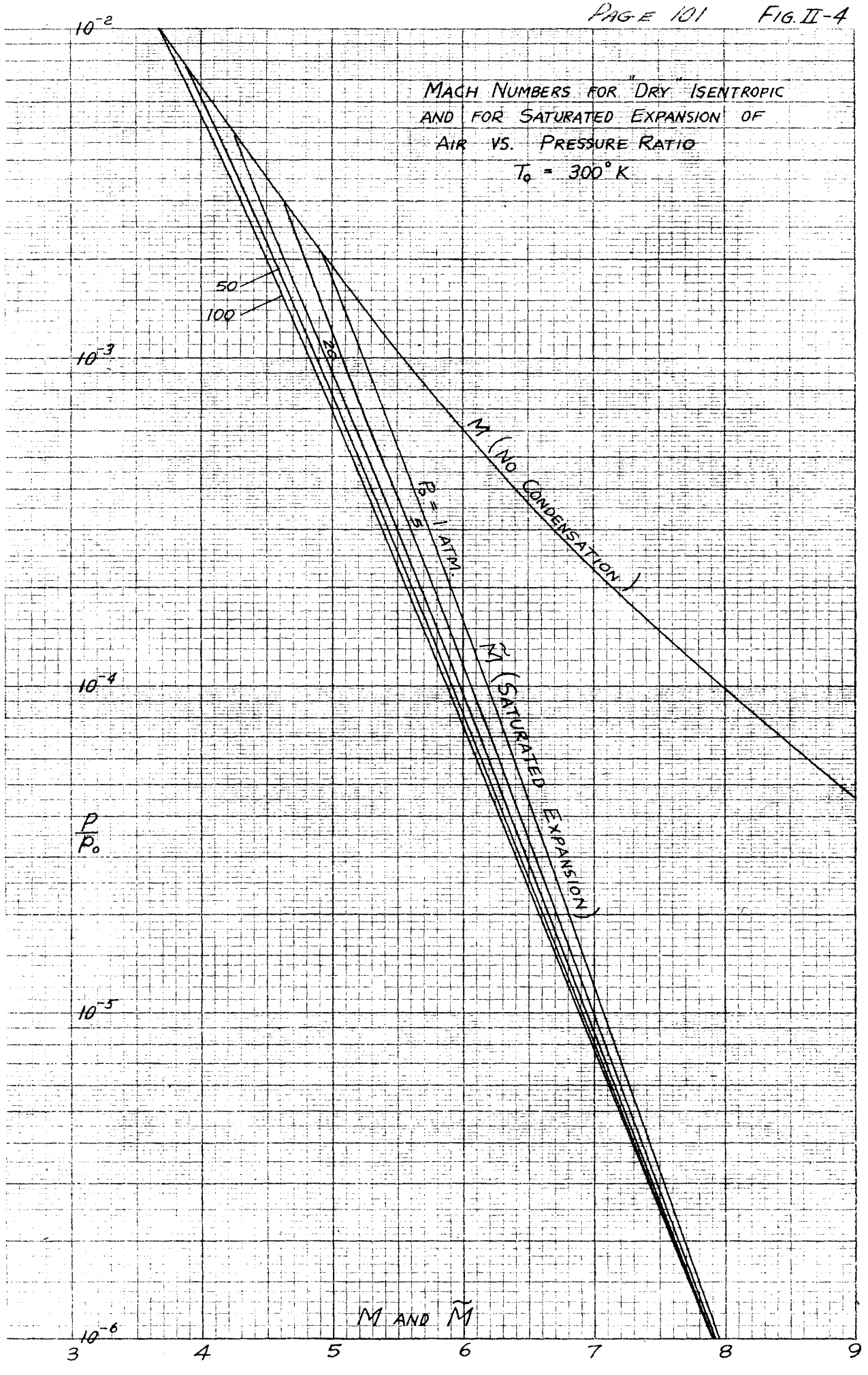
MACH NUMBERS FOR "DRY" ISENTROPIC AND FOR SATURATED EXPANSION OF AIR VS. PRESSURE RATIO
$T_0 = 300°K$
10^{-2}
10^{-3}
10^{-4}
10^{-5}
10^{-6}
$\frac{P}{P_0}$
50
100
20
5
P_0 = 1 ATM.
M (NO CONDENSATION)
$\tilde{M}$ (SATURATED EXPANSION)
3
4
5
6
7
8
9
M AND $\tilde{M}$

$\frac{\mathring{M}}{\tilde{M}}$ VS. EXPANSION RATIO
SATURATED EXPANSION OF AIR
$T_o = 300°K$

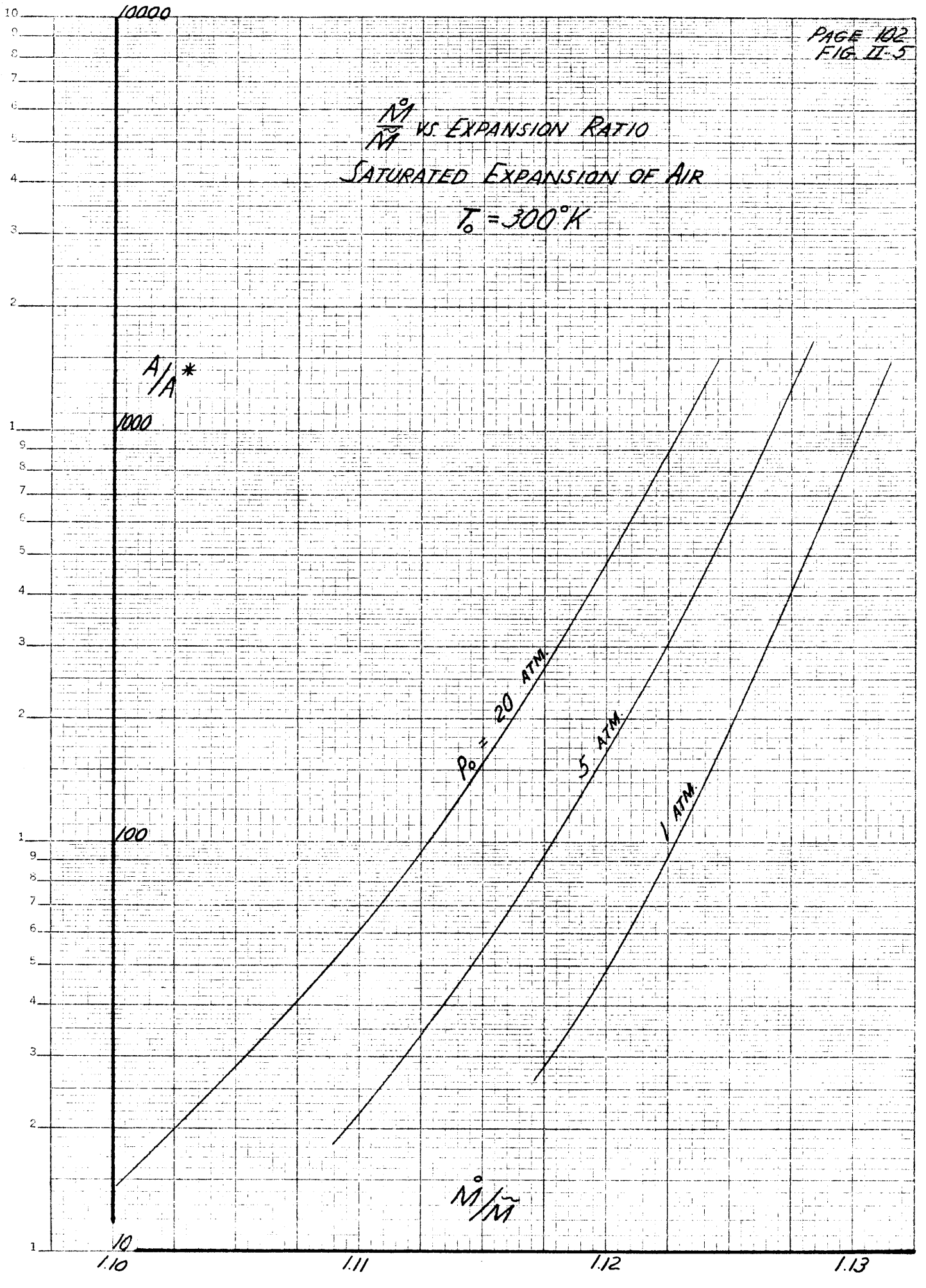

$\tilde{M}_{N_2}$, NORMAL MACH NUMBER AHEAD OF SHOCK VS. M_{N_3}, NORMAL MACH NUMBER BEHIND SHOCK.

SHOCK INVARIANT $\tilde{\phi}(\tilde{M}_N, E)$

$\tilde{\phi}(\tilde{M}_N, E)$

E = 0
-1
-2
-3
-4
-5
-6
-7
-8

.10 .20 .30 .40 .50 .60 .70 .80 .90 1.0

M_{N_3}

1.0 1.5 2.0 2.5 3.0 3.5 4.0

$\tilde{M}_{N_2}$

9-5-50

P.H.J.

FIG. III-2

EVAPORATION PARAMETER

$$E = \frac{2g_2}{1-g_2}\left(\frac{1}{\gamma-1} - \frac{L}{\mathcal{R}T_2}\right)$$

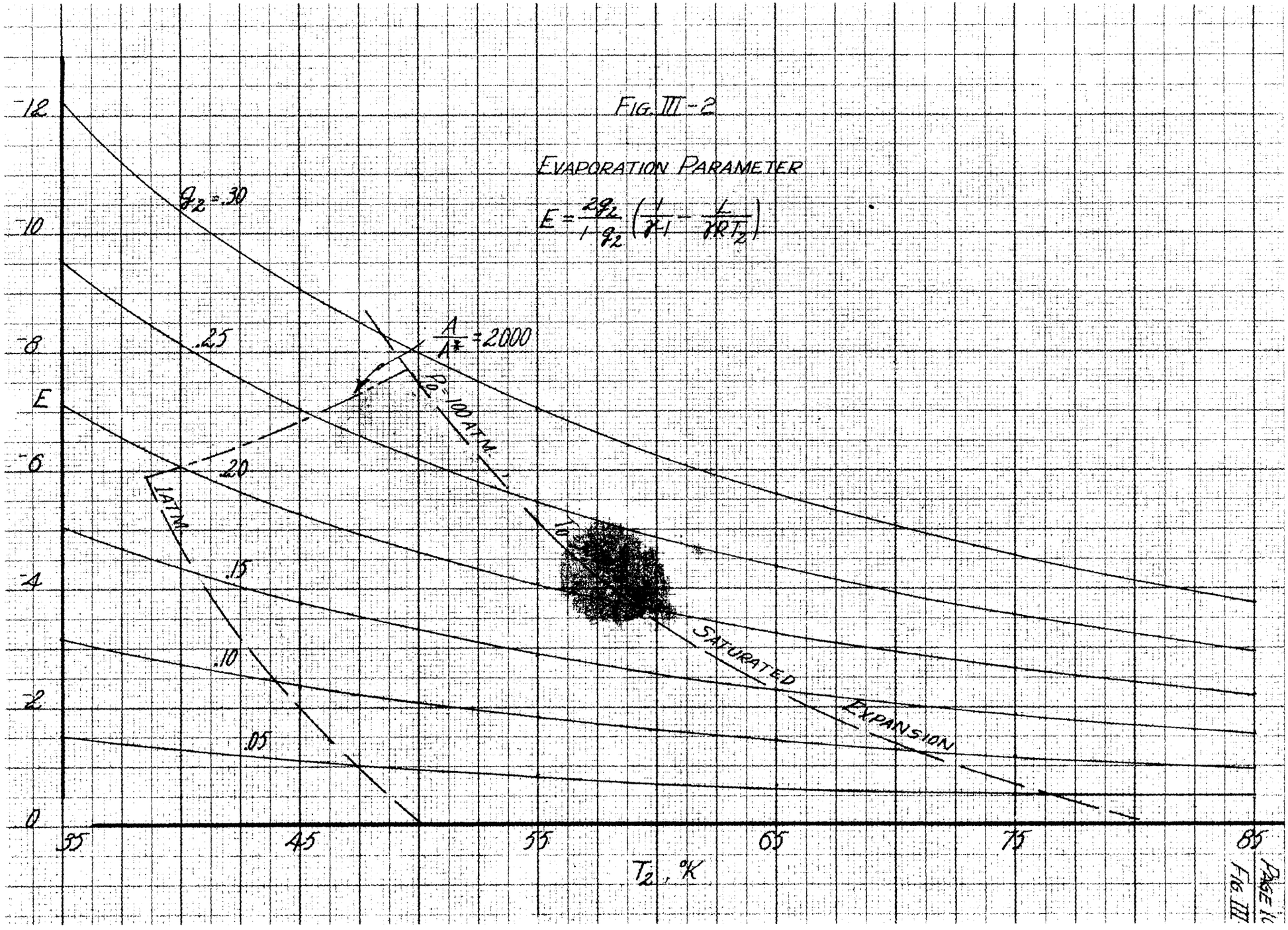

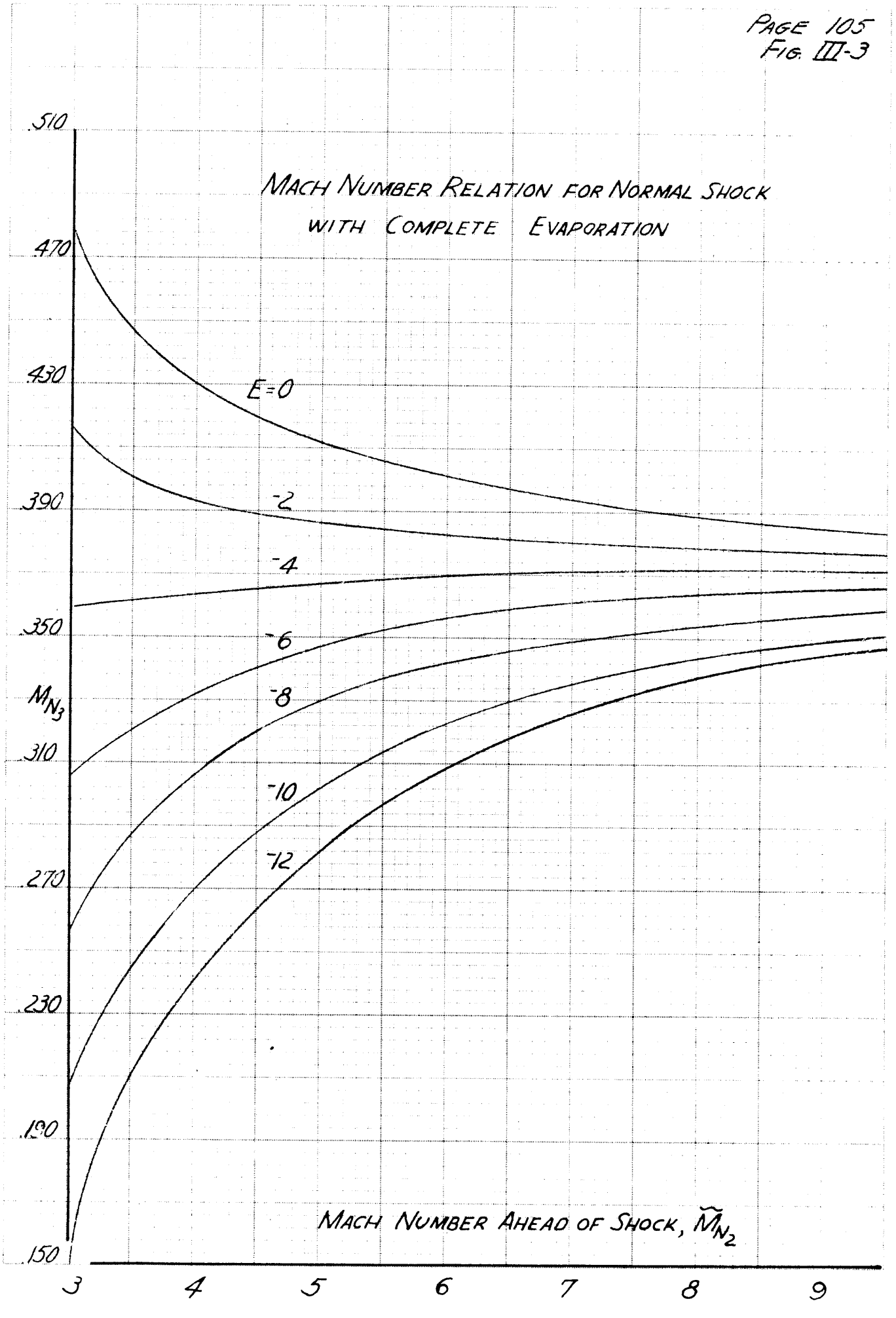
MACH NUMBER RELATION FOR NORMAL SHOCK
WITH COMPLETE EVAPORATION
.510
.470
.430
.390
.350
.310
.270
.230
.190
.150
M_{N_3}
E=0
-2
-4
-6
-8
-10
-12
3
4
5
6
7
8
9
MACH NUMBER AHEAD OF SHOCK, $\tilde{M}_{N_2}$

EVAPORATION CORRECTION FACTOR FOR STATIC PRESSURE RATIO ACROSS NORMAL SHOCK

$$r\left(E, \tilde{M}_N\right) = \frac{p_3/p_2\ (E, \tilde{M}_N)}{p_3/p_2\ (0, \tilde{M}_N)}$$

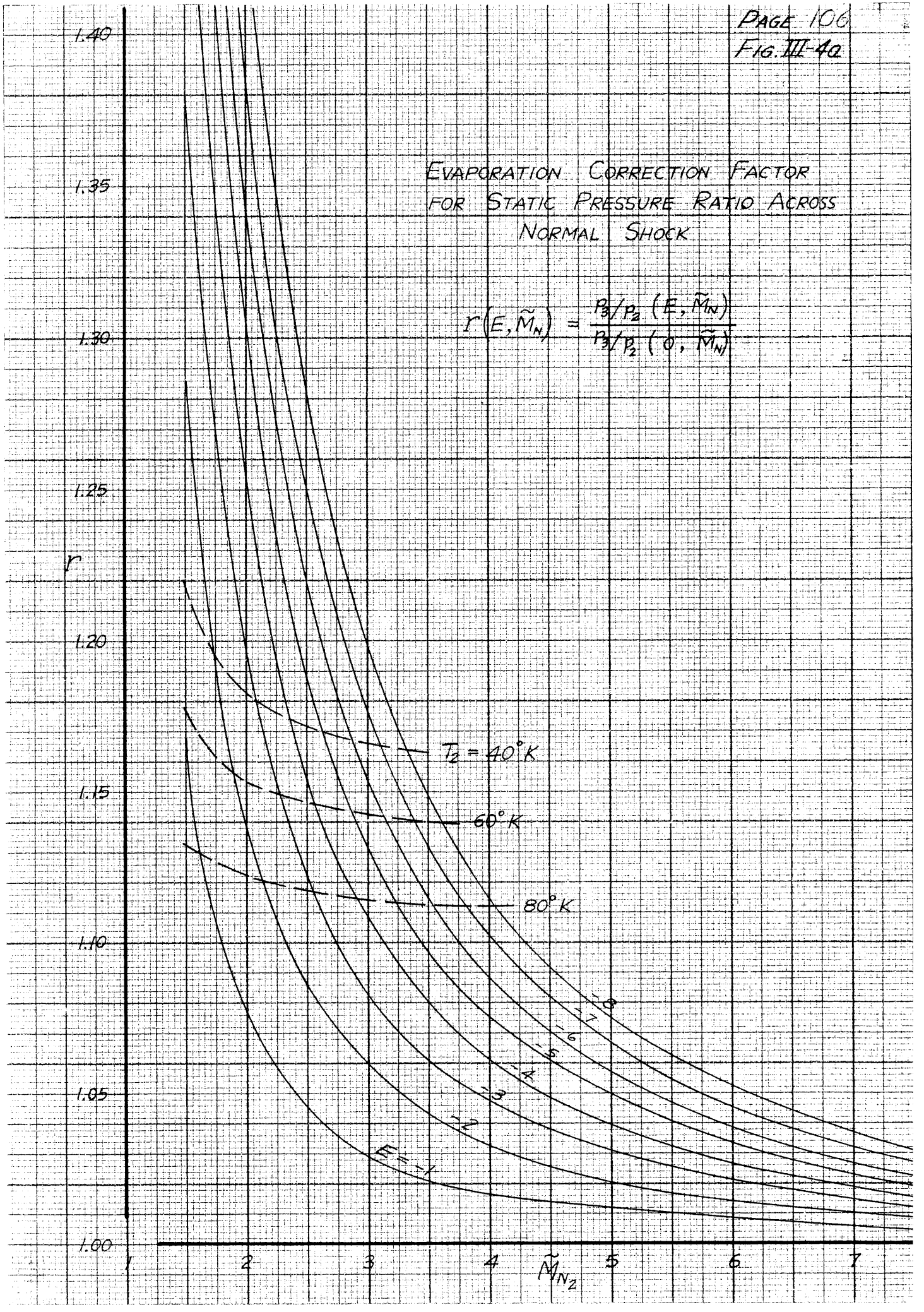

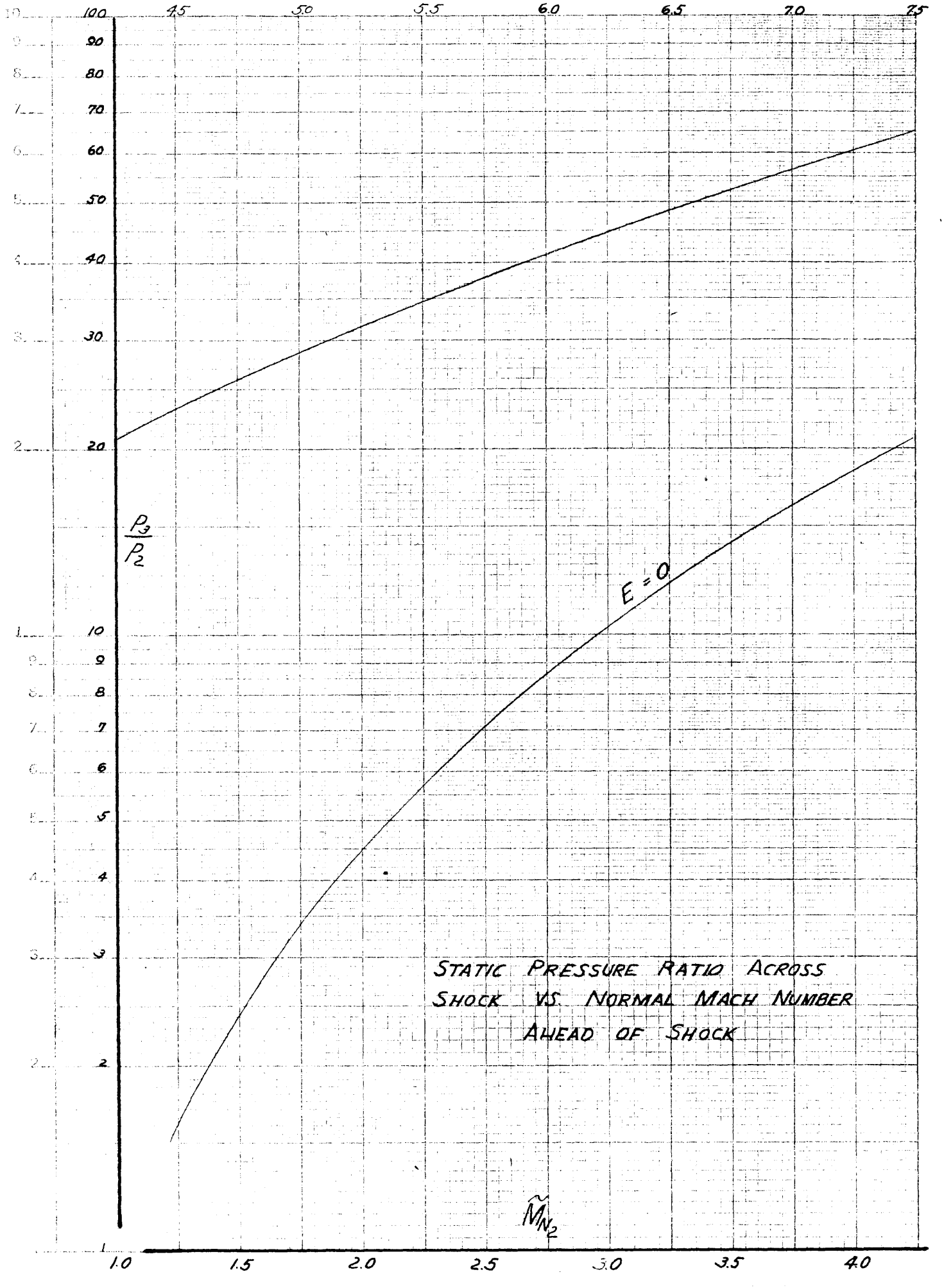
$\frac{P_3}{P_2}$
E = 0
$\tilde{M}_{N_2}$
STATIC PRESSURE RATIO ACROSS SHOCK VS. NORMAL MACH NUMBER AHEAD OF SHOCK

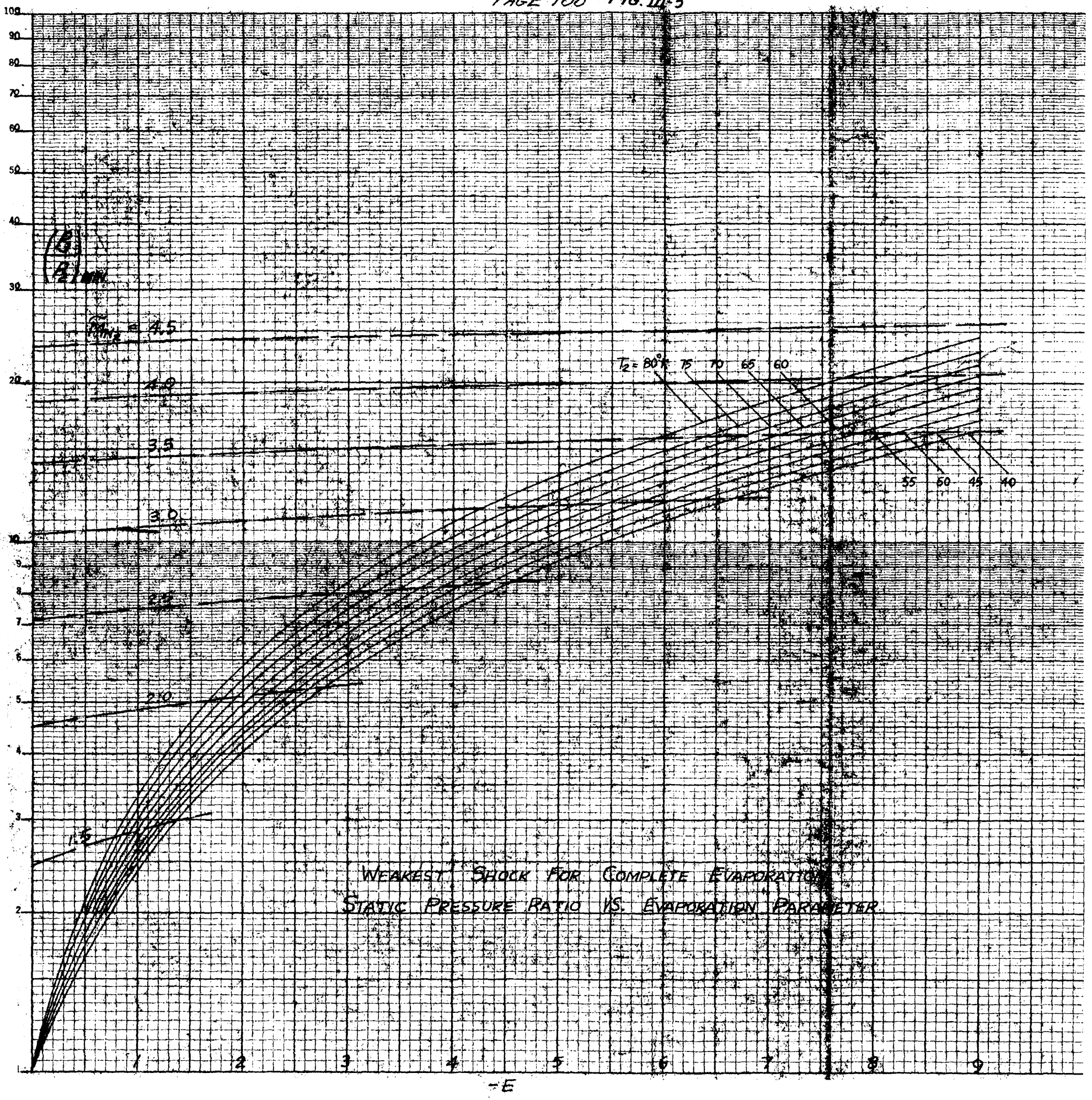

WEAKEST SHOCK FOR COMPLETE EVAPORATION
STATIC PRESSURE RATIO VS. EVAPORATION PARAMETER

FIG. III-6

STATIC PRESSURE RATIO ACROSS SHOCK, P_3/P_2 VS.
MACH NUMBER AHEAD OF SHOCK, M_2
COMPLETE EVAPORATION

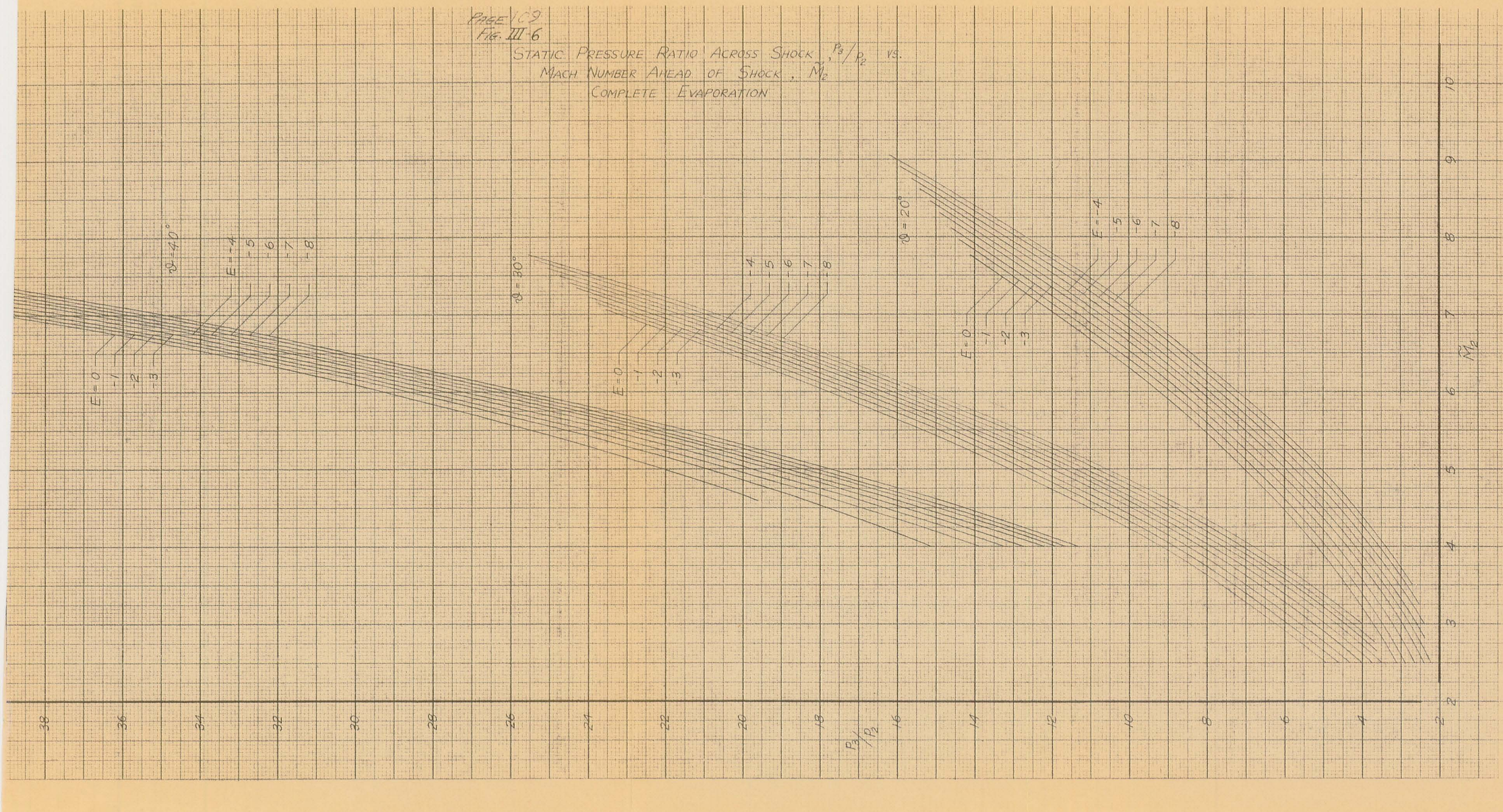

FIG. III-7

WAVE ANGLE δ VS. MACH NUMBER AHEAD OF SHOCK $\tilde{M}_2$ WITH COMPLETE EVAPORATION

$\vartheta = 30°$

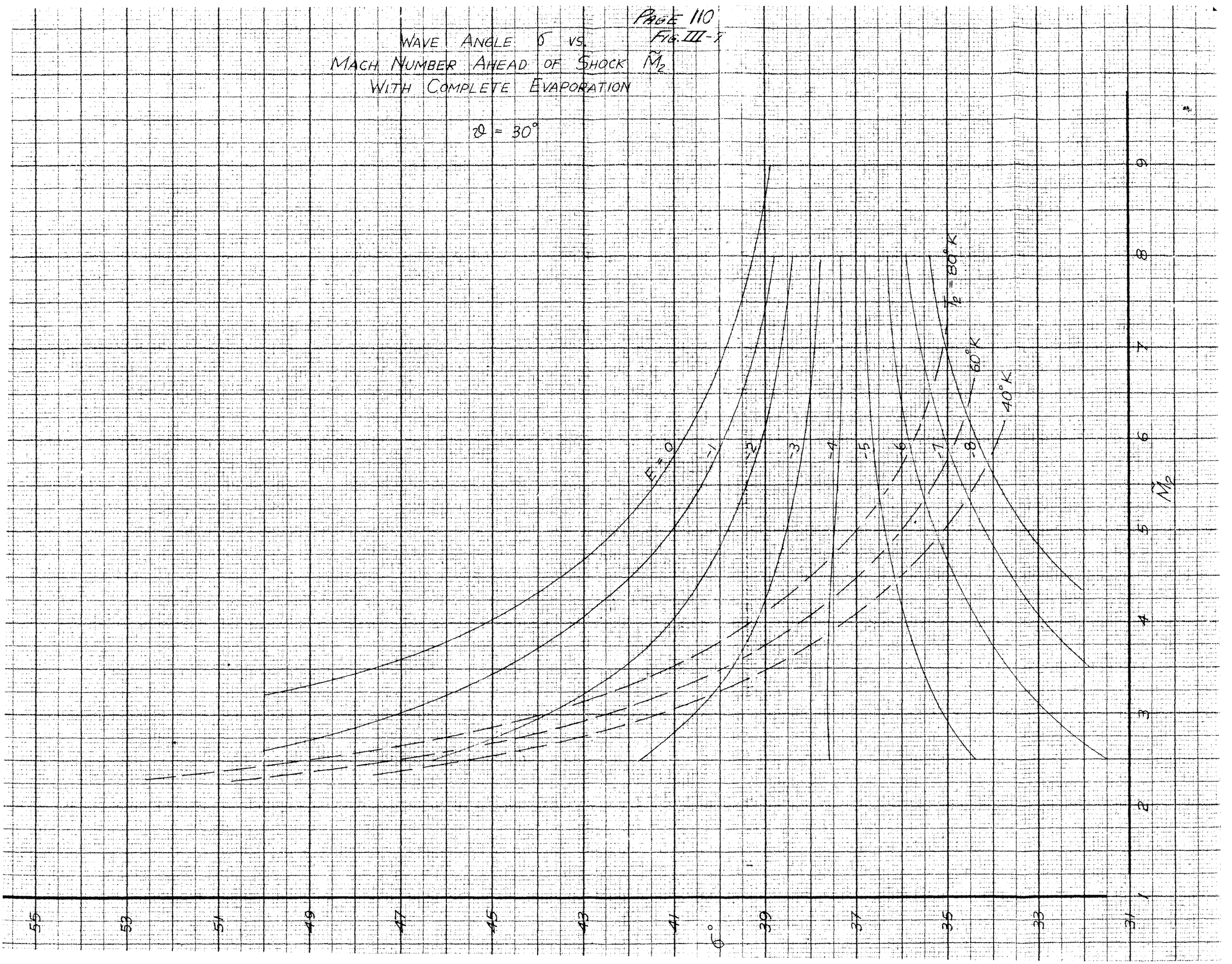

FIG III-8

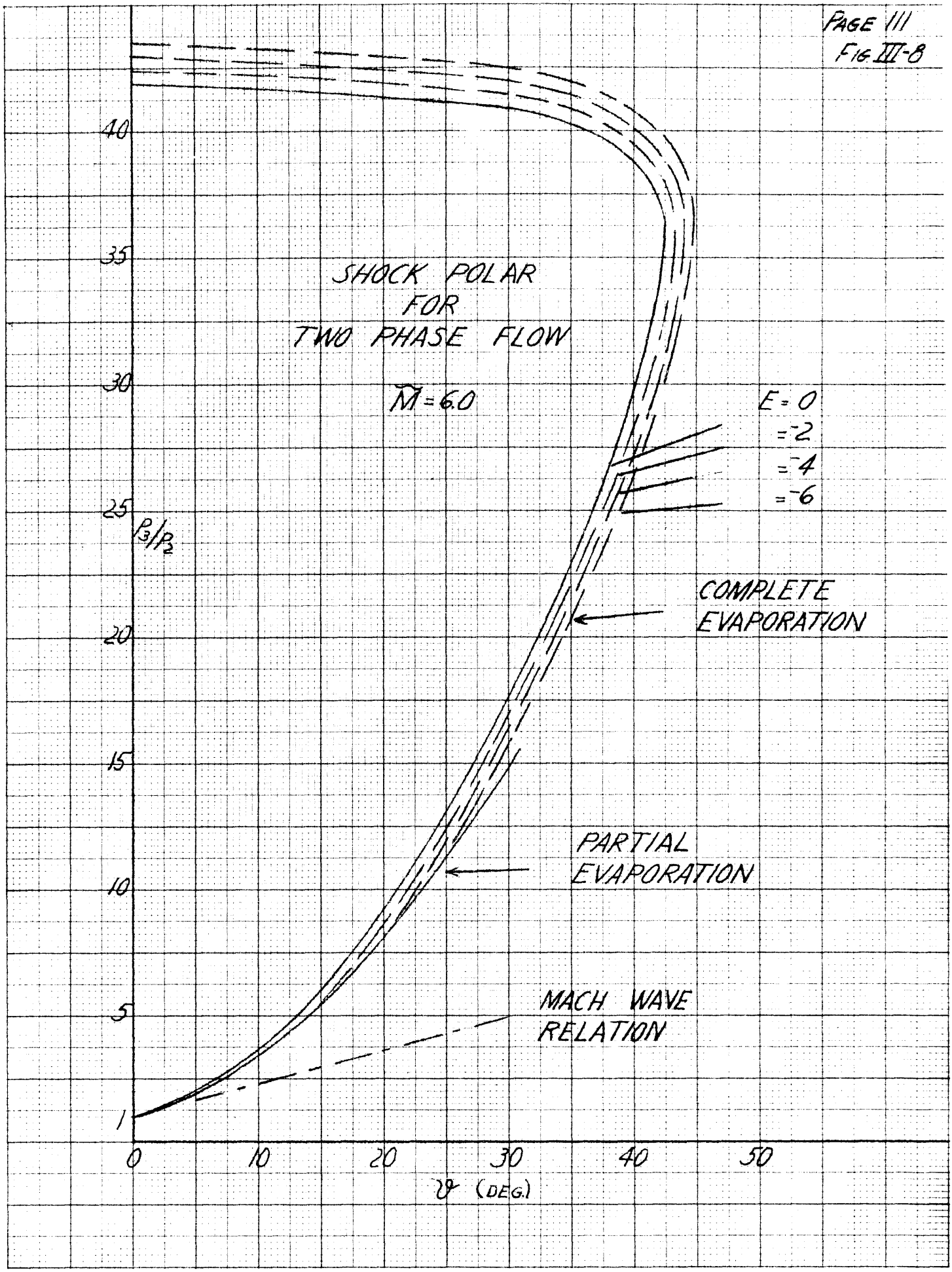
SHOCK POLAR
FOR
TWO PHASE FLOW
$\bar{M} = 6.0$
E = 0
= -2
= -4
= -6
COMPLETE
EVAPORATION
PARTIAL
EVAPORATION
MACH WAVE
RELATION
P_3/P_2
40
35
30
25
20
15
10
5
1
0
10
20
30
40
50
θ (DEG.)

FIG. III-9

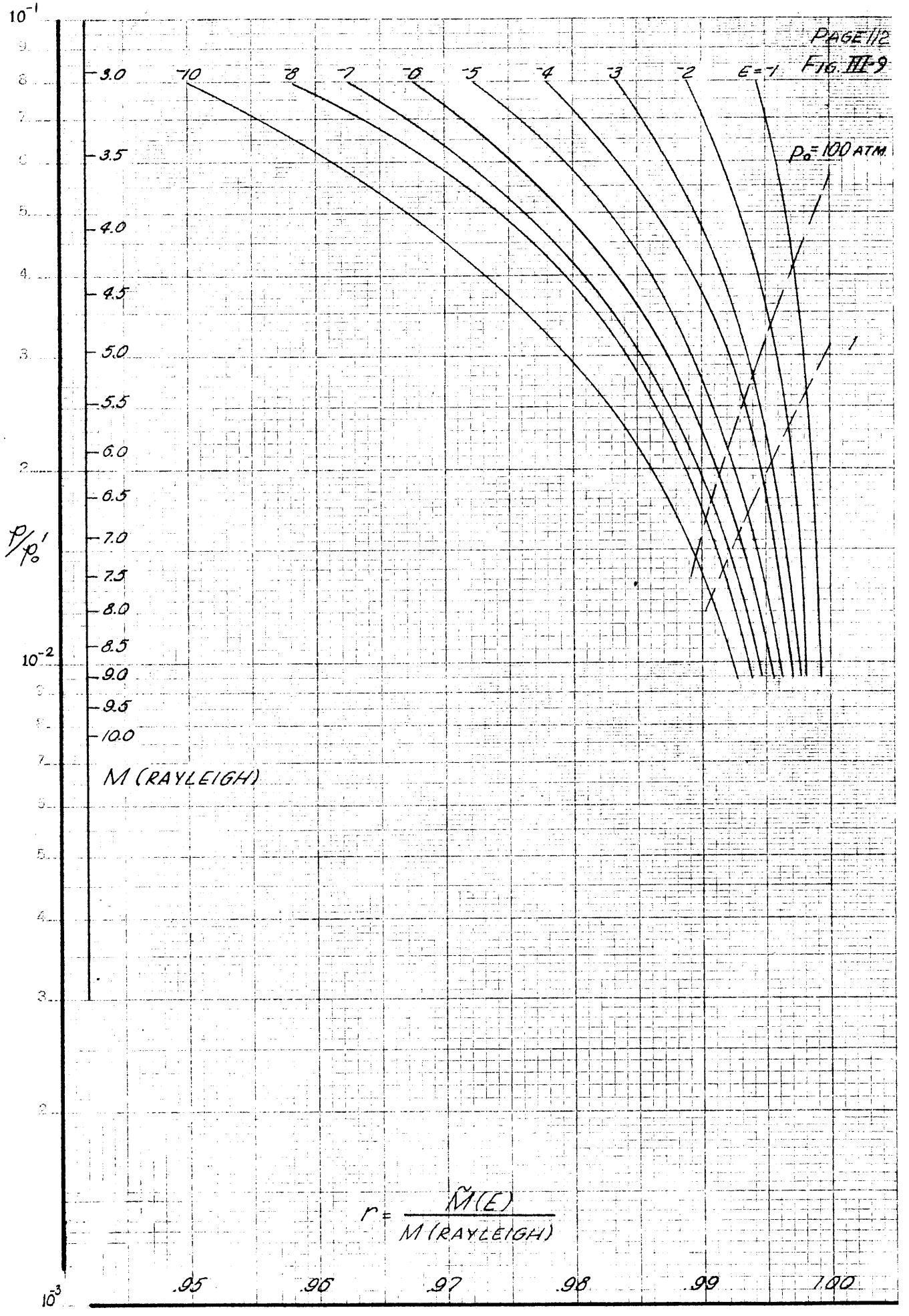
10^{-1}
9
8
7
6
5
4
3
2
10^{-2}
9
8
7
6
5
4
3
2
10^{-3}
3.0
3.5
4.0
4.5
5.0
5.5
6.0
6.5
7.0
7.5
8.0
8.5
9.0
9.5
10.0
M (RAYLEIGH)
P/P₀'
-10
-8
-7
-6
-5
-4
-3
-2
E=-1
P₀=100 ATM.
1
.95
.96
.97
.98
.99
1.00
r = M̃(E) / M (RAYLEIGH)

FIGURE III-10

STATIC-PITOT PRESSURE RATIO VS. PITOT-STAGNATION PRESSURE RATIO

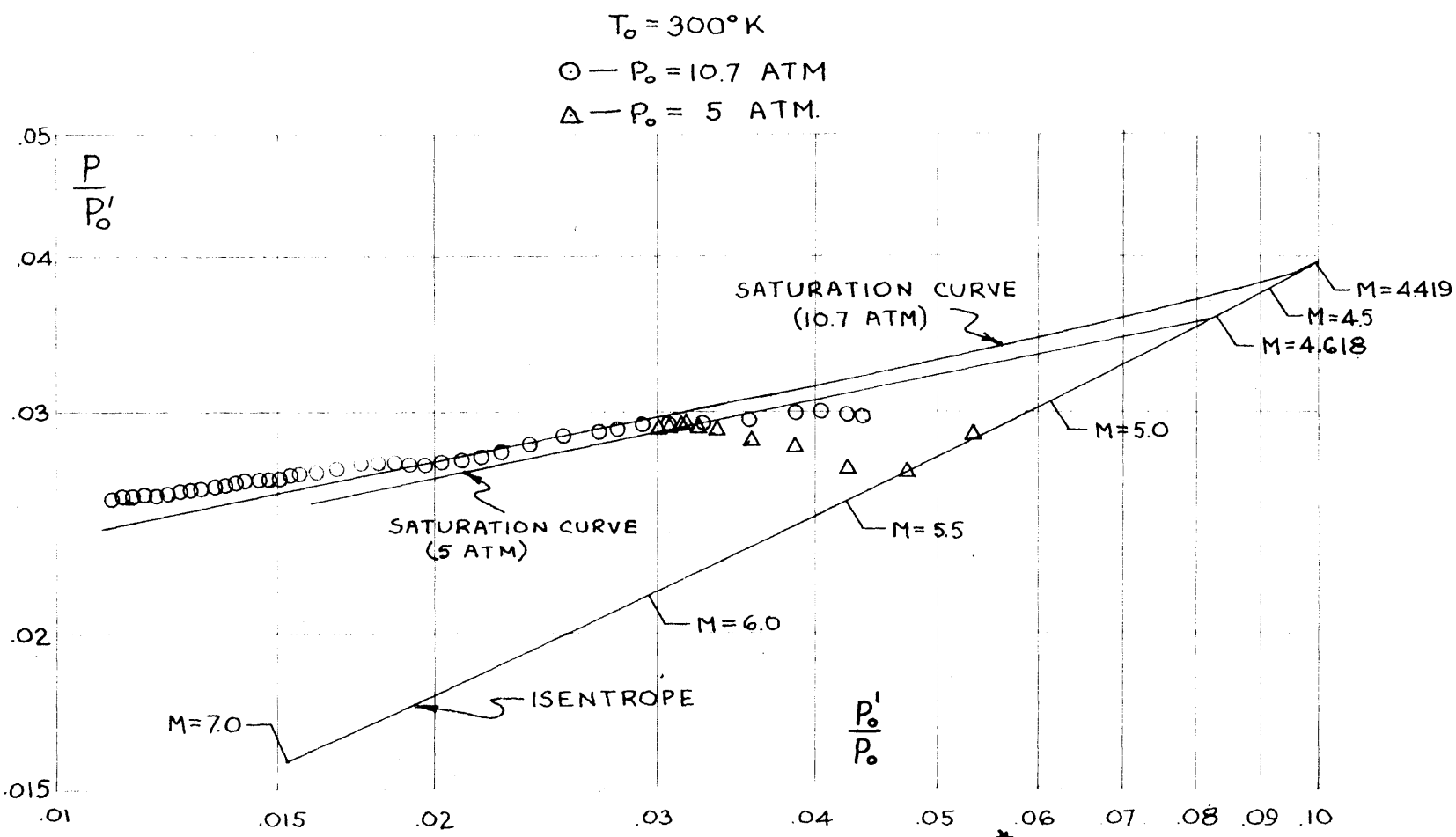

COMPARISON OF SATURATED EXPANSION WITH DATA* FOR AIR

5X5 INCH TUNNEL

* GREY AND NAGAMATSU, REF. 17

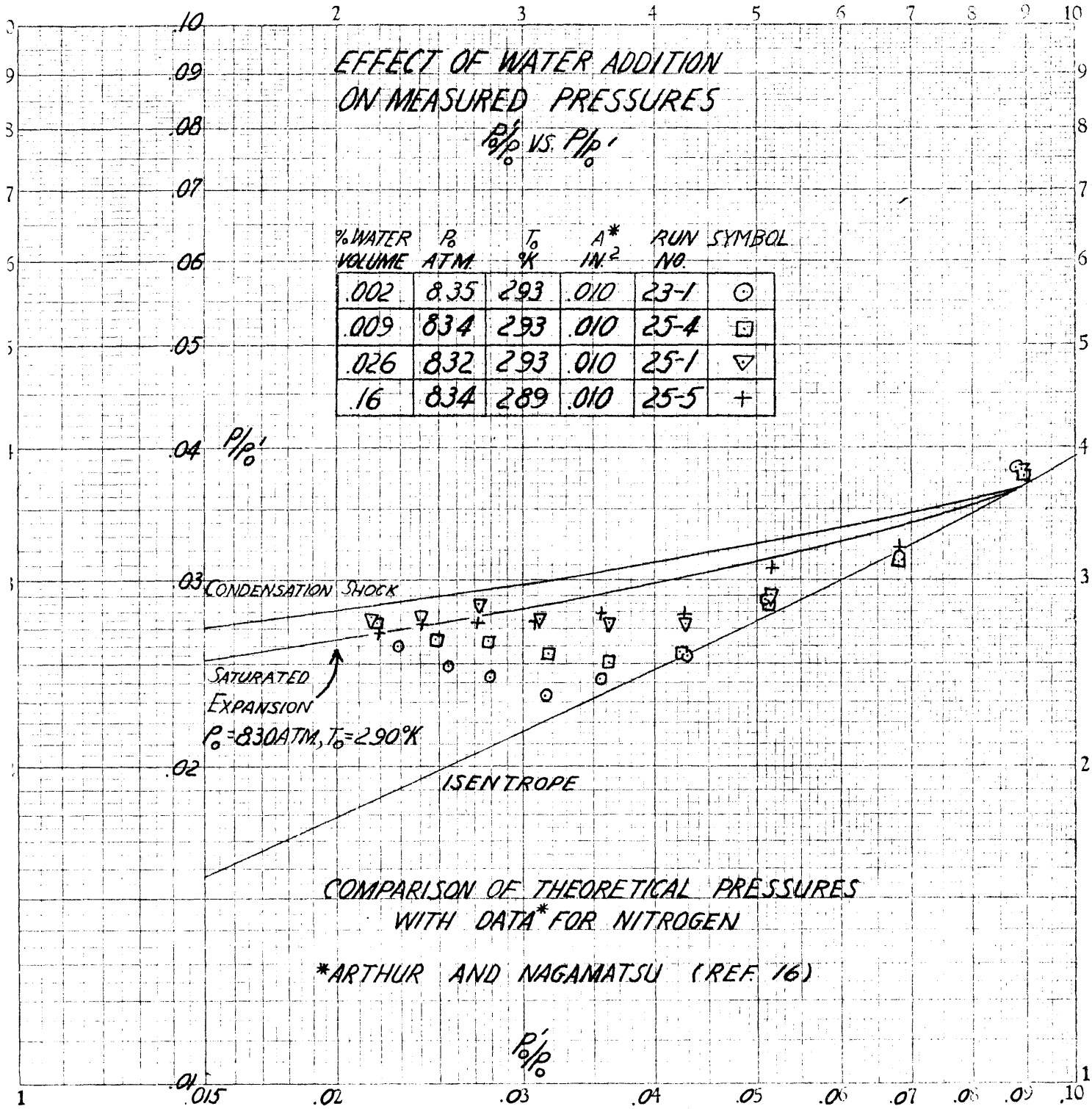

COMPARISON OF THEORETICAL PRESSURES WITH DATA* FOR NITROGEN

*ARTHUR AND NAGAMATSU (REF. 16)

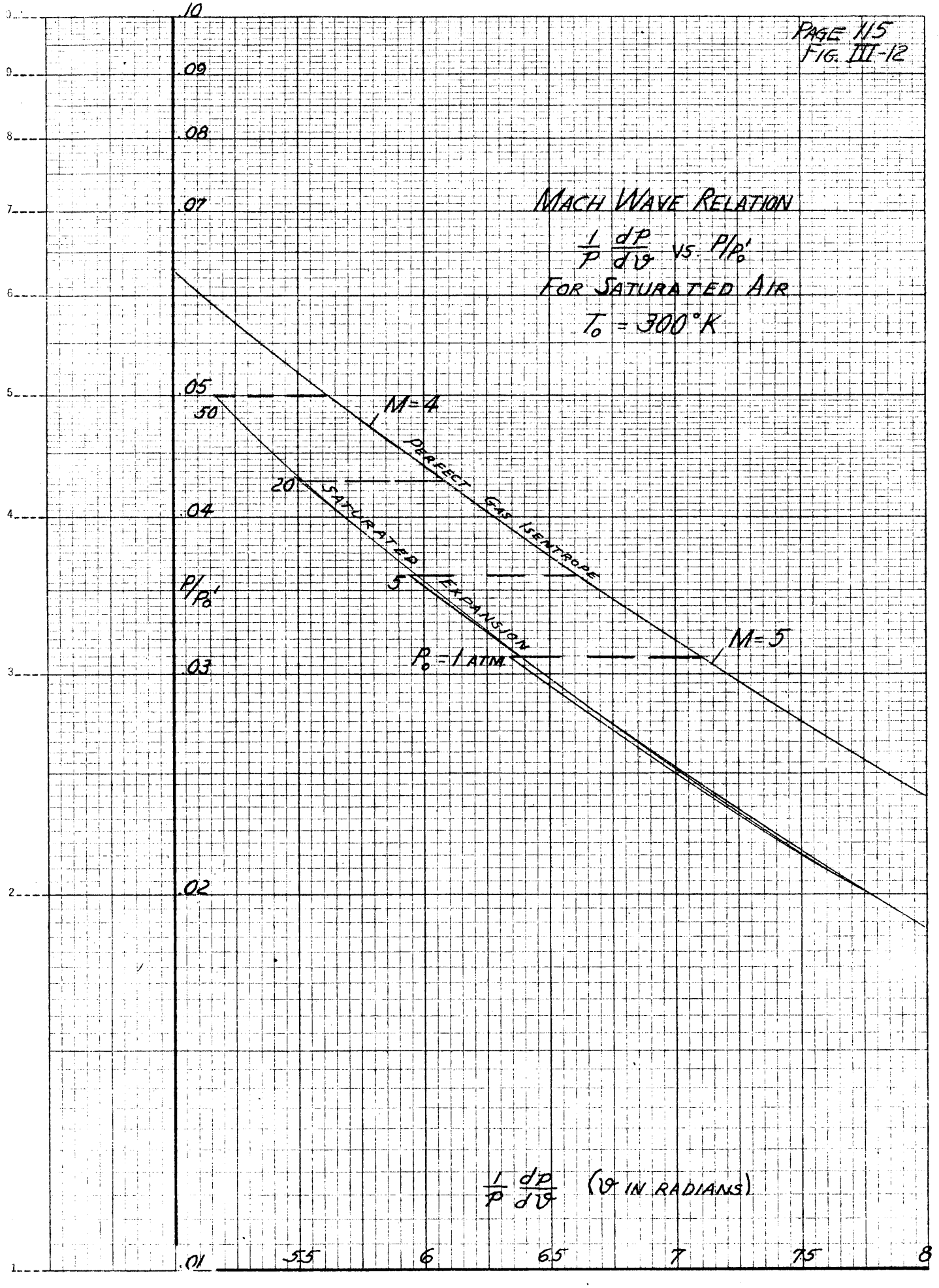
MACH WAVE RELATION
$\frac{1}{P}\frac{dP}{d\vartheta}$ VS P/P_0'
FOR SATURATED AIR
$T_0 = 300°K$
M=4
M=5
PERFECT GAS ISENTROPE
SATURATED EXPANSION
$P_0 = 1$ ATM
P/P_0'
$\frac{1}{P}\frac{dP}{d\vartheta}$ (ϑ IN RADIANS)
10
09
08
07
05
30
20
04
03
02
01
5
55
6
65
7
75
8

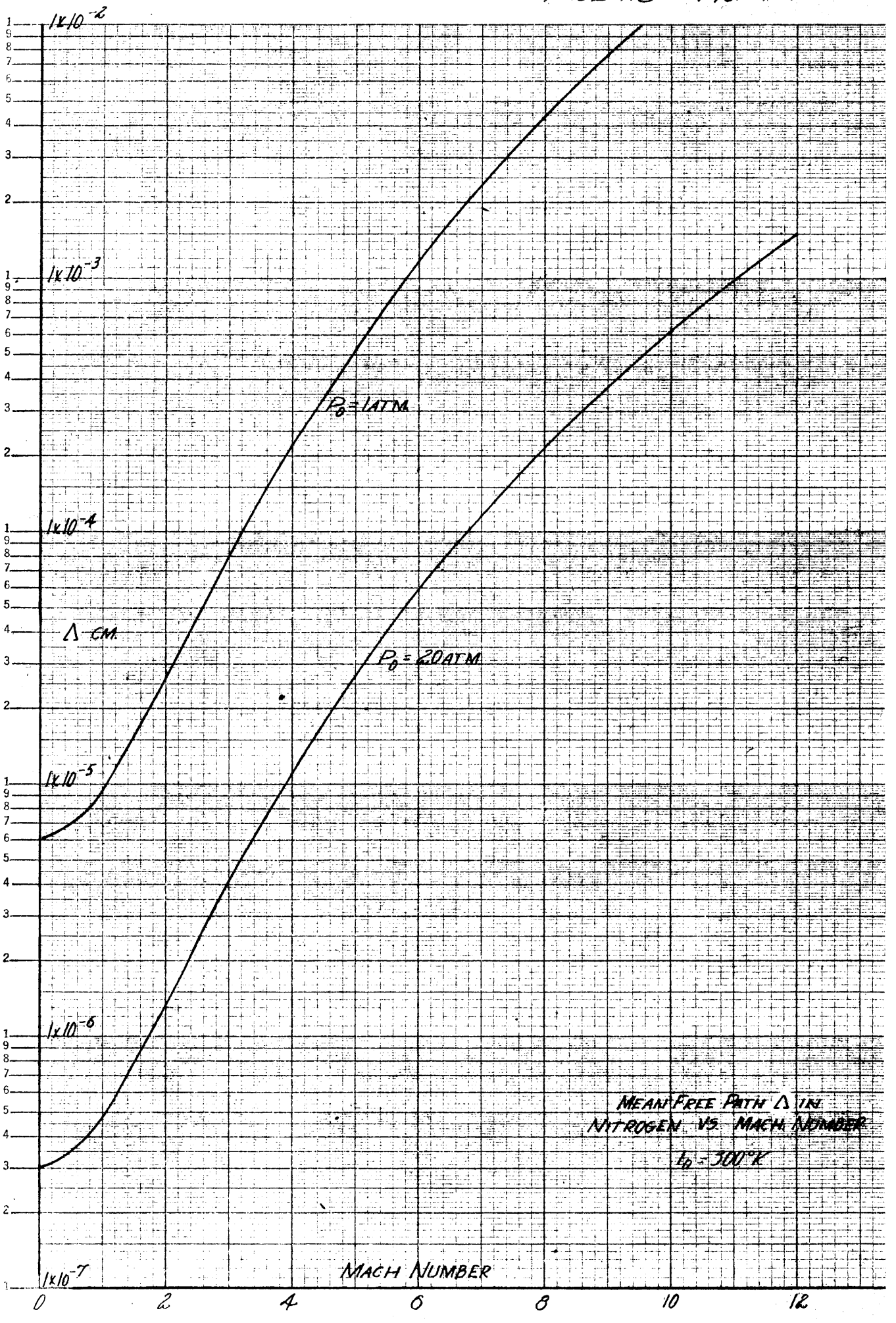

Semi-Logarithmic, 5 Cycles X 10 to the inch, 5th lines accented.
MADE IN U. S. A.

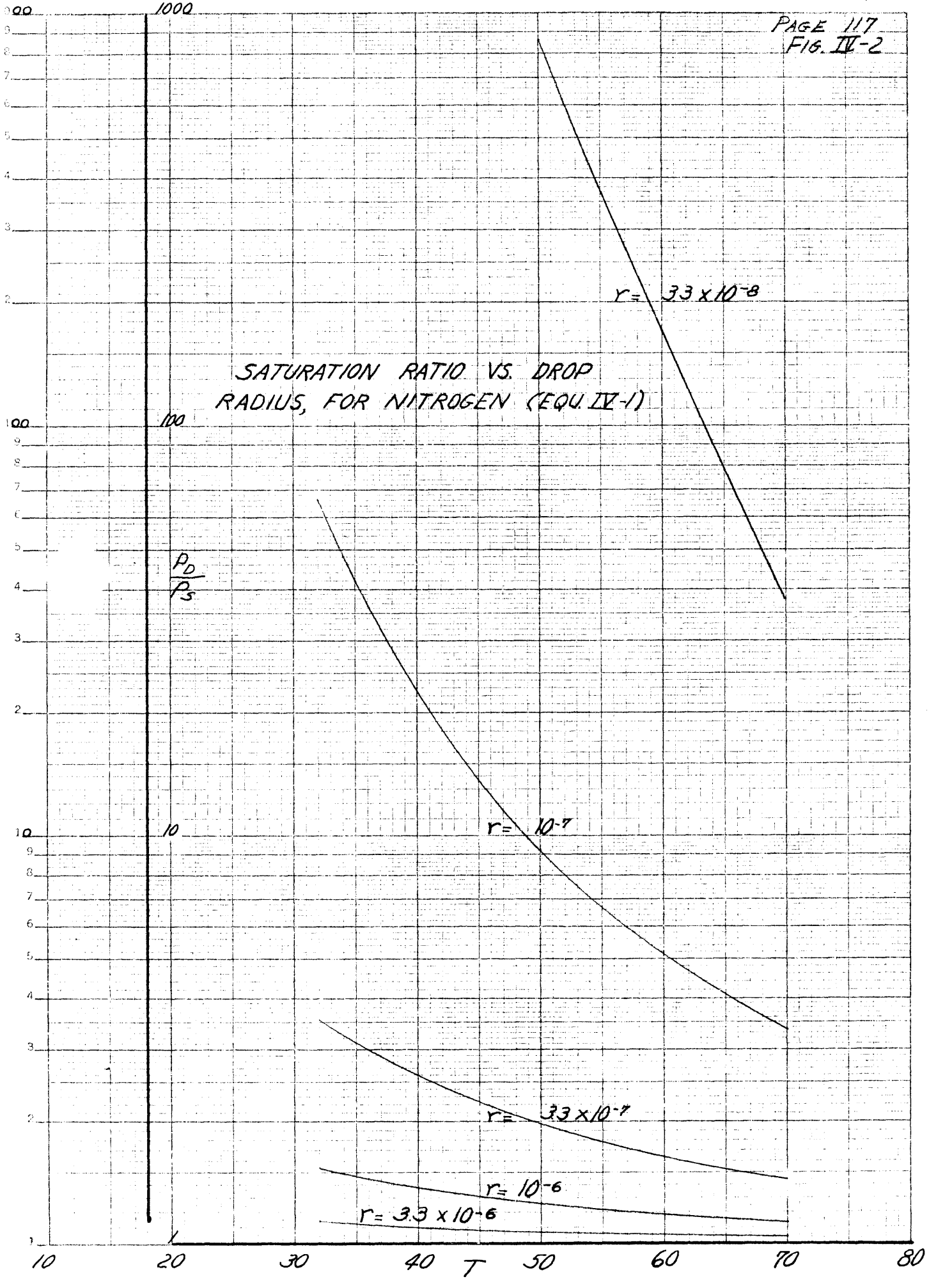
SATURATION RATIO VS. DROP RADIUS, FOR NITROGEN (EQU. IV-1)
$\frac{P_D}{P_S}$
r= 3.3 x 10⁻⁸
r= 10⁻⁷
r= 3.3 x 10⁻⁷
r= 10⁻⁶
r= 3.3 x 10⁻⁶
1000
100
10
1
10
20
30
40
T
50
60
70
80

PAGE 116
FIG. IV-3

SOLUTION OF EQUATION IV-13
FOR QUASI-STEADY EQUILIBRIUM
TEMPERATURE OF NITROGEN

$P_0 = 20$ ATM.

$M = 4.3$
$M = 4.5$
$M = 4.7$
$M = 5.0$
$M = 5.5$
$M = 6.0$
$M = 7.0$
$M = 9.0$
$M = 11.0$

$\tau = 10^{-7}$ CM.
$\tau = 3.3 \times 10^{-7}$ CM.
$\tau = 10^{-6}$ CM.
$\tau = 10^{-5}$ CM.

$\frac{P}{\sqrt{T}}$ P IN ATM.
T IN °K

QUASI-STEADY EQUILIBRIUM TEMPERATURE, T_E ~ °K

SOLUTION OF EQUATION IV-13

$\frac{P_E}{\sqrt{T_E}}$

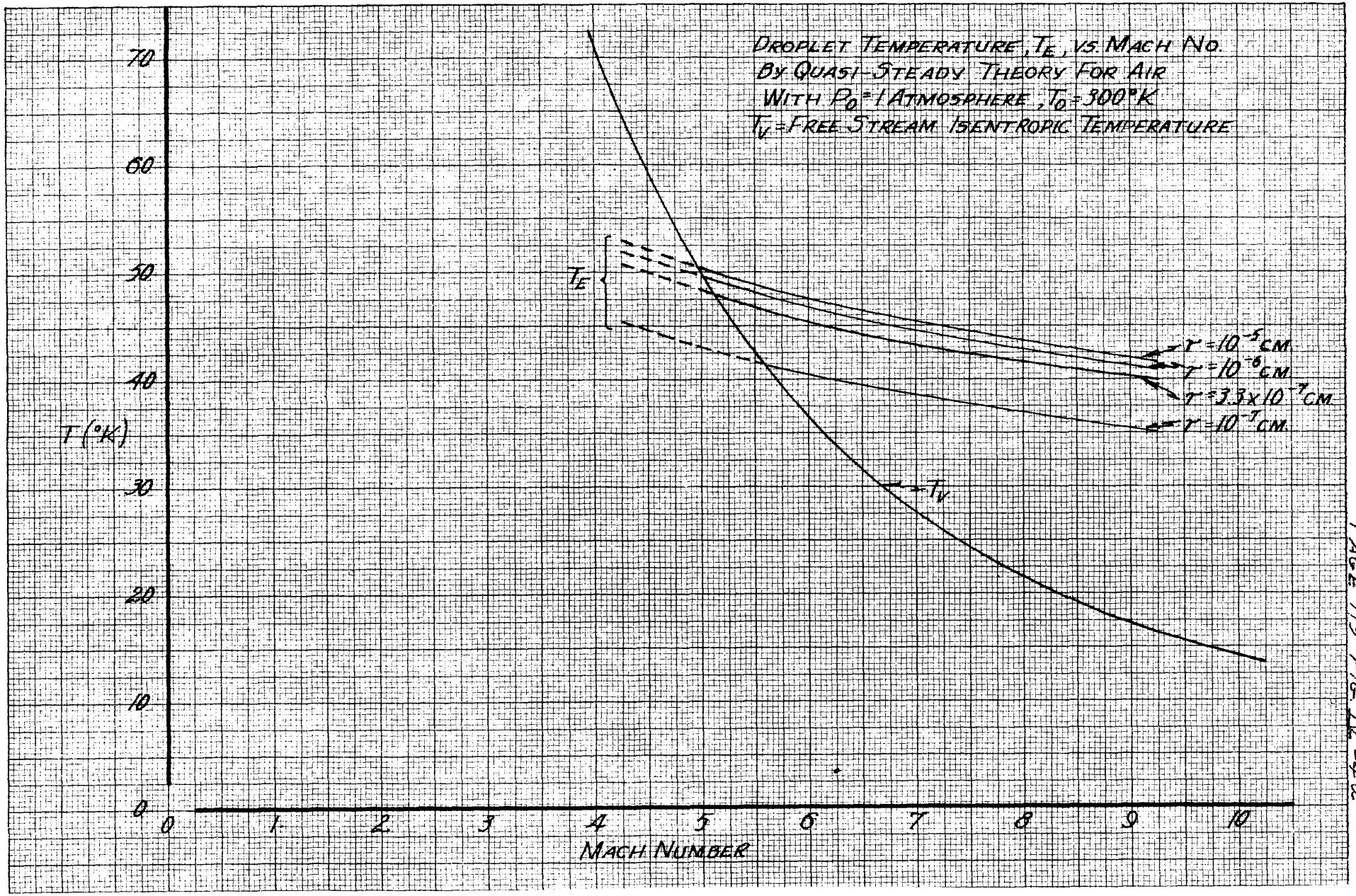

PAGE 119 FIG. IV-42

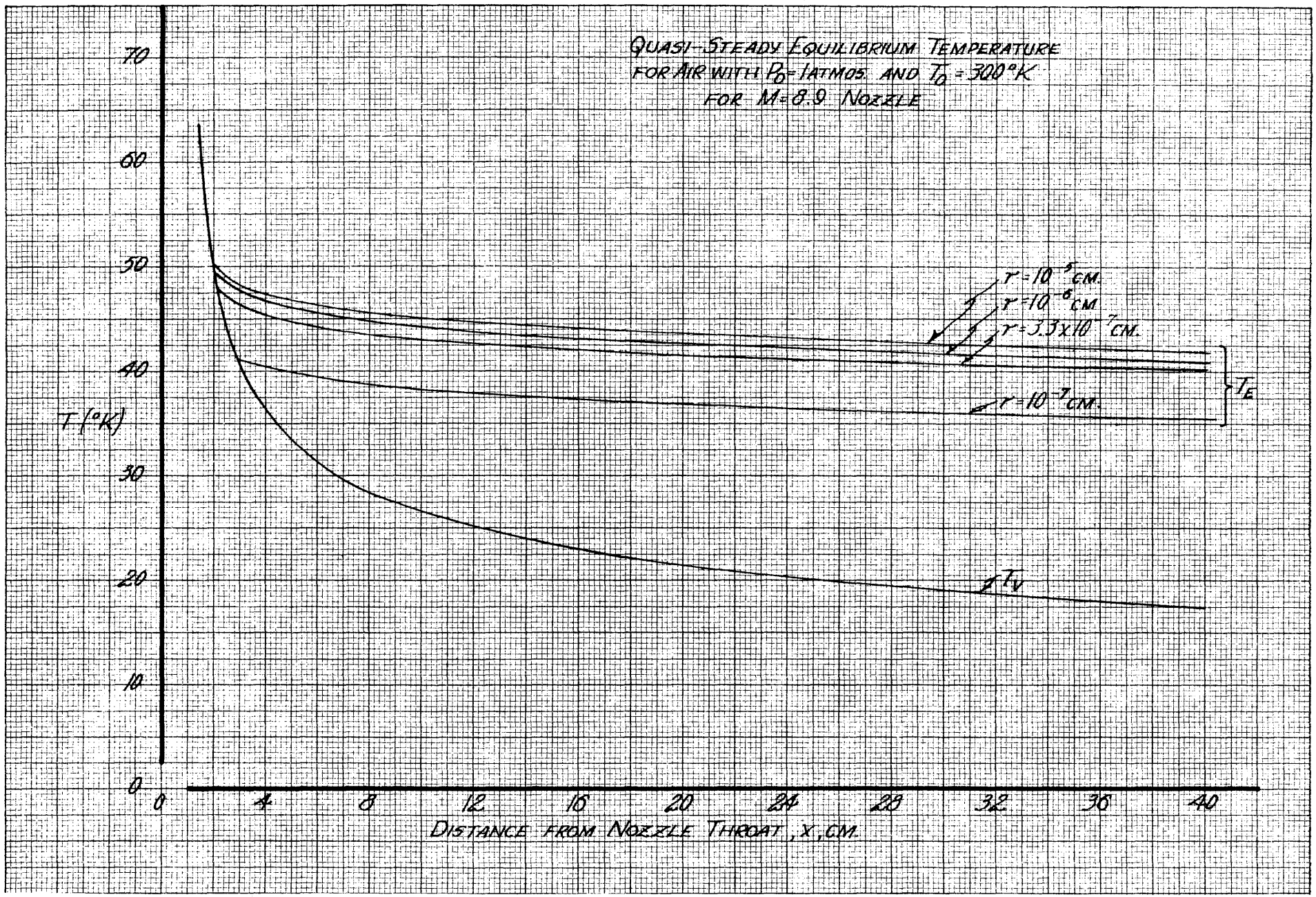

PAGE 120 FIG. 17.10

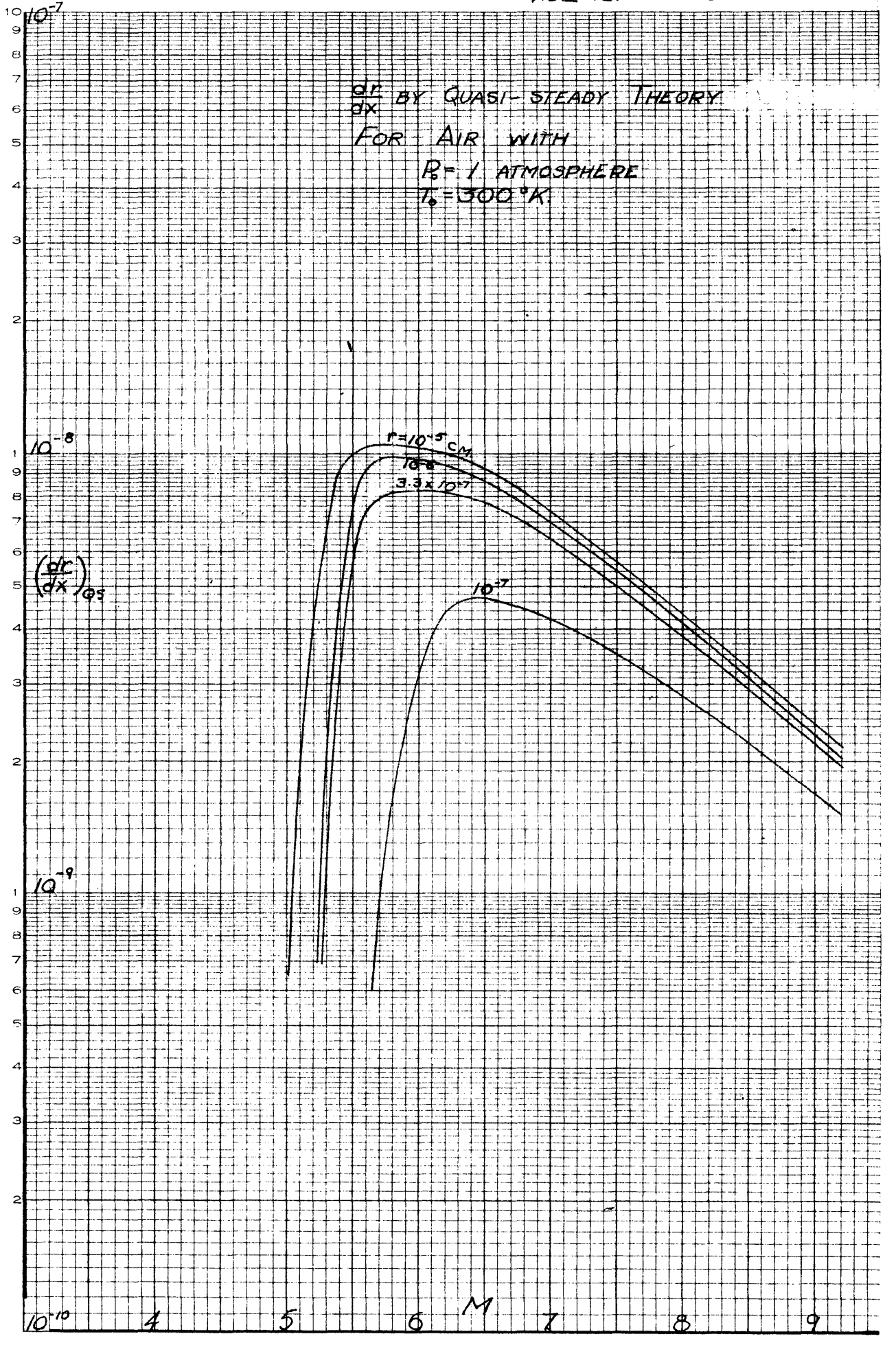

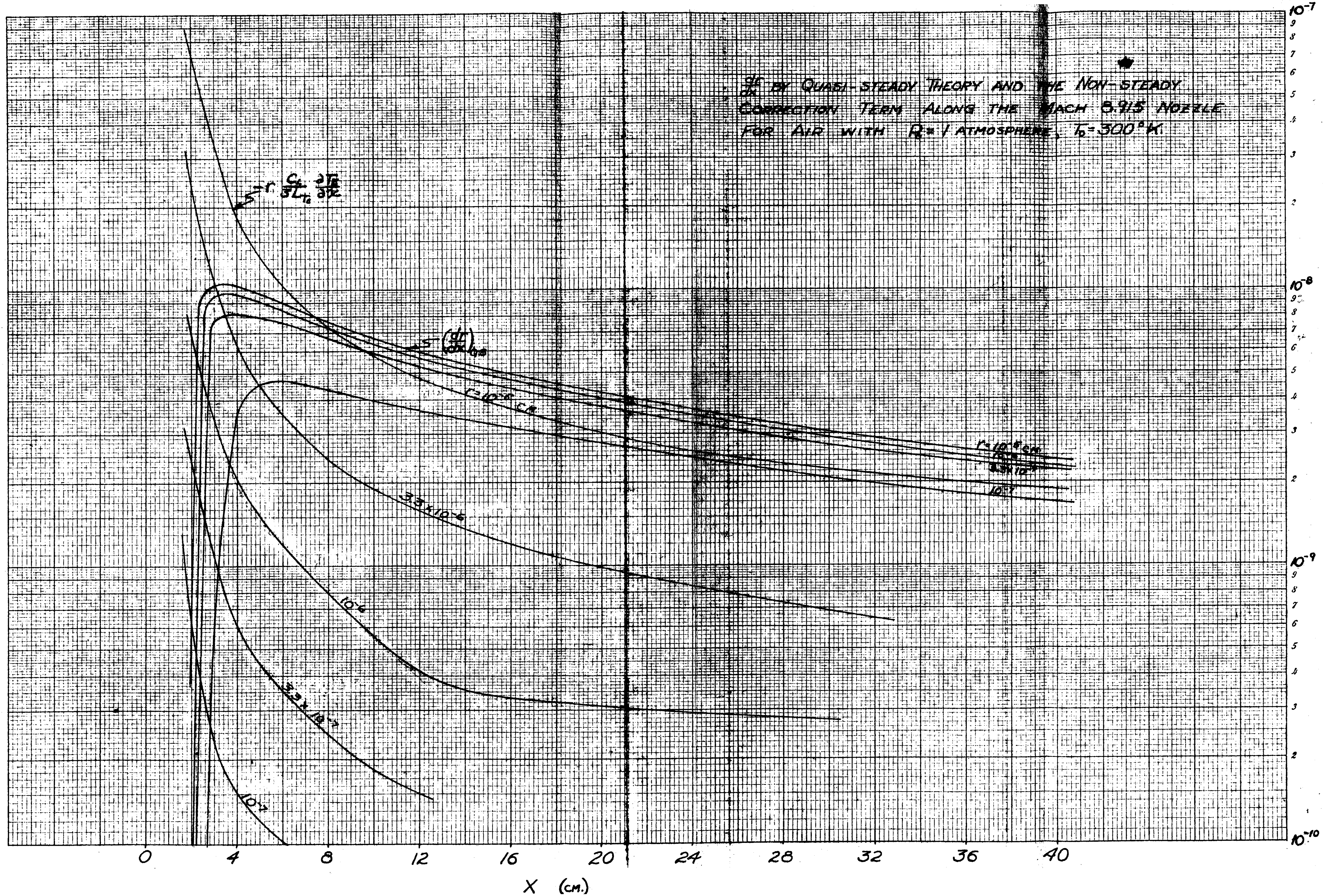
$\frac{dr}{dx}$ BY QUASI-STEADY THEORY AND THE NON-STEADY CORRECTION TERM ALONG THE MACH 8.915 NOZZLE FOR AIR WITH P_0 = 1 ATMOSPHERE, T_0 = 300° K.
$r \cdot \frac{C_t}{3L_{T_0}} \frac{\partial T_R}{\partial x}$
$\left(\frac{dr}{dx}\right)_{QS}$
r = 10^{-5} cm
3.3×10^{-6}
10^{-6}
3.3×10^{-7}
10^{-7}
10^{-7}
10^{-8}
10^{-9}
10^{-10}
0
4
8
12
16
20
24
28
32
36
40
X (CM.)

DROPLET GROWTH ALONG THE MACH 8.915 NOZZLE FOR AIR WITH P_o = 1 ATMOS., T_o = 300° K.

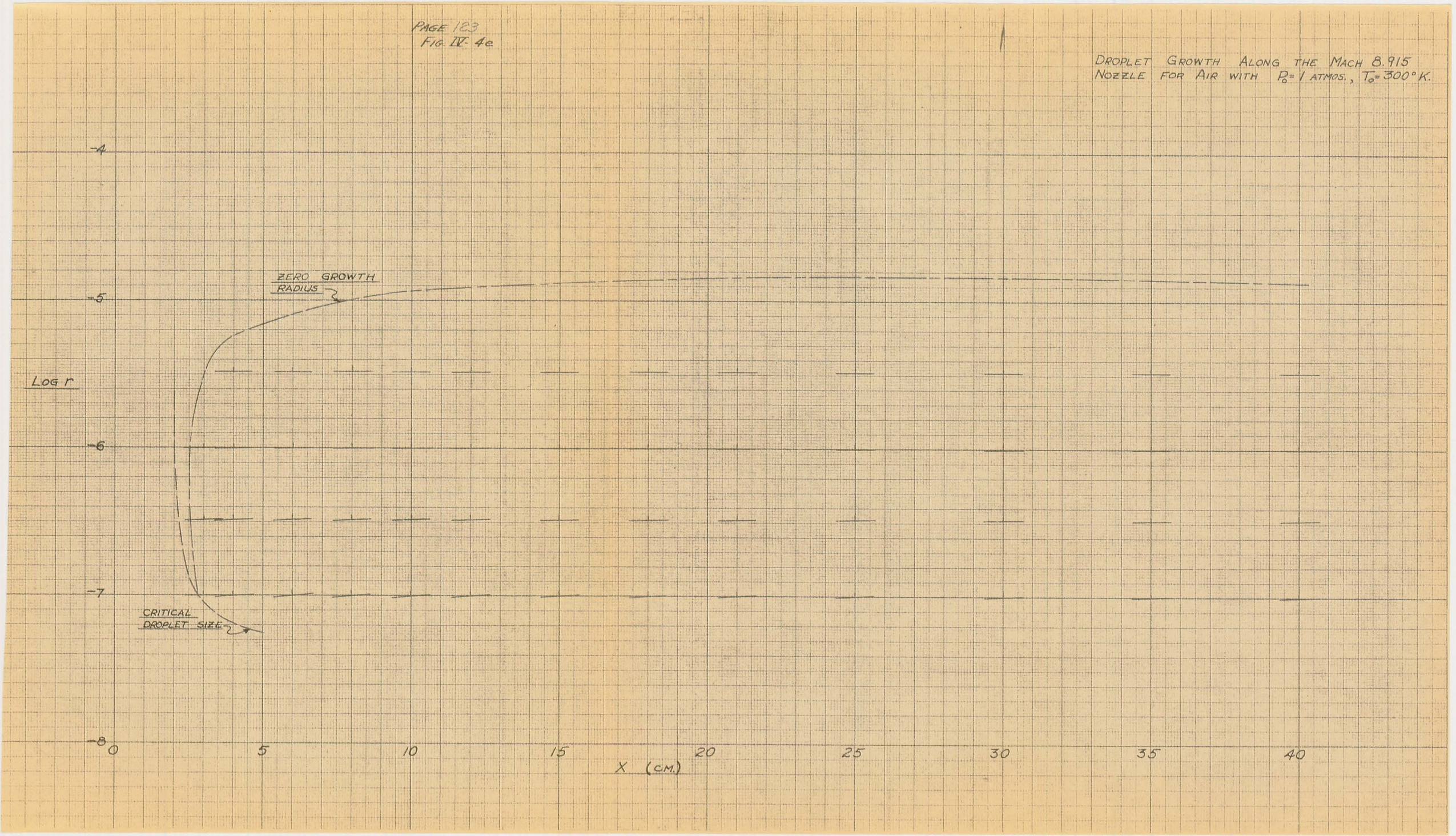

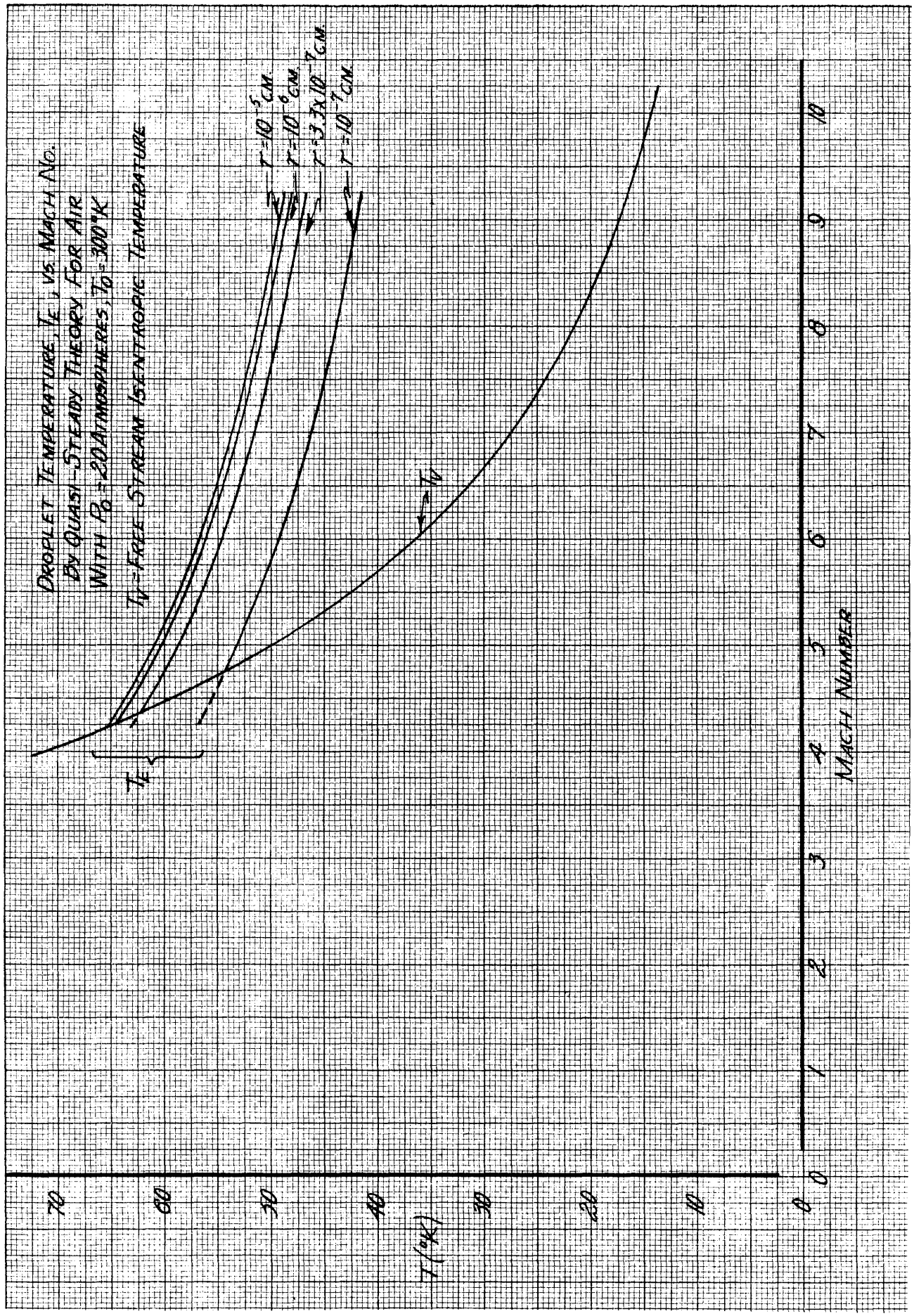
DROPLET TEMPERATURE, T_E, VS. MACH NO.
BY QUASI-STEADY THEORY FOR AIR
WITH P_0 = 20 ATMOSPHERES, T_0 = 300°K
T_W = FREE STREAM ISENTROPIC TEMPERATURE
$r = 10^{-5}$ GM.
$r = 10^{-6}$ GM.
$r = 3.3 \times 10^{-7}$ GM.
$r = 10^{-7}$ GM.
T_E
T_W
T (°K)
MACH NUMBER
0
1
2
3
4
5
6
7
8
9
10
20
30
40
50
60
70

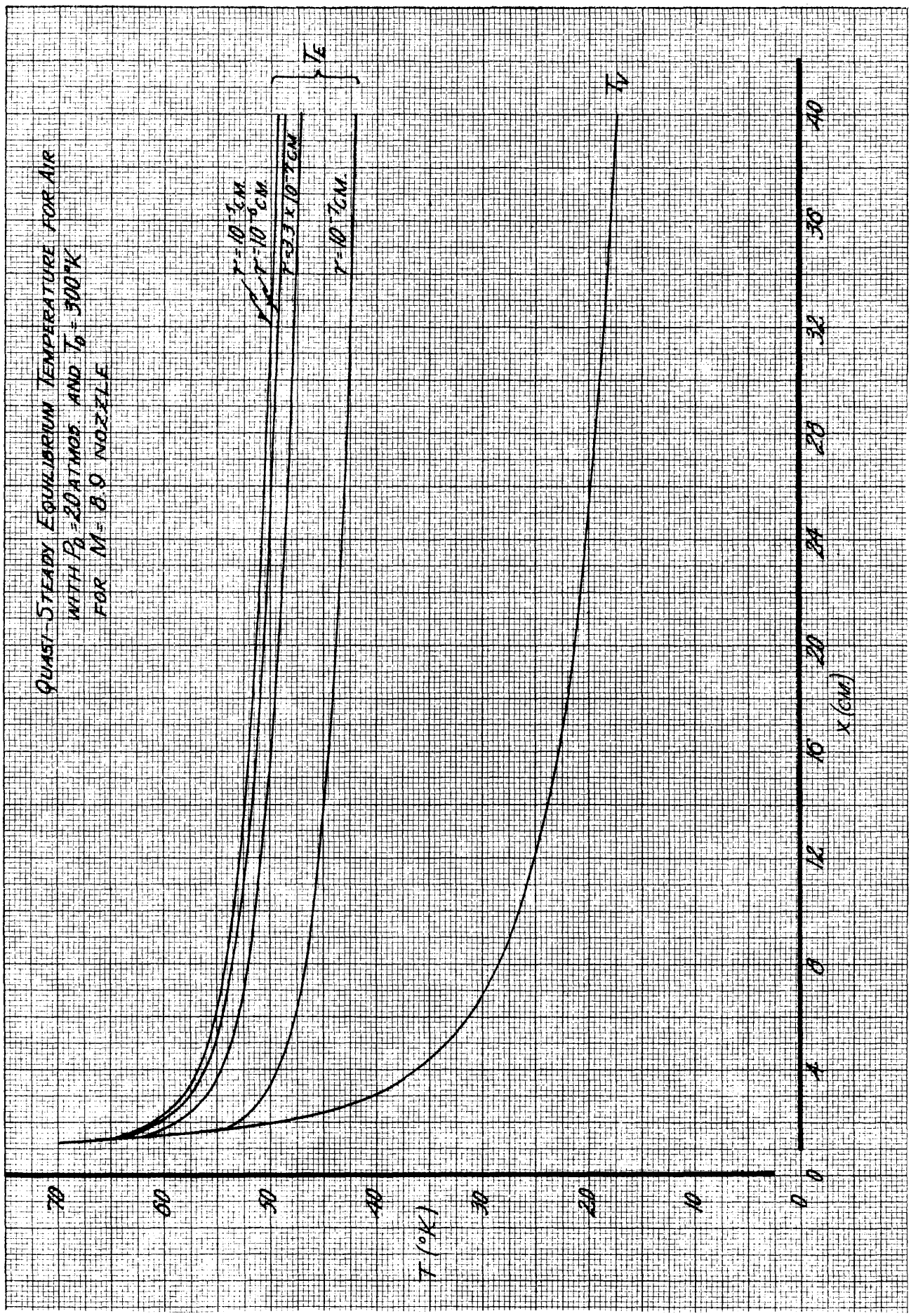
QUASI-STEADY EQUILIBRIUM TEMPERATURE FOR AIR
WITH P_0 = 20 ATMOS. AND T_0 = 300°K
FOR M = 8.9 NOZZLE
$\tau = 10^{-5}$ G.M.
$\tau = 10^{-6}$ G.M.
$\tau = 3.3 \times 10^{-7}$ G.M.
$\tau = 10^{-7}$ G.M.
T_E
T_V
T (°K)
x (CM)
70
60
50
40
30
20
10
0
0
4
8
12
16
20
24
28
32
36
40

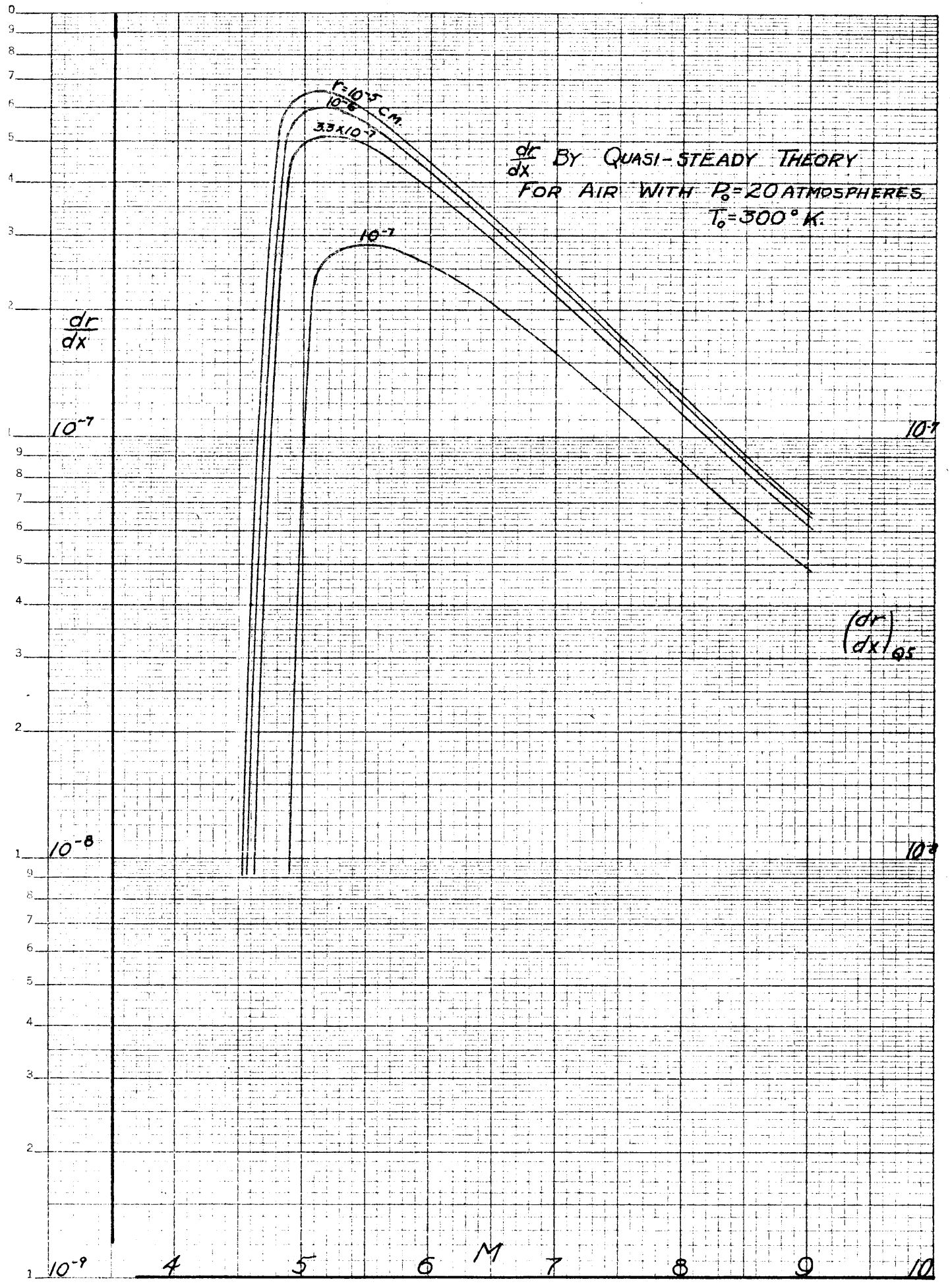
$\frac{dr}{dx}$ BY QUASI-STEADY THEORY
FOR AIR WITH P_0=20 ATMOSPHERES
T_0=300° K.
r=10⁻⁵ CM.
10⁻⁶
3.3x10⁻⁷
10⁻⁷
$\frac{dr}{dx}$
$\left(\frac{dr}{dx}\right)_{QS}$
10⁻⁷
10⁻⁸
10⁻⁹
4
5
6
M
7
8
9
10

$\frac{dr}{dx}$ BY QUASI-STEADY THEORY AND THE NON-STEADY CORRECTION TERM ALONG THE MACH 8.915 NOZZLE FOR AIR WITH $P_0 = 20$ ATMOSPHERES, $T_0 = 300°K$.

$-r\frac{C_L}{SL_{TE}}\frac{\partial T_E}{\partial x}$

$\frac{dr}{dx}$

$r = 3.3 \times 10^{-5}$ CM.

10^{-5}

3.3×10^{-6}

$r = 10^{-5}$ CM.

3.3×10^{-6}

10^{-6}

10^{-7}

10^{-5} 10^{-6} 10^{-7} 10^{-8}

0 4 8 12 16 20 24 28 32 36 40

X (CM.)

DROPLET GROWTH ALONG THE MACH 8.915 NOZZLE
FOR AIR WITH P_o = 20 ATMOS., T_o = 300° K.

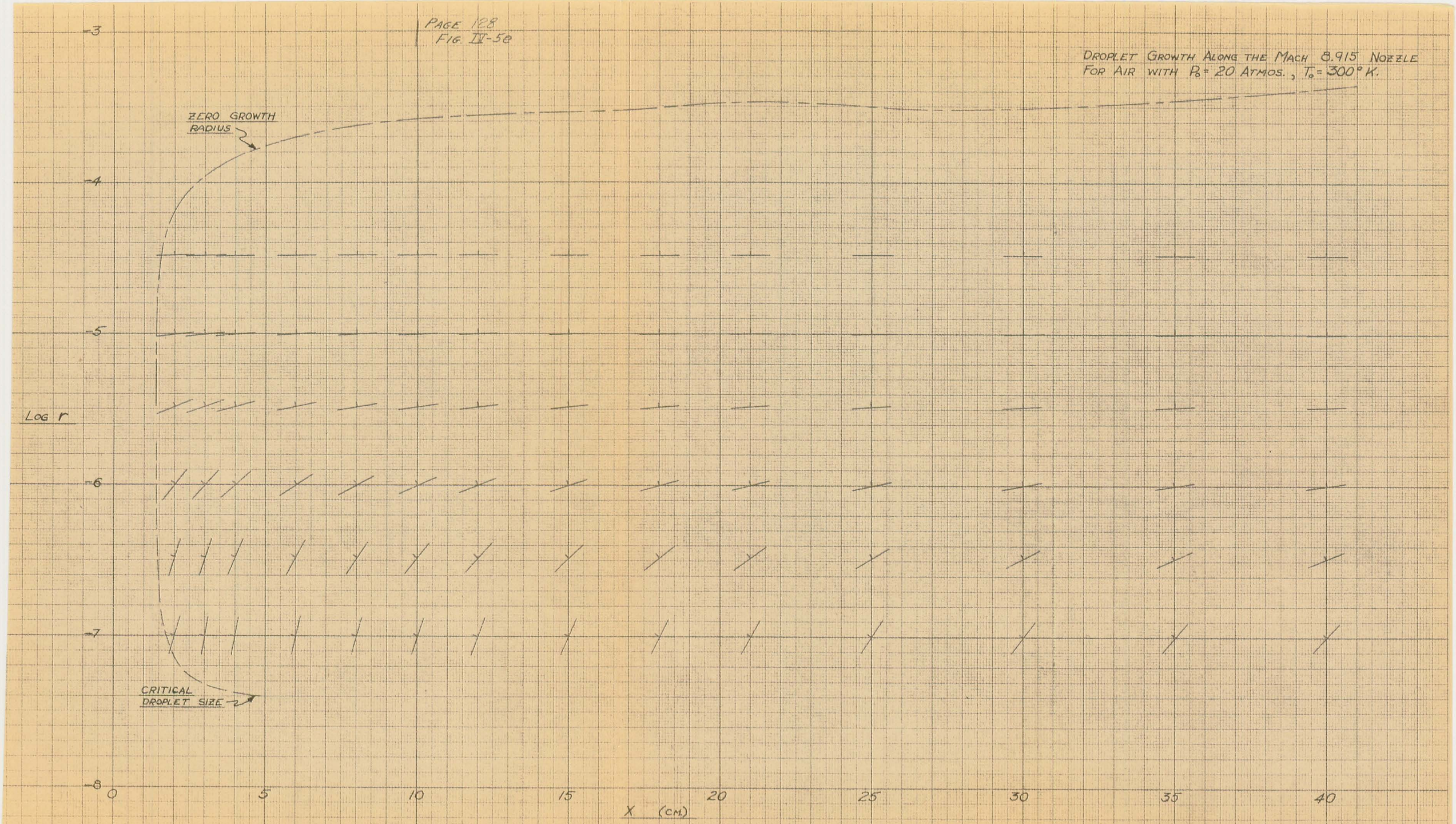

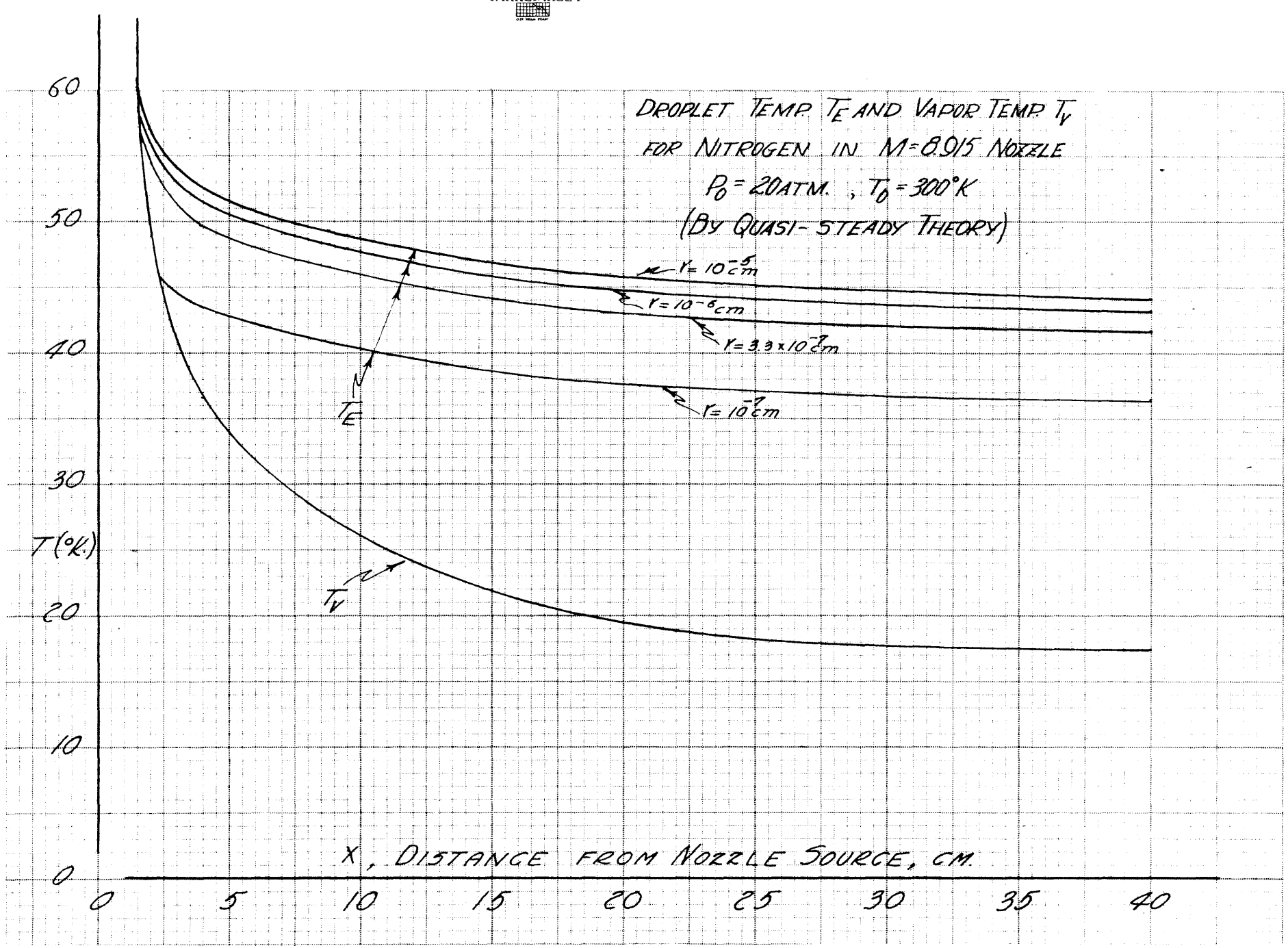

PAGE 129
FIG. III-6a

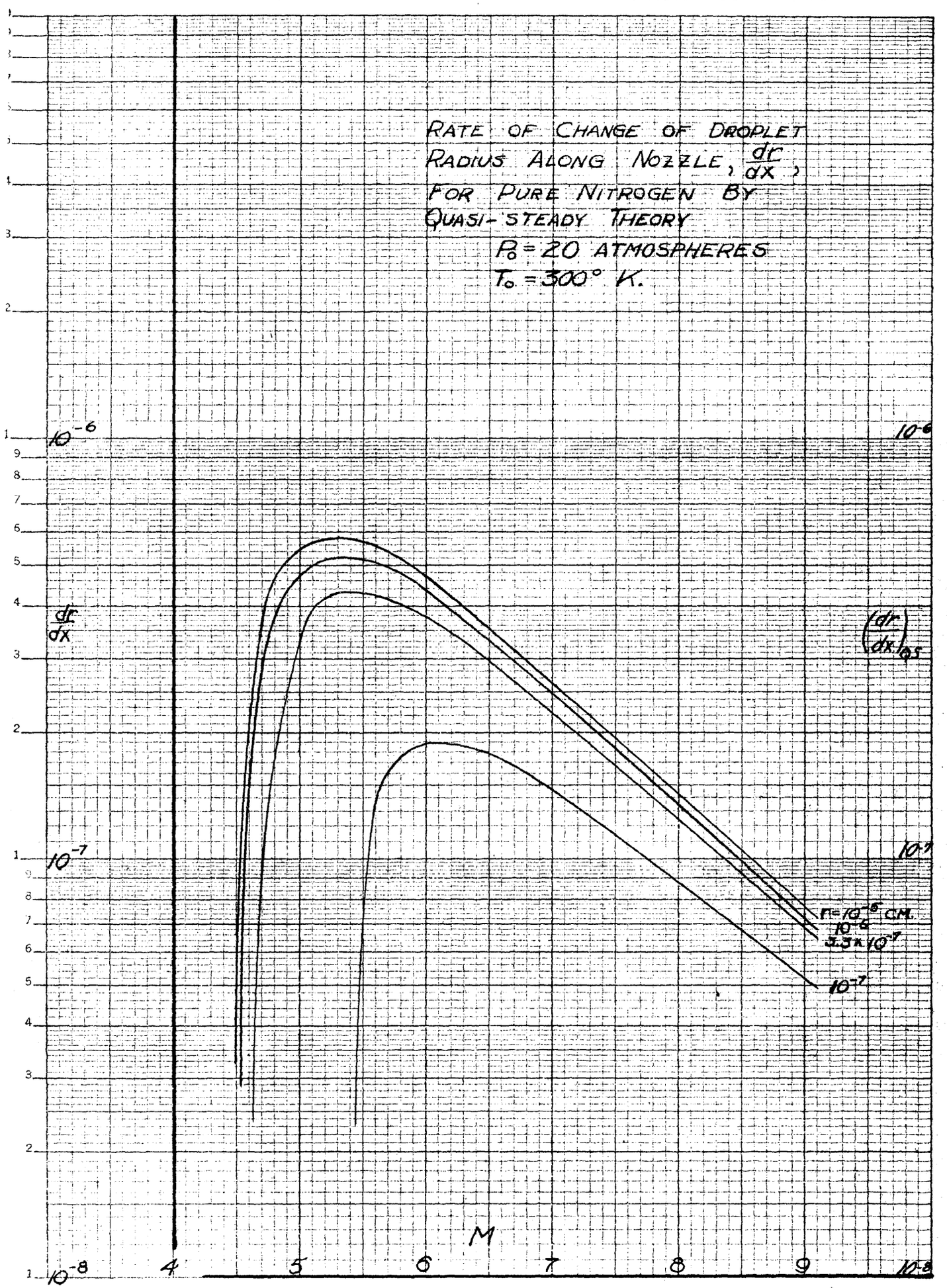
RATE OF CHANGE OF DROPLET RADIUS ALONG NOZZLE, $\frac{dr}{dx}$, FOR PURE NITROGEN BY QUASI-STEADY THEORY
$P_o = 20$ ATMOSPHERES
$T_o = 300°$ K.
10^{-6}
10^{-7}
10^{-8}
$\frac{dr}{dx}$
$\left(\frac{dr}{dx}\right)_{QS}$
$r = 10^{-5}$ CM.
10^{-6}
3.3×10^{-7}
10^{-7}
M
4
5
6
7
8
9

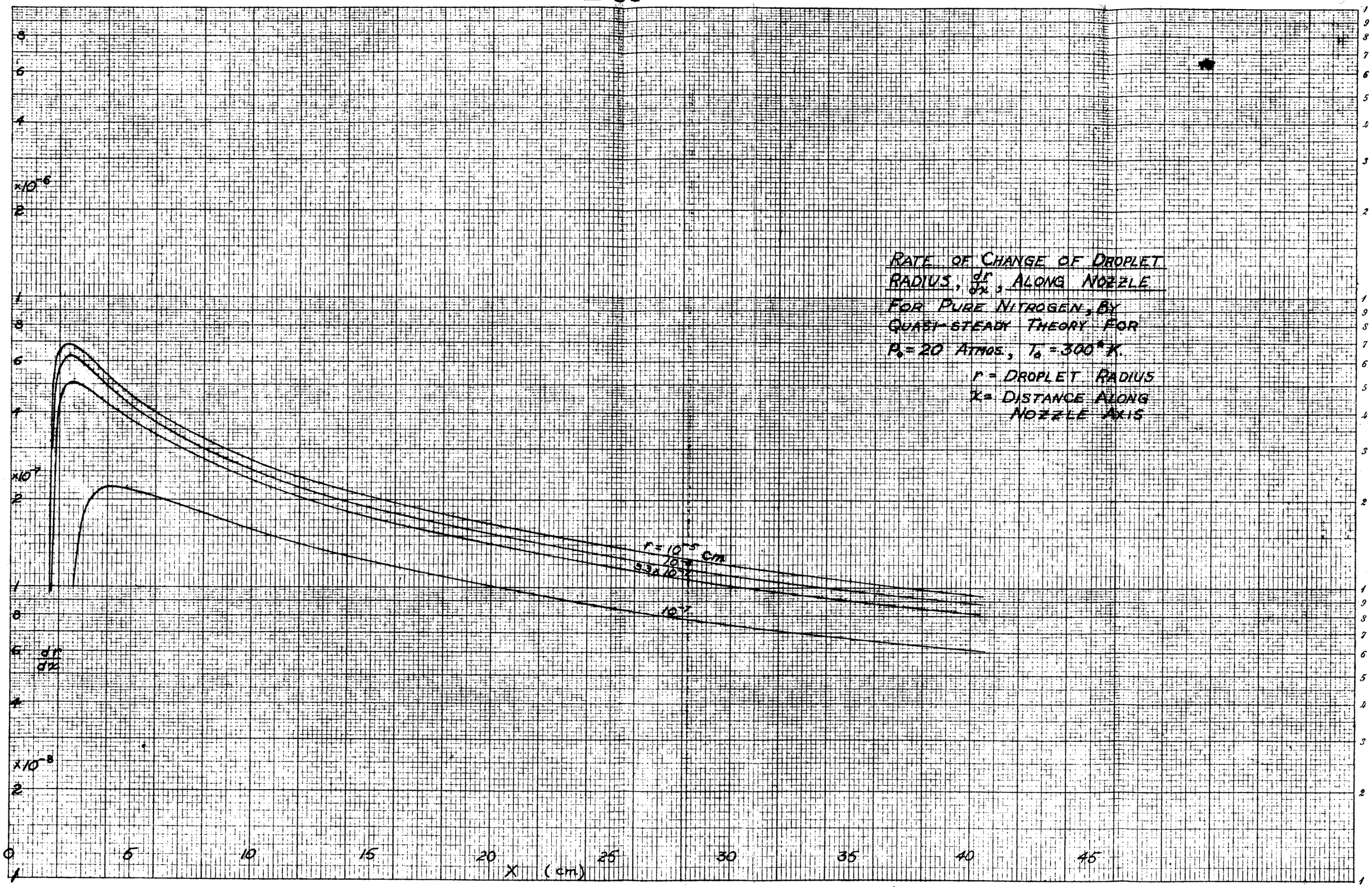
RATE OF CHANGE OF DROPLET RADIUS, $\frac{dr}{dx}$, ALONG NOZZLE FOR PURE NITROGEN, BY QUASI-STEADY THEORY FOR P_0 = 20 ATMOS., T_0 = 300°K.
r = DROPLET RADIUS
x = DISTANCE ALONG NOZZLE AXIS
$r = 10^{-5}$ cm
9.3×10^{-6}
10^{-6}
10^{-7}
$\frac{dr}{dx}$
$\times 10^{-6}$
$\times 10^{-7}$
$\times 10^{-8}$
0
5
10
15
20
25
30
35
40
45
x (cm.)

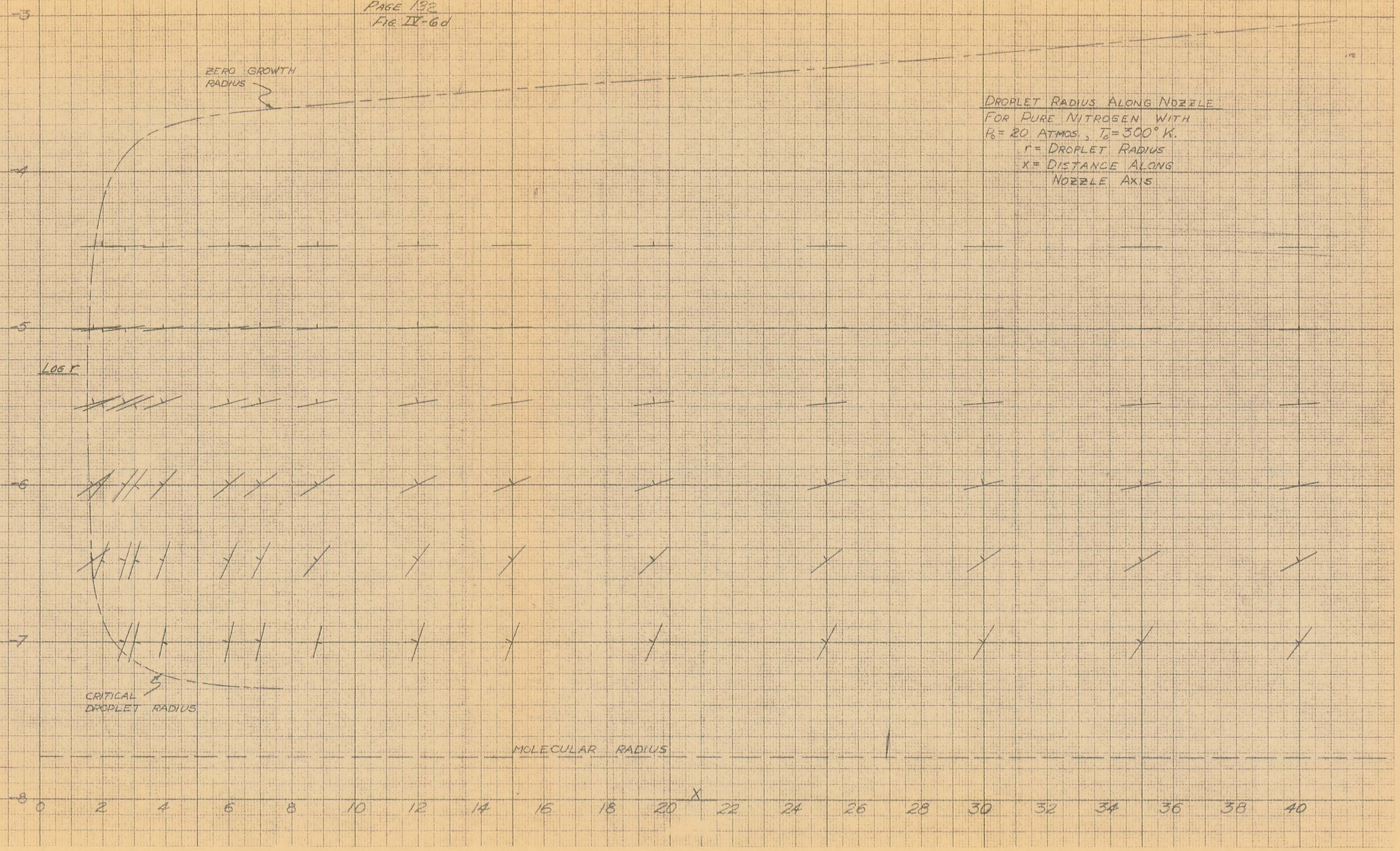

DROPLET RADIUS ALONG NOZZLE
FOR PURE NITROGEN WITH
P_o = 20 ATMOS., T_o = 300° K.
r = DROPLET RADIUS
x = DISTANCE ALONG
NOZZLE AXIS

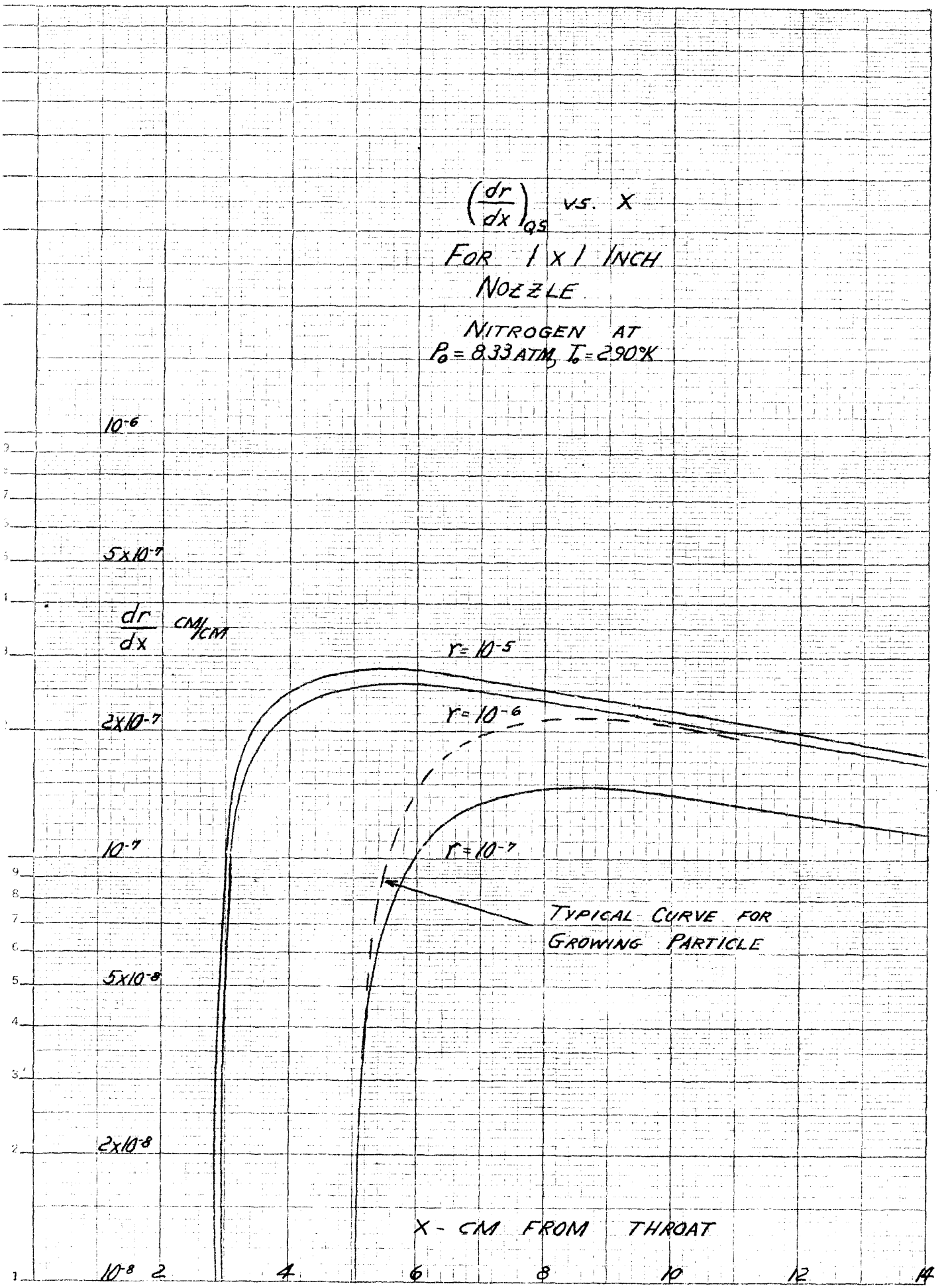
$\left(\frac{dr}{dx}\right)_{QS}$ VS. X
FOR 1 X 1 INCH NOZZLE
NITROGEN AT $P_o = 8.33$ ATM, $T_o = 290°K$
10^{-6}
5×10^{-7}
$\frac{dr}{dx}$ CM/CM
$r = 10^{-5}$
$r = 10^{-6}$
2×10^{-7}
10^{-7}
$r = 10^{-7}$
TYPICAL CURVE FOR GROWING PARTICLE
5×10^{-8}
2×10^{-8}
X - CM FROM THROAT
10^{-8}
2
4
6
8
10
12
14

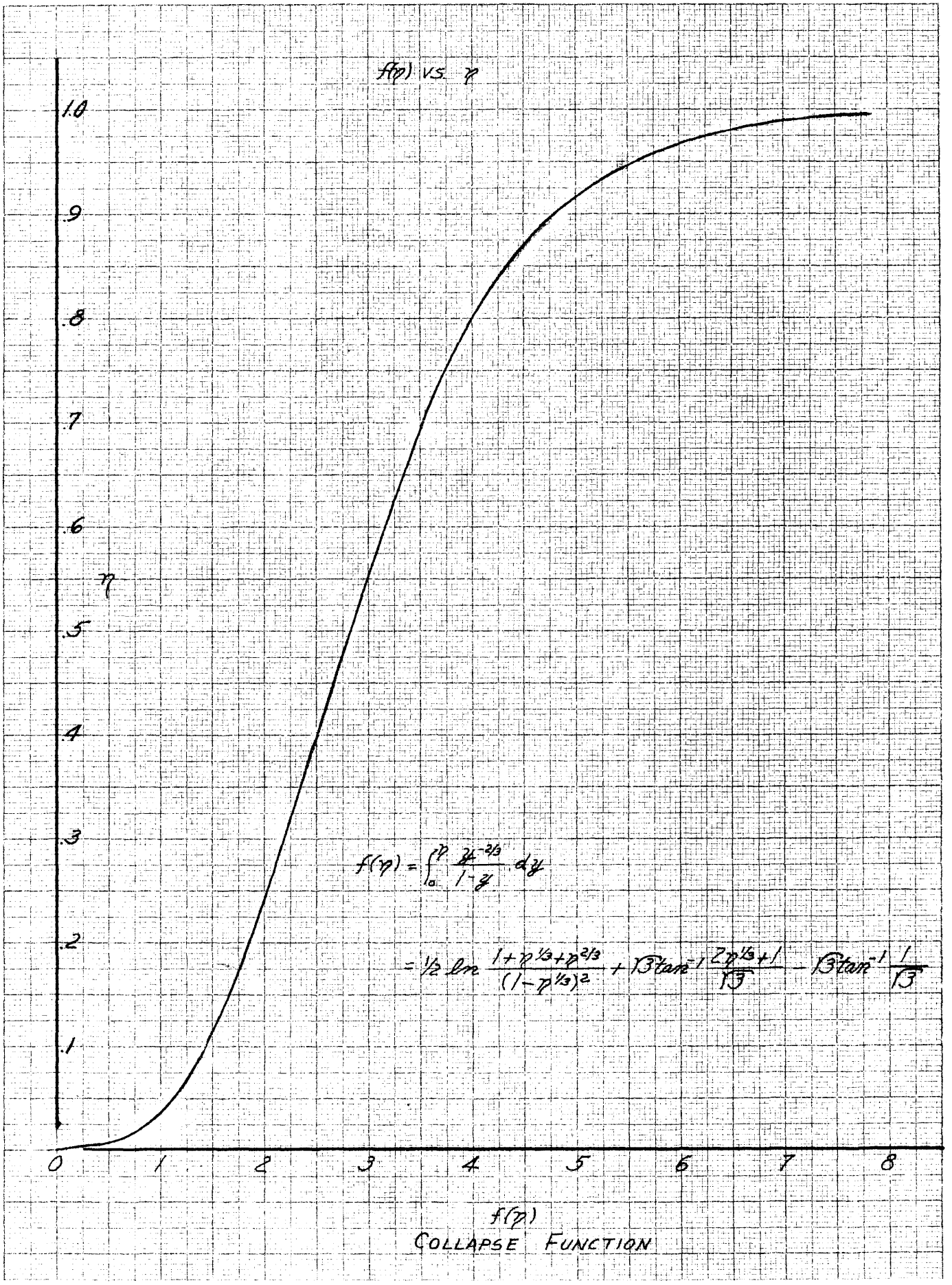

$f(\eta)$
COLLAPSE FUNCTION

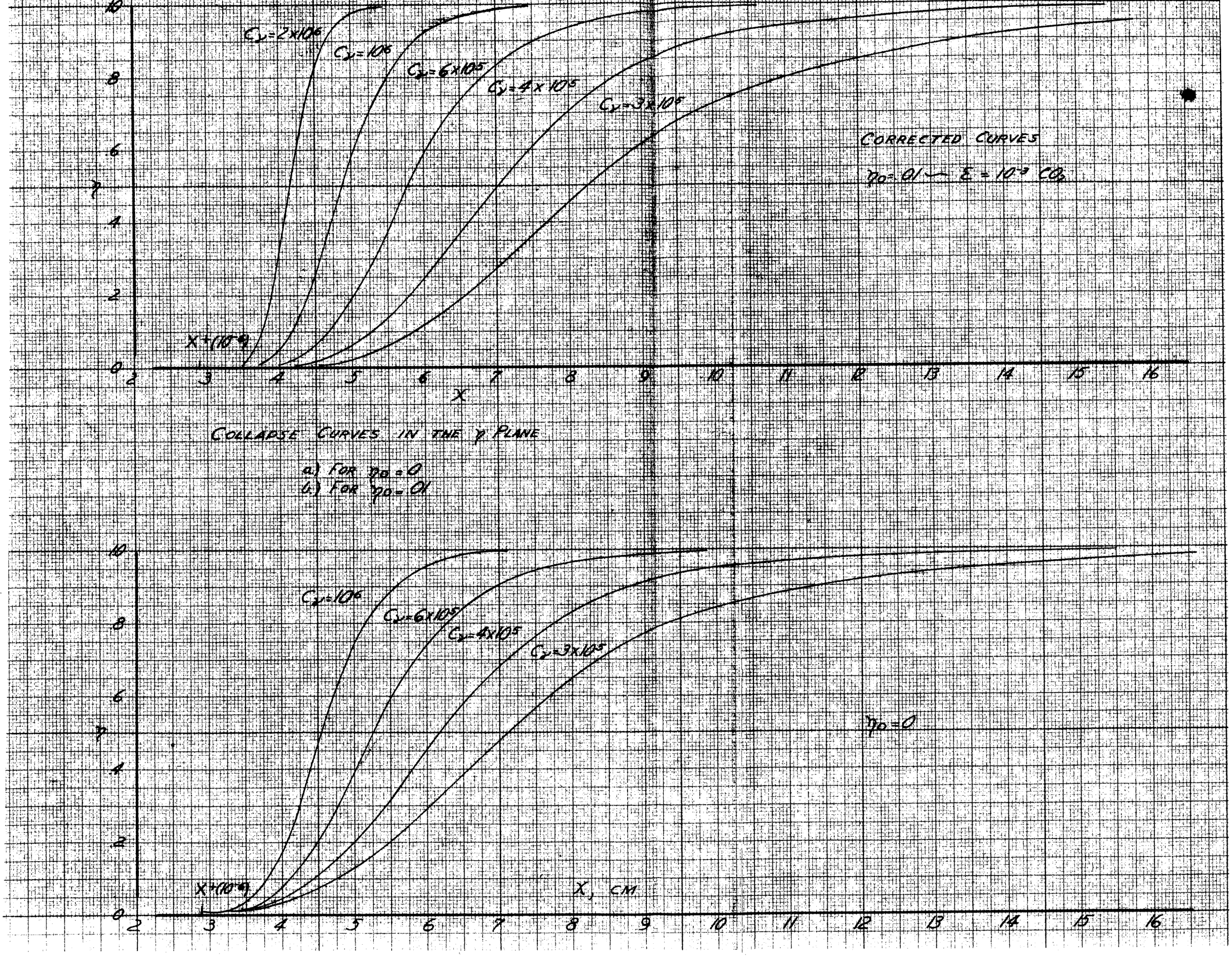
$C_y = 2\times10^6$
$C_y = 10^6$
$C_y = 6\times10^5$
$C_y = 4\times10^5$
$C_y = 3\times10^5$
CORRECTED CURVES
$\eta_0 = 0$ — $\xi = 10^{-3}$ CO_2
$X+(10^{-4})$
X
COLLAPSE CURVES IN THE η PLANE
a) FOR $\eta_0 = 0$
b) FOR $\eta_0 = 01$
$C_y = 10^6$
$C_y = 6\times10^5$
$C_y = 4\times10^5$
$C_y = 3\times10^5$
$\eta_0 = 0$
$X+(10^{-4})$
X, CM

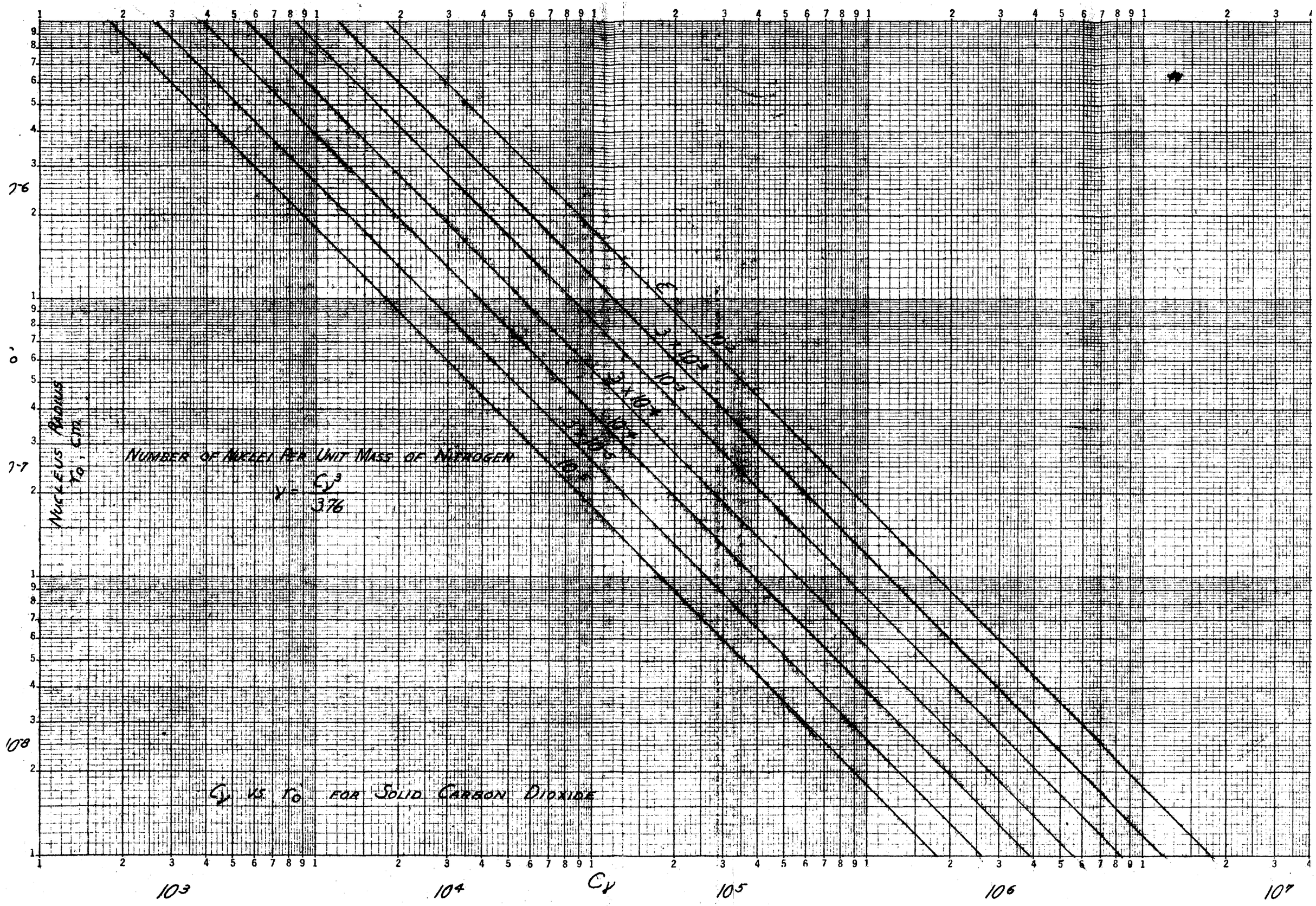
NUMBER OF NUCLEI PER UNIT MASS OF NITROGEN
$\gamma = \frac{C_\gamma^3}{3T_0}$
NUCLEUS RADIUS r_0, CM.
C_γ VS. T_0 FOR SOLID CARBON DIOXIDE
C_γ
10^3
10^4
10^5
10^6
10^7
10^8
7·6
7·7
3×10^{-6}
10^{-6}
3×10^{-7}
10^{-7}
3×10^{-8}
10^{-8}

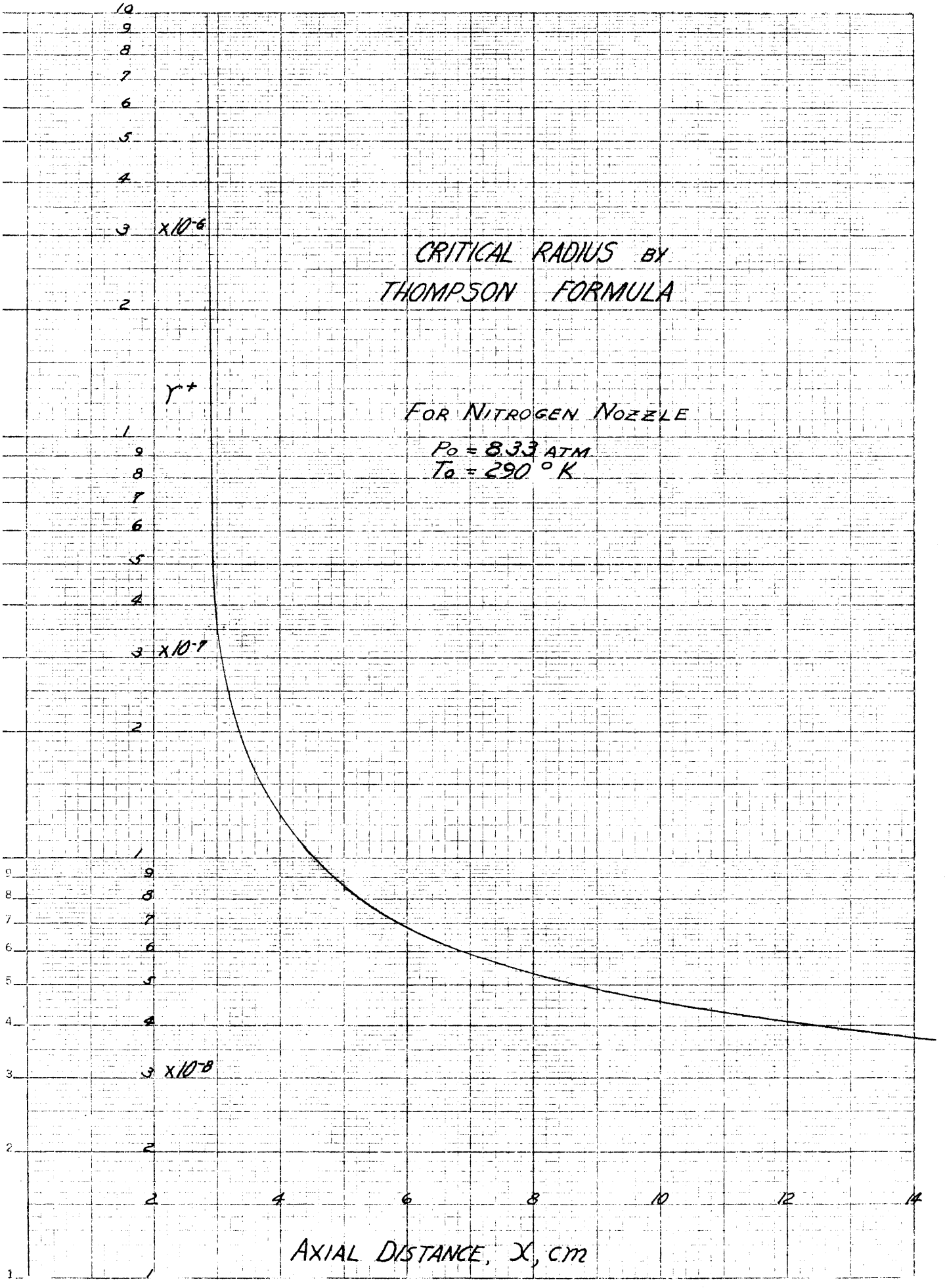
CRITICAL RADIUS BY
THOMPSON FORMULA
FOR NITROGEN NOZZLE
P_o = 8.33 ATM
T_o = 290 °K
r^*
10
9
8
7
6
5
4
3 x10⁻⁶
2
1
9
8
7
6
5
4
3 x10⁻⁷
2
1
9
8
7
6
5
4
3 x10⁻⁸
2
1
2
4
6
8
10
12
14
AXIAL DISTANCE, X, cm

CORRECTED FOR $\eta_0 = .01$

$\varepsilon = 10^{-3}$ $\eta = 0.5$

$\varepsilon = 10^{-3}$ $\eta = 0.8$

$\varepsilon = 10^{-3}$ $\eta = 0.5$

$\varepsilon = 10^{-3}$ $\eta = 0.8$

$\varepsilon = 10^{-4}$ $\eta = 0.5$

$\varepsilon = 10^{-4}$ $\eta = 0.8$

$\varepsilon = 10^{-5}$ $\eta = 0.5$

$\varepsilon = 10^{-5}$ $\eta = 0.8$

THOMPSON CRITICAL RADIUS

NUCLEUS RADIUS r_0, CM

X, CM

THEORETICAL COLLAPSE POSITION FOR DIFFERENT NUCLEUS SIZES (FOR NITROGEN NOZZLE OF REF 16)

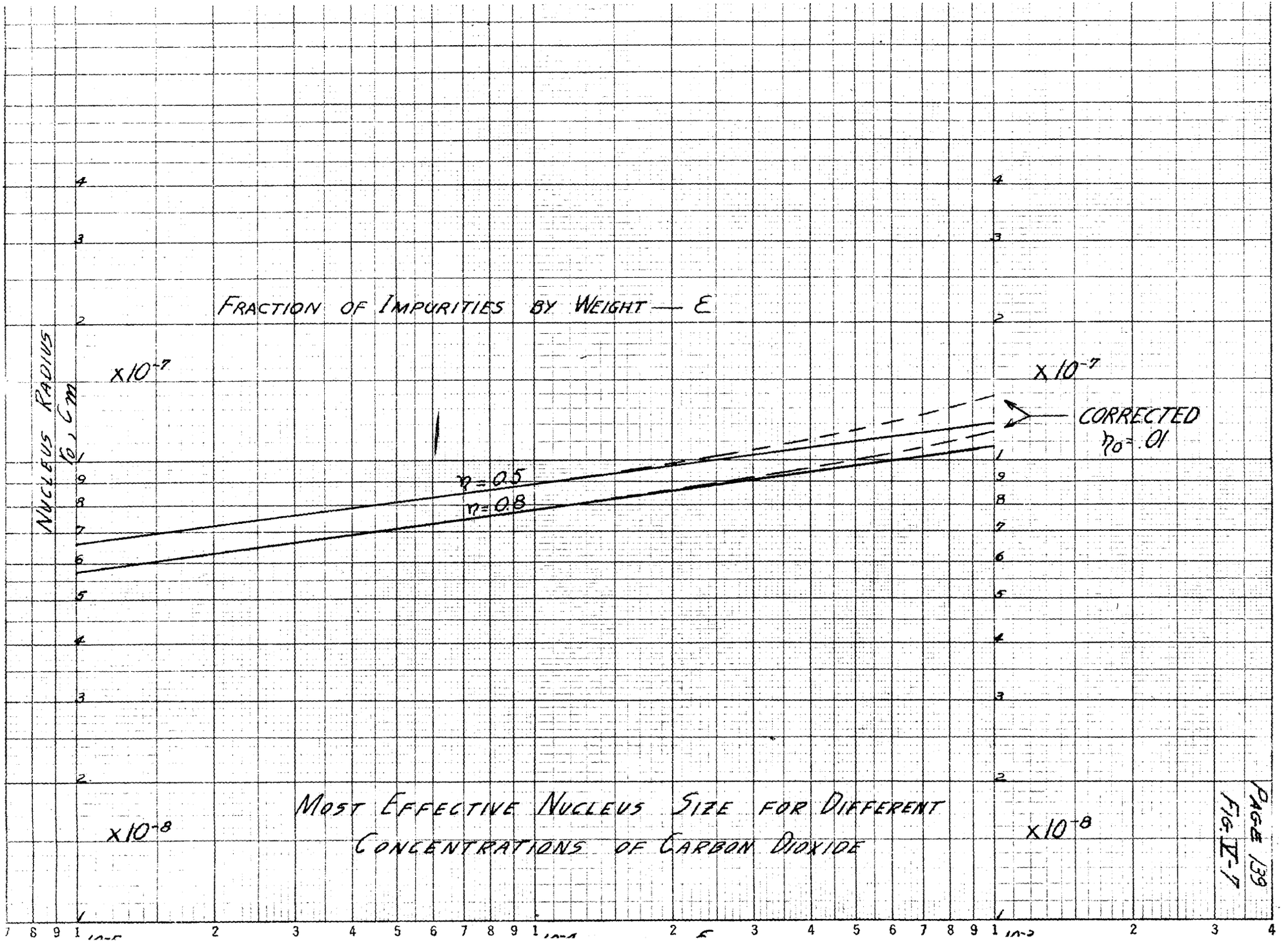

MOST EFFECTIVE NUCLEUS SIZE FOR DIFFERENT CONCENTRATIONS OF CARBON DIOXIDE

PAGE 139
FIG. II-1

PAGE 140
FIG. V-8

EXPERIMENTS BY ARTHUR (REF 26)

SYMBOL	RUN No	IMPURITIES, BY WEIGHT, ε CO_2	H_2O	REMARKS
●	23-1	3.3×10^{-5}	1.5×10^{-5}	COMMERCIAL BOTTLED NITROGEN
◉	27-1	$< 6.3 \times 10^{-5}$	$< 4.5 \times 10^{-6}$	
◉	34-1	$< 1.1 \times 10^{-4}$	$< 1.4 \times 10^{-5}$	
⊡	23-2	1.2×10^{-4}	1.5×10^{-5}	
×	23-3	1.1×10^{-3}	"	
▲	23-4	2.8×10^{-4}	"	
■	23-5	6.8×10^{-4}	"	

CONDENSATION SHOCK LOCUS

SATURATED EXPANSION

$\varepsilon = 10^{-3}$ $(C_Y = 1.35 \times 10^5)$

$\varepsilon = 10^{-4}$ $(C_Y = 2.5 \times 10^5)$

$\varepsilon = 10^{-5}$ $(C_Y = 3.15 \times 10^5)$

ISENTROPE (NO CONDENSATION)

$\gamma = 1$

$\gamma = 0$

$\frac{P}{P_0'}$

.035
.03
.025
.02

THEORETICAL COLLAPSE ESTIMATES COMPARED WITH EXPERIMENT

AXIAL DISTANCE FROM THROAT, CM.

0 1 2 3 4 X 5 6 7 8 9 10 11 12 13 14 15 16

.9 .8 .7 .6 .5 .4 .3 .2 .1

FIG V-9

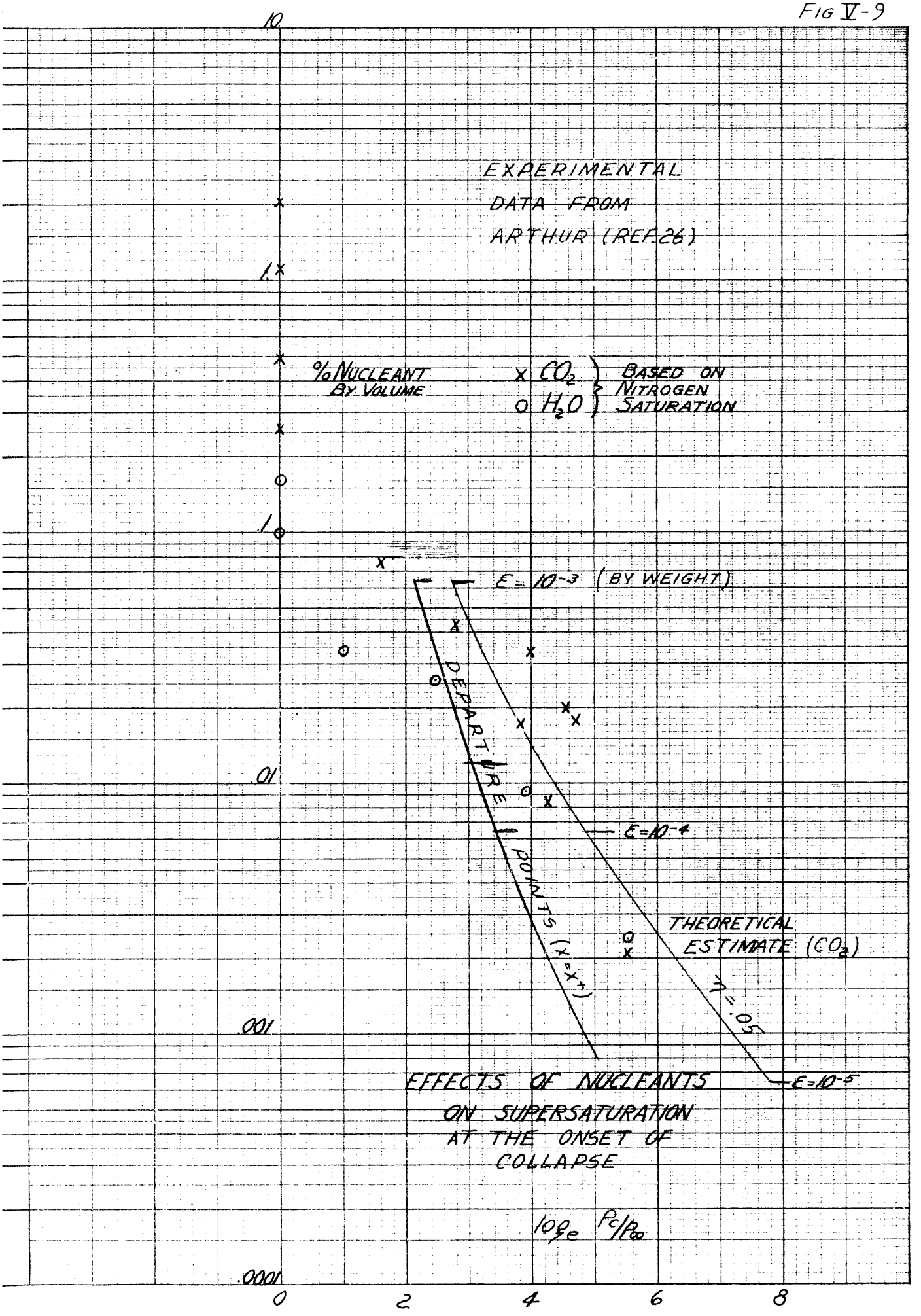

EFFECTS OF NUCLEANTS ON SUPERSATURATION AT THE ONSET OF COLLAPSE

FIG. A-1

VAPOR PRESSURE OF AIR

WAGNER (REF. 1)

$$\ln \frac{P_2}{P_1} = \frac{L}{R}\left[\frac{1}{T_1} - \frac{1}{T_2}\right]$$

⊙ MATCHED TO WAGNER'S CURVE AT $T = 40°, 60°$

◉ " " " " " " $T = 47.5°, 75°$

△ " " " " " $T_1 = 85°$

$L/R = T_2$

$L/R = 632.09$

$L/R = 823.64$

WAGNER'S CURVE

P_s

T (°K)

10^{-1} 10^{-2} 10^{-3} 10^{-4} 10^{-5}

30 40 50 60 70 80 90

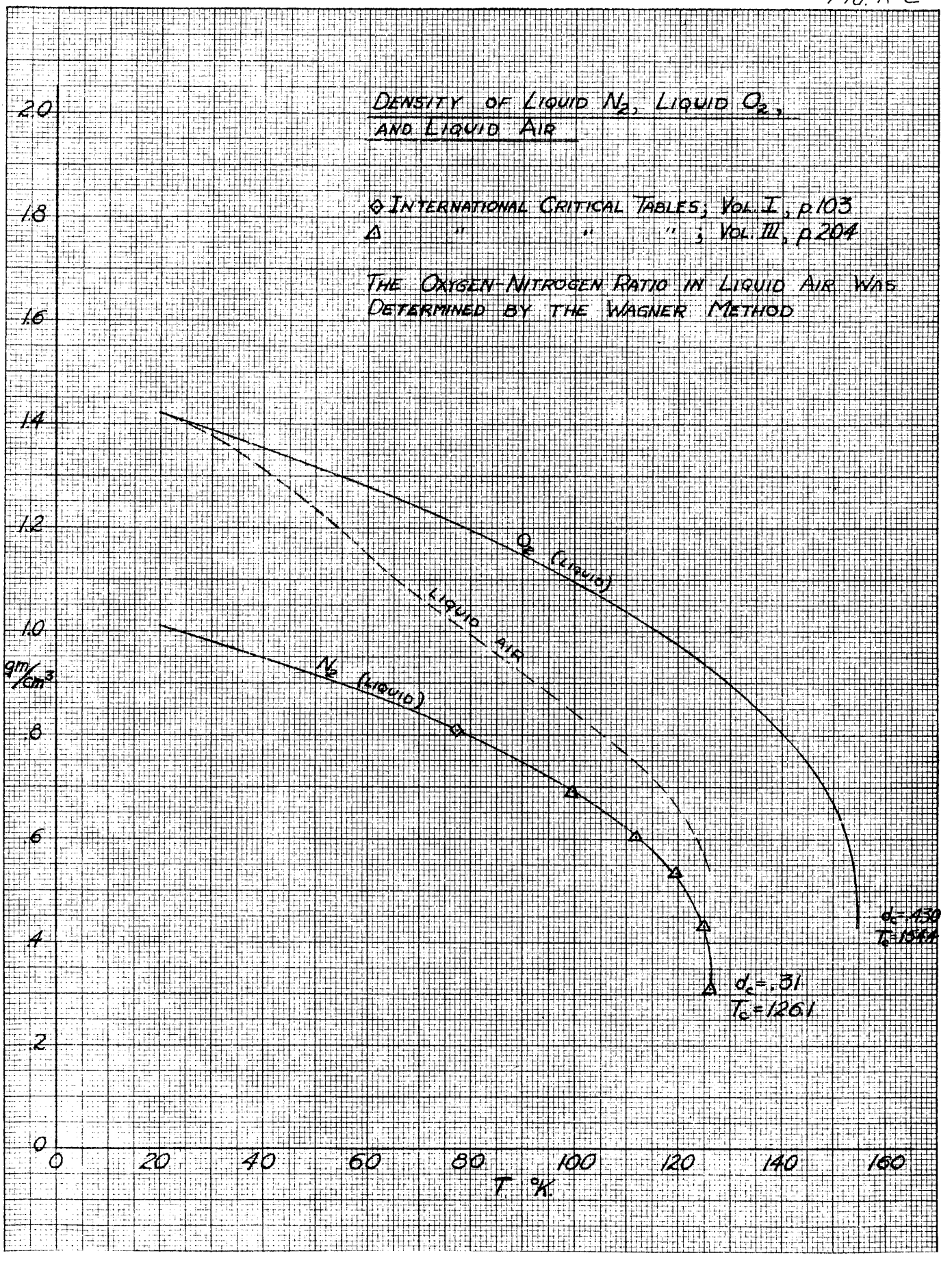
DENSITY OF LIQUID N_2, LIQUID O_2, AND LIQUID AIR
◇ INTERNATIONAL CRITICAL TABLES; VOL. I, p 103
Δ " " " ; VOL. III, p 204
THE OXYGEN-NITROGEN RATIO IN LIQUID AIR WAS DETERMINED BY THE WAGNER METHOD
O_2 (LIQUID)
LIQUID AIR
N_2 (LIQUID)
d_c=.430
T_c=154.4
d_c=.31
T_c=126.1
gm/cm³
2.0
1.8
1.6
1.4
1.2
1.0
.8
.6
.4
.2
0
0
20
40
60
80
100
120
140
160
T °K.

FIG. A-3

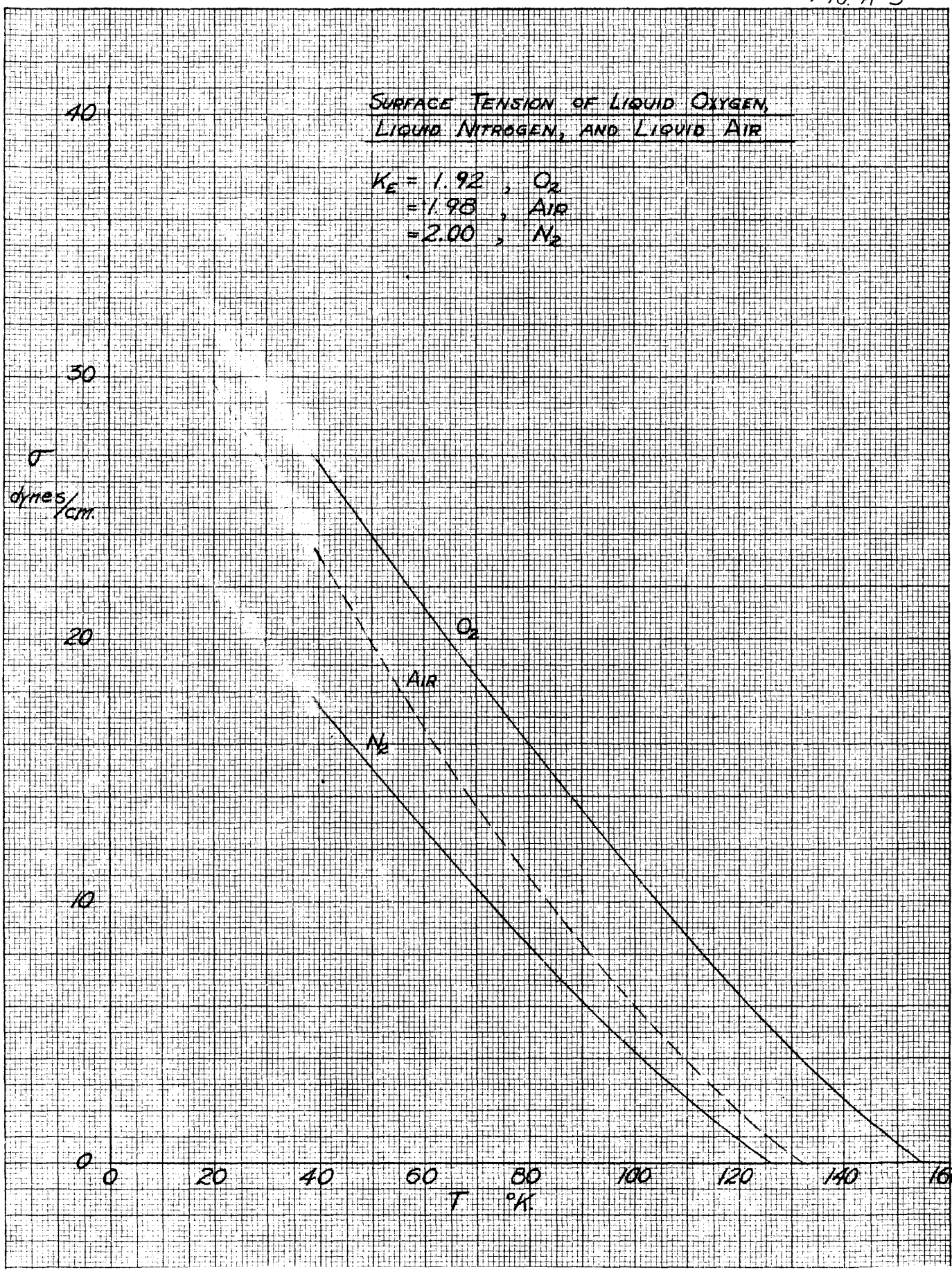
SURFACE TENSION OF LIQUID OXYGEN, LIQUID NITROGEN, AND LIQUID AIR
K_E = 1.92 , O_2
= 1.98 , AIR
= 2.00 , N_2
40
30
20
10
0
σ
dynes/cm.
O_2
AIR
N_2
0
20
40
60
80
100
120
140
160
T °K.

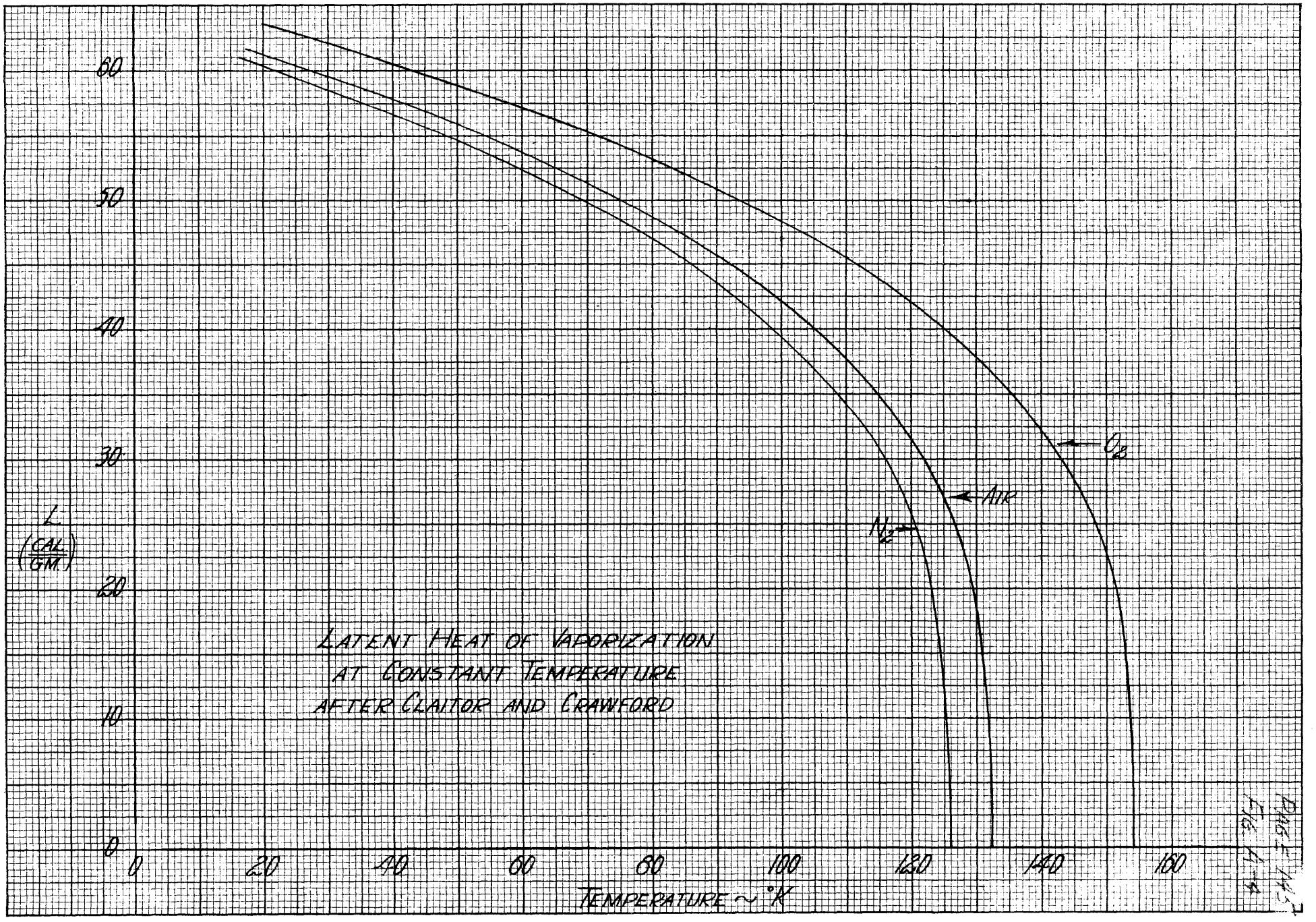

LATENT HEAT OF VAPORIZATION
AT CONSTANT TEMPERATURE
AFTER CLAITOR AND CRAWFORD

FIG. 4-4

PAGE 145